FINITE ELEMENT ANALYSIS AND COMPUTATIONAL MODELING OF SOME NON-LINEAR PARABOLIC PDEs

Ph. D. THESIS

by

OM PRAKASH YADAV

DEPARTMENT OF MATHEMATICS
INDIAN INSTITUTE OF TECHNOLOGY ROORKEE
ROORKEE - 247 667 (INDIA)
DECEMBER, 2018

FINITE ELEMENT ANALYSIS AND COMPUTATIONAL MODELING OF SOME NON-LINEAR PARABOLIC PDEs

A THESIS

Submitted in partial fulfilment of the requirements for the award of the degree

of

DOCTOR OF PHILOSOPHY

in

MATHEMATICS

by

OM PRAKASH YADAV

DEPARTMENT OF MATHEMATICS
INDIAN INSTITUTE OF TECHNOLOGY ROORKEE
ROORKEE - 247 667 (INDIA)
DECEMBER, 2018

INDIAN INSTITUTE OF TECHNOLOGY ROORKEE
ROORKEE

CANDIDATE'S DECLARATION

I hereby certify that the work which is being presented in the thesis entitled **"FINITE ELEMENT ANALYSIS AND COMPUTATIONAL MODELING OF SOME NON-LINEAR PARABOLIC PDEs"** in partial fulfilment of the requirements for the award of the Degree of Doctor of Philosophy and submitted in the Department of Mathematics of the Indian Institute of Technology Roorkee, Roorkee is an authentic record of my own work carried out during a period from December, 2014 to December, 2018 under the supervision of Dr. Ram Jiwari, Assistant Professor, Department of Mathematics, Indian Institute of Technology Roorkee, Roorkee.

The matter presented in this thesis has not been submitted by me for the award of any other degree of this or any other Institution.

(OM PRAKASH YADAV)

This is to certify that the above statement made by the candidate is correct to the best of my knowledge.

(Ram Jiwari)
Supervisor

The Ph.D. Viva-Voce Examination of **Mr. Om Prakash Yadav**, Research Scholar, has been held on.....

Chairman, SRC External Examiner

This is to certify that the student has made all the corrections in the thesis.

Signature of Supervisor Head of the Department

Dated:.....

In the memory of my late mother

Abstract

This work deals with analysis and approximations of some non-linear parabolic partial differential equations (PDEs) using finite element method. Such differential equations arise frequently in science and engineering. For instance, heat conduction, weather prediction, option pricing, gas dynamics in an exhaust pipe, waves in deep water, some chemical reactions like BZ reaction, iodine clock reaction *etc.* give rise to non-linear parabolic PDEs. The non-linearity in these equations poses a difficult task in analysing and approximating the solutions to such differential equations. With the advent of high speed computers, however, engineers and mathematicians are devising techniques which enable us to approximate solutions to such differential equations to a sufficient degree of accuracy. In this work, we consider some problems of non-linear nature and try to establish their existence, uniqueness and also approximate their solutions using Galerkin finite element method. A priori error estimates are also derived for such approximations.

In Chapter 1, some basic concepts regarding this work are introduced and a brief literature survey is presented.

In Chapter 2, we consider Burgers′-Fisher equation. The existence and uniqueness of the solution is proved using Faedo-Galerkin approximations. Further, some a priori error estimates are given for semi-discrete and fully-discrete solutions. Also, since we often model a physical situation by this differential equation, it is, therefore, desirable to require a positive solution in such cases. Hence, we present a positivity analysis of the solution and give a bound on time step to ensure the solution remains positive if started with a positive initial solution. The time discretization of the system is done using Euler backward scheme which is unconditionally stable. The non-linearity in the system is resolved by lagging it to the previous known level. Some numerical examples are also considered and the results are compared with the results from literature.

In Chapter 3, a coupled version of the non-linear parabolic PDEs is considered. Using Banach fixed point theorem, the existence and uniqueness of the solution is established. We also prove an a priori error estimate for the approximation. Neumann type boundary conditions are taken in this chapter. The time discretization of the system is done using Crank-Nicolson scheme (C-N scheme) and the non-linearity is resolved by the predictor-corrector scheme (P-C scheme). Since the C-N scheme and the P-C scheme are second order convergent, we get an overall second order convergence which is demonstrated in numerical examples.

In Chapter 4, we consider the Brusselator model where the cross-diffusion is allowed. The presence of cross-diffusion affects the stability of equilibrium. As we know, the diffusion in reaction diffusion equations may destabilize the equilibrium, which is called 'Turing instability'. Similarly, we investigate the effect of cross-diffusion on the stability. We find that the cross-diffusion increases the wave number associated to the solution. Some Turing patterns of the model are also plotted in the chapter.

In Chapter 5, we consider the Schrödinger equation. Some new soliton-type solutions are given for the equation. Further, since these soliton-type solutions peter out for large spatial values, we may truncate the infinite domain to some finite sub-domain. Therefore, the truncation analysis is performed for the soliton solutions so that we may truncate the domain without loosing much information about the solution. Some examples are also considered in this chapter where we see the interaction of solitons. The C-N scheme together with P-C scheme is used for this purpose.

In Chapter 6, a general reaction diffusion advection equation is considered and is analyzed for the existence of solution. Further, a priori error estimates are discussed for approximation error and second order convergence is found. Some 1D and 2D examples are considered in this chapter and their computational aspects are discussed.

Publications

Published Papers

1. O. P. Yadav and R. Jiwari, "Finite element analysis and approximation of Burgers'-Fisher equation," **Numerical Methods for Partial Differential Equations**, vol. 33, no. 5, pp. 1652-1677, 2017.

2. O. P. Yadav and R. Jiwari, "A finite element approach for analysis and computational modelling of coupled reaction diffusion models," **Numerical Methods for Partial Differential Equations**, vol. 35, no. 2, pp. 830-850, 2019.

3. O. P. Yadav and R. Jiwari, "A finite element approach to capture Turing patterns of autocatalytic Brusselator model", **Journal of Mathematical Chemistry**, vol. 57, no. 3, pp. 769-789, 2019.

4. O.P. Yadav and R. Jiwari, "Some soliton-type analytical solutions and numerical simulation of nonlinear Schrdinger equation", **Nonlinear Dynamics**, pp. 1-12, 2018.

Submitted Papers

1. O. P. Yadav and R. Jiwari, "A priori L^2 error estimates for Galerkin approximations to reaction-diffusion-advection equations", *communicated*.

Acknowledgement

Completion of this thesis was possible with the support of several people. I would like to express my sincere gratitude to all of them.

First of all, I thank my thesis supervisor, Dr. Ram Jiwari, for his continuous support and encouragement throughout my Ph.D. work. My discussions with him regarding research work proved fruitful and his suggestions were beneficial in solving problems. I am grateful to him for his assistance in academic and non-academic matters.

I am thankful to my Student Research Committee members, Prof. Rama Bhargava, Prof. Shishir Sinha, Prof. R. C. Mittal and Prof. S. P. Yadav for carefully scrutinizing my progress and providing helpful suggestions.

I am thankful to the University Grants Commission (UGC), Government of India and IIT Roorkee for providing me financial support to carry out this work.

Also, I am grateful to the Head; Chairman, DRC; faculty members; research scholars and non-academic staff of the Department for their help and support. I thank my friends for their support and for making my stay memorable and enjoyable at IIT Roorkee.

I dedicate this thesis to my family and friends for their unconditional love, encouragement and support throughout my life and, in particular, during the course of my thesis work.

Om Prakash Yadav

Contents

Abstract **i**

Publications **iii**

Acknowledgments **v**

Notations **ix**

1 Introduction **1**

1.1 A General Introduction

1.2 Literature Survey

1.3 Inequalities

2 Burgers′-Fisher Equation **11**

2.1 Introduction

2.2 Weak Formulation

2.3 Existence and Uniqueness of Weak Solution

2.4 Semi-discretization of the Problem

2.5 Fully Discretization of the Problem

2.6 Numerical Examples

3 Coupled Reaction Diffusion Models **33**

3.1 Introduction

3.2 Weak Formulation

3.3 Existence and Uniqueness of Weak Solution

3.4 A Priori Error Estimates and Convergence

3.5 Fully Discretization

3.6 Numerical Demonstrations and Discussions

4 Brusselator Model **53**

4.1 Introduction

4.2 Weak Formulation

4.3 A Priori Error Estimate

4.4 Stability Analysis

4.5 Numerical Demonstrations and Discussions

5 Schrödinger Equation **73**

5.1 Introduction

5.2 Some Soliton-Type Analytical Solutions

5.3 Truncation of Domain

5.4 Numerical Demonstrations and Discussions

6 Reaction Diffusion Advection Models **87**

6.1 Introduction

6.2 Weak Formulation

6.3 Existence and Uniqueness of Solution

6.4 A Priori Error Estimates

6.5 Fully Discretization of the Problem

6.6 Numerical Demonstrations

7 Conclusions and Future Scopes **99**

7.1 Conclusions

7.2 Future Scopes

Bibliography **103**

Notations

Abbreviations:

PDE(s)	Partial differential equation(s)
RDE(s)	Reaction diffusion equation(s)
FEM	Finite element method
Fig./Figs.	Figure/Figures
Eq./Eqs.	Equation/Equations
Sec.	Section
C-N	Crank-Nicolson
P-C	predictor-corrector
w.r.t.	with respect to

Notations:

Ω	a domain in $\mathbb{R}^n$, $n = 1, 2$; *i.e.*, an open bounded connected set with sufficiently regular boundary $\partial\Omega$
Ω_T	$= [0, T] \times \Omega$, $T > 0$
$L^p(\Omega)$	set of measurable functions $\{f : \Omega \to \mathbb{R}\}$ s.t. $\int_\Omega \lvert f(x)\rvert^p d\Omega < \infty$
$\lvert\lvert.\rvert\rvert_{L^p(\Omega)}$	$=\left(\int_\Omega \lvert f(x)\rvert^p d\Omega\right)^{1/p}$, norm for $L^p(\Omega)$ space
$\lvert\lvert.\rvert\rvert$	norm for $L^2(\Omega)$
$(.,.)$	inner product on L^2
L^1_{loc}	$= \{f : \Omega \to \mathbb{R}\ s.t.\ f\lvert_K \in L^1(K)$ for each compact set $K \subset \Omega\}$
$D^\alpha f(\mathbf{x})$	$= \frac{\partial^{\lvert\alpha\rvert} f(\mathbf{x})}{\partial x_1^{\alpha_1} \partial x_2^{\alpha_2} ... \partial x_n^{\alpha_n}}$, α^{th} derivative of f, for multi-index $\alpha = (\alpha_1, \alpha_2, ..., \alpha_n)$,
supp f	= closure of $\{x : f(x) \neq 0,\ f : \Omega \to \mathbb{R}\}$

$C_c^\infty(\Omega)$	$= \{f \in C^\infty(\Omega) : \exists$ a compact set $K \subset \Omega$ such that supp $f \subset K\}$
$W_p^k(\Omega)$	Sobolev spaces of order k in $L^p(\Omega)$
$H^k(\Omega)$	Hilbert spaces of order k in $L^2(\Omega)$
$\|.\|_k$	$= \left(\sum_{\|\alpha\| \leq k} \int_\Omega (D^\alpha f)^2 d\Omega \right)^{1/2}$, norm for $H^k(\Omega)$
$\|.\|_k$	$= \left(\sum_{\|\alpha\| = k} \int_\Omega (D^\alpha f)^2 d\Omega \right)^{1/2}$, semi-norm for $H^k(\Omega)$
$H_0^1(\Omega)$	completion of $C_c^\infty(\Omega)$ in H^1 norm
$H^{-1}(\Omega)$	dual space of $H_0^1(\Omega)$
$< ., . >$	duality product on Hilbert spaces, particularly between $H_0^1(\Omega)$ and $H^{-1}(\Omega)$
$L^q(0,T;W_p^k(\Omega))$	$= \left\{ f : (0,T) \to W_p^k(\Omega) \; s.t. \; f \text{ is measurable and } \int_0^T \|f(t)\|_{W_p^k(\Omega)}^q dt < \infty \right\}$
	for every integer $k \geq 0$, $1 \leq q < \infty$, $1 \leq p \leq \infty$
$\|f\|_{L^q(0,T;W_p^k(\Omega))}$	$= \left(\int_0^T \|f(t)\|_{W_p^k(\Omega)}^q dt \right)^{1/q}$
$W(0,T;H(\Omega))$	$= \left\{ f \in L^2(0,T;H_0^1(\Omega)) \; : \; f_t \in L^2(0,T;H^{-1}(\Omega)) \right\}$
$\|f\|_{W(0,T;H(\Omega))}$	$= \{\|f\|^2_{L^2(0,T;H_0^1(\Omega))} + \|f_t\|^2_{L^2(0,T;H^{-1}(\Omega))}\}^{1/2}$
u'	$= \frac{du}{dt}$.

We usually use u_t and u_{xx} to mean $\frac{\partial u}{\partial t}$ and $\frac{\partial^2 u}{\partial x^2}$ respectively. However, u_m represents semi-discrete solution in finite dimensional space V_m. Furthermore, $u_{m,t}$ and $u_{m,x}$ stand for $\frac{\partial u_m}{\partial t}$ and $\frac{\partial u_m}{\partial x}$ respectively. Since, we use t, x and y as the independent variables in problems, therefore, partial derivatives of unknown function w.r.t. these variables figure in the problems. Therefore, wherever x, y, t appear in the subscript these always represent partial derivatives unless mentioned otherwise.

For computational purpose, we have used MATLAB 2012B on an i5 personal computer with 4GB RAM to run the simulations.

Chapter 1

Introduction

1.1 A General Introduction

Analysis of partial differential equations (PDEs) in general and of nonlinear PDEs in particular poses a challenging task to the mathematicians. Many theories in the present form, for instance, functional analysis, Fourier analysis *etc.*, are the consequences of developing tools to analyze such PDEs [18]. The finite element method (FEM), though initially developed by engineers for solving problems of engineering and mathematical physics, later proved to be a crucial tool for solving such PDEs. FEM originated around 1960's when structural engineers combined the well established framework analysis with variational methods in continuum mechanics into a discretization method in which a structure is thought of as consisting of elements with locally defined strains or stresses [113]. The method was applied to elliptic problems at first but later extended to parabolic problems also in 1970's holding time fixed at different levels.

While approximating solution of a partial differential equation (PDE) by finite element method, there are three main components which we need to have a clear understanding of — Variational formulation; finite element space and its basis; and norm for error estimation.

A solution is said to be the classical solution or the strong solution if it has the enough regularity and it satisfies the differential equation at each point of its domain. However, in many practical situations, as demonstrated in [95] (Chapter 3), a function may satisfy a differential equation at each point but may not have enough regularity. Therefore, it becomes

necessary to seek an alternative formulation which weakens the regularity requirement for solutions. This is achieved by interpreting a given equation in distributional sense, *i.e.*, converting a differential equation into its weak form or variational form.
The standard solution spaces for weak formulations of PDEs are the Sobolev spaces of different orders depending upon the derivatives involved in the weak form.

General procedure:
After having the weak form and the appropriate solution space, we prove the existence of the solutions to the problems taken up in this work. To accomplish this, two strategies are used. First, by showing convergence of Faedo-Galerkin approximations to the original solution. Second, by applying the Banach fixed point theorem in appropriate setting.
We take a finite dimensional subspace of the solution space where the existence is established. And approximate the solution in the subspace. We find a priori estimates for the error committed in such an approximation for semi-discrete solution and fully discrete solution.
Finally, some numerical examples are considered in each chapter to verify the results proved theoretically in the respective chapters. Since, our problems have non-linearity, therefore, it must be removed to find an approximation. Two techniques are used in this regard: first by lagging the non-linearity and second by using the P-C scheme.

Demonstration of the procedure to a general problem:

In this work, we consider the following non-linear problem in different forms:

$$u_t - \Delta u = f(t, x, u, \nabla u),\ (t, x) \in (0, T] \times \Omega, \tag{1.1}$$

$$u(0, x) = u_0,\ x \in \Omega, \tag{1.2}$$

with some Dirichlet or Neumann boundary conditions to be specified wherever required.
For Dirichlet case, we may always consider homogeneous boundary conditions, since non-homogeneous boundary conditions are reducible to the homogeneous case by some appropriate transformation [95]. Therefore, for Dirichlet problem we seek a space in which the functions vanish at boundary. We will elaborate it later.

To interpret the Eq. (1.1) in the distributional sense, let us first define distributions.

Distributions: [95]

Let T be a linear transformation from C_c^∞ to $\mathbb{R}$ and $< T, \phi >$ represents the value taken by T on the element $\phi \in C_c^\infty$. We call *distributions on* Ω any linear and continuous transformation T from C_c^∞ into $\mathbb{R}$. The space of distributions is therefore given by the dual space $(C_c^\infty(\Omega))'$ of $C_c^\infty(\Omega)$.

To each function f in L^2 or $Ł^1_{loc}$, we may associate a distribution T_f defined as

$$T_f(\phi) = \int_\Omega f\phi d\Omega, \ \forall \phi \in C_c^\infty.$$

This calls upon us to multiply the equation (1.1)-(1.2) by $\phi \in C_c^\infty$ and integrate over Ω. We consider only 1D case. A 2D case is considered in coming chapters. Thus we get,

$$\int_\Omega u_t \phi d\Omega + \int_\Omega \nabla u \nabla \phi d\Omega = \int_\Omega f\phi d\Omega, \tag{1.3}$$

$$\int_\Omega u(x,0)\phi d\Omega = \int_\Omega u_0 \phi d\Omega, \tag{1.4}$$

for every $\phi \in C_c^\infty$. In obtaining (1.3), we have used the integration by parts formula and the compactness of ϕ, hence the boundary term does not appear. The formulation (1.3)-(1.4) is called the weak form of the problem (1.1)-(1.2) under homogeneous Dirichlet conditions. In the inner product form, (1.3)-(1.4) may be written as,

$$(u_t, \phi) + (\nabla u, \nabla \phi) = (f, \phi), \tag{1.5}$$

$$(u(0,x), \phi) = (u_0, \phi), \tag{1.6}$$

for every $\phi \in C_c^\infty$. We see that this formulation involves only one derivative of functions, therefore, the space H^1 is enough to discuss the existence of solution for (1.5). We have seen for the case of Dirichlet boundary conditions the solution vanishes at boundary, therefore, we consider H_0^1 as the required solution space and for Neumann boundary conditions we consider H^1 as the solution space to make sure the boundary conditions are satisfied, since functions of H_0^1 space do not see boundary values. It is opportune to point out that these are the spaces for spatial discretization. Since we are considering time dependent problems, therefore, time dependent Sobolev spaces will be used. However, the above calculations are

done by fixing time at a particular instant. Therefore, we only need to worry about the spaces used for spatial discretizaton.

Since $u(t) \in H^1$, implying $\nabla u(t) \in L^2$ and since $\phi \in C_c^\infty \subset H_0^1(\Omega)$, so we have $\nabla\phi \in L^2$, therefore from Cauchy-Schwartz inequality $\nabla u \nabla\phi$ is in L^1. Similarly, if we take $u_t(t) \in L^2$, we get $u_t\phi \in L^1$. Moreover, we may take a much bigger space for u, that is, $W(0,T;H(\Omega))$, where $u_t(t) \in H^{-1}$, for which we have to replace the inner product (u_t, ϕ) by the duality bracket $< u_t, \phi >$. We also want $f\phi \in L^1$. For $f \in L^2$, this is easily accomplished; but, if f depends on u non-linearly then the issue complicates.

Theorem 1.1.1. *[95] If Ω is open set of $\mathbb{R}^n$, $n \geq 1$ provided with a sufficiently smooth boundary, then*

$$H^k(\Omega) \subset C^m(\bar{\Omega}),\ if\ m < k - \frac{n}{2}.$$

We see from Theorem 1.1.1 that if $u \in H^1(\Omega)$ then $u \in C^0(\bar{\Omega})$ for $n = 1$. In fact, in 1D, H^1 functions are absolutely continuous. And therefore by the algebra of continuous functions, $f(u)$ is continuous and hence integrable. For higher dimensions, say in 2D, H^1 functions are not continuous, therefore, we must ensure that $f(u)$ is L^2 for such cases to ensure integrability of non-linear part. This will be seen in Chapter 3.

Now we have the appropriate setting to discuss existence. But before that, first we look into the literature for existence of solution.

1.2 Literature Survey

Existence:

Existence and uniqueness of the reaction diffusion equation $u_t - d\Delta u = f(u)$ with $f(u)$ being Lipschitz continuous in u is discussed using Banach theorem in appropriate Sobolev spaces by Evans [30]. For a more general case $b(u)_t = \nabla.a(u, \nabla u) + f$, existence and uniqueness is studied in [4, 14] under some conditions on a and b, using the concept of mild solutions and weak solutions. We may note that f is not non-linear so this is still not very general case. Further, Friendman gave a semigroup approach for existence of at most one solution to even more general equation $u_t - d\Delta u = f(u, \nabla u)$, with f being Lipschitz continuous in u or monotonically decreasing in u or Hölder continuous in u [32]. The semi-group approach depends on establishing complicated a priori estimates for the solution. This again is not

very general as $f(u, \nabla u)$ varies w.r.t. first argument only. A more recent work on existence of solution to a semi-linear PDE may be found in [73].

A priori error estimates:

Next, we consider the approximate problem of (1.5)-(1.6) in a finite dimensional subspace, say V_m, of the solution space, say $\mathcal{S}$. V_m is such that, for small h [113],

$$\inf_{\chi \in V_m} \{||v - \chi|| + h||\nabla(v - \chi)||\} \leq Ch^2||v||_2, \tag{1.7}$$

for all $v \in H^2 \cap H_0^1$. The discretization parameter h in 1D is given by:

$$h = \max_{i \in \{1,2,...,m-1\}} (x_{i+1} - x_i),$$

where $\{x_i\}_{i=1}^m$ is a partition of $\Omega = (a, b)$, say. In 2D, for some triangulation T_h of Ω, h is maximum of diameters of triangles $\{T : T \in T_h\}$. Therefore, the approximate version of (1.5)-(1.6) becomes,

$$(u_{m,t}, \phi_m) + (\nabla u_m, \nabla \phi_m) = (f, \phi_m), \tag{1.8}$$

$$(u_m(0, x), \phi_m) = (u_{0m}, \phi_m), \ \forall \phi_m \in V_m. \tag{1.9}$$

We take a basis for V_m, say $\{\phi_1, \phi_2, ..., \phi_m\}$, then u_m may be written as

$$u_m = \sum_{i=1}^{m} c_i(t)\phi_i(x). \tag{1.10}$$

Our task now reduces to finding out the coefficients $c_i's$. The Eq. (1.8) is true for every $\phi_m \in V_m$ so it will be true in particular for every ϕ_i and hence putting from (1.10) into (1.8), we get a system of ordinary differential equations in t. The $u_m(t)$ so obtained is called the 'semi-discrete' solution. The error $u_m - u$ is known as the semi-discrete error. We attempt to find a bound on this error for our particular problems in the chapters to come. The pervading strategy is to break $u_m - u$ into $(u_m - U) + (U - u)$, where U is some element of V_m. There are two strategies to proceed further. Either we take U to be the

elliptic projection of u [113], defined as

$$(\nabla(U-u),\nabla\phi)=0,\ \forall\phi\in V_m; \tag{1.11}$$

or we take U to be an arbitrary element of V_m and use the orthogonality of Galerkin method to derive an error estimate in terms of U [27]. For the former case, we have estimates of $(U-u)$ quoted in the following theorem. For the latter case, we will see in Chapter 2 that U will be replaced by interpolant of u and again available estimates of $(U-u)$ are used to derive an estimate for $(u-u_m)$.

Theorem 1.2.1. *For the space V_m which satisfies* (1.7)*, and for the projection U of u defined in* (1.11)*, we have*

$$||U-u||+h||\nabla(U-u)||\leq Ch^2||u||_2,\ \forall u\in H^2\cap H_0^1. \tag{1.12}$$

We have used here that $u\in H^2$; but we had only assumed u to be H^1. This is answered by the following theorem [30]:

Theorem 1.2.2. *Assume $f\in L^2(\Omega)$. Suppose that $u\in H_0^1(\Omega)$ is a weak solution of the elliptic boundary value problem,*

$$-\Delta u=f,\ x\in\Omega\ ;\ u=0,\ x\in\partial\Omega.$$

If $\partial\Omega$ is C^2 then $u\in H^2$.

Further, if u is not vanishing on the boundary, so $u\in H^1$, then $u\in H^2_{loc}$.
In this work, our aim will be to establish an estimate of (1.12) type for $||u_m-u||$ when $f(u,\nabla u)$ is non-linear. Let us look into some of the developments in literature regarding a priori error estimates for non-linear $f(u)$.
The first comprehensive a priori error estimate for semi-linear parabolic problem was found by Douglas and Dupont in [27]. These estimates were in H^1 or the energy norm. Wheeler [123] extended these results to L^2 norm and found the optimal order convergence. The effect of non-smoothness in initial data for Galerkin approximations and associated errors was studied by Thomée et al. in [58]. The book by Thomée [113] gives a good account of the results in this direction.

Fully-discretization:

Lastly, we perform time discretization of (1.8) by using some time stepping scheme. For instance, in Chapter 2 we use Euler backward method for the purpose and in later chapters, we use C-N scheme. The crucial part in these calculations will be to resolve the non-linearity. In this regard we resort to two techniques – the first being lagging of non-linearity and the second by using P-C scheme.

Next, we list some inequalities and formulae which will be used throughout the thesis.

1.3 Inequalities

Generalized Hölder inequality: For $r \in (0, \infty]$ and $p_1, p_2, ...p_n \in (0, \infty]$ such that $\sum_{k=1}^{n} \frac{1}{p_k} = \frac{1}{r}$, then

$$f_k \in L^{p_k}(\Omega),\ k = 1, 2, ..., n \implies \prod_{k=1}^{n} f_k \in L^r(\Omega). \tag{1.13}$$

For $r = 1$, the above inequality is the Hölder inequality. Also, the inequality (1.13) reduces to Cauchy-Schwarz inequality for $n = 2$ and $p_1 = 2 = p_2$.

Gronwall inequality: Let $a(s)$ be a non-negative integrable function in $[0, T]$. Suppose f and g be two continuous functions on $[0, T]$. If f satisfies

$$f(t) \leq g(t) + \int_0^t a(s)f(s)ds,\ \forall t \in [0, T],$$

then, if g is non-decreasing,

$$f(t) \leq g(t)e^{\int_0^t a(s)ds},\ \forall t \in [0, T].$$

Young inequality: For every a, $b \in \mathbb{R}$,

$$ab \leq \frac{\epsilon}{2}a^2 + \frac{1}{2\epsilon}b^2,\ \forall \epsilon > 0.$$

Poincaré inequality: Let Ω be a bounded set of $\mathbb{R}^n$, then there exists a constant $C(\Omega)$

such that,

$$||f|| \leq C||\nabla f||, \ \forall f \in H_0^1(\Omega).$$

Some Embedding Results

A topological space X is said to be embedded into another space Y if there exists a continuous injective structure preserving map f from X to Y. Since we primarily work with Sobolev spaces in this work, therefore, the Sobolev embedding theorem is particularly important to us. Essentially we want to see if a function belongs to a Sobolev space $W_k^p(\Omega)$, $\Omega \subset \mathbb{R}^n$ then what other spaces this function may also belong to. This is given by the Sobolev embedding theorem and depends on four factors: n, p, k and bounded/unbounded-ness of Ω.

Case 1: $1 \leq p < n$

Assume Ω is a bounded open subset of $\mathbb{R}^n$. Suppose $u \in W_0^{1,p}(\Omega)$ for some $1 \leq p < n$. Then

$$||u||_{L^q(\Omega)} \leq C||Du||_{L^p(\Omega)}$$

for each $q \in [1, p^*]$, $p^* = \frac{np}{n-p}$, the constant C depending only on p, q, n, Ω. In other words, in this case $W_0^{1,p}(\Omega) \hookrightarrow L^q(\Omega)$ holds.

Case 2: $p = n$

Let $\Omega \subset \mathbb{R}^n$ be a regular bounded domain. Then, for $u \in W^{1,n}(\Omega)$,

$$||u||_{L^q(\Omega)} \leq C||u||_{W^{1,n}(\Omega)}$$

for some fixed $q \in [1, \infty)$. Note that q can not be ∞, for example $f(x) = \text{loglog}\left(1 + \frac{1}{|x|}\right)$ belongs to $W^{1,n}(\Omega)$, $n \geq 2$, but does not belong to $L^\infty(\Omega)$.

Case 2: $p > n$

Let $\Omega \subset \mathbb{R}^n$ be a domain with at least Lipschitz boundary. Suppose $p > n$ and $\mu = 1 - \frac{n}{p}$. Then $W^{1,p}(\Omega) \subset C^{0,\mu}(\Omega)$. $C^{0,\mu}$ are μ-Hölder continuous maps, which are contained in the class of continuous maps.

Error formulae

L^2 error in an approximation $u_m(t)$ of the solution $u(t)$ is defined by

$$\begin{aligned}||u(t) - u_m(t)||^2 &= \int_\Omega (u(t,x) - u_m(t,x))^2 dx \\ &= \sum_{i=1}^{m-1} \int_{x_i}^{x_{i+1}} (u(t,x) - u_m(t,x))^2 dx \\ &\approx \sum_{i=1}^{m-1} (x_{i+1} - x_i)(u(t,x_i) - u_m(t,x_i))^2.\end{aligned}$$

If the exact solution is known at the mid points also then we can use even more accurate approximation for L^2 error as

$$\sum_{i=1}^{m-1} (x_{i+1} - x_i) \left(u(t, \frac{x_i + x_{i+1}}{2}) - \frac{u_m(t,x_i) + u_m(t,x_{i+1})}{2} \right)^2.$$

L^∞ error in an approximation $u_m(t)$ of the solution $u(t)$ is defined by

$$\begin{aligned}||u(t) - u_m(t)||_{L^\infty} &= ess\_sup_\Omega \ |u(t,x) - u_m(t,x)| \\ &\approx \max_{1 \le i \le m} |u(t,x_i) - u_m(t,x_i)|.\end{aligned}$$

Relative error for an approximation u_m of a solution u is given by

$$u^r = \left(\frac{\sum_{i=1}^m (u(t,x_i) - u_m(t,x_i))^2}{\sum_{i=1}^m u(t,x_i)^2} \right)^{1/2} \approx \left(\frac{\sum_{i=1}^m (u(t,x_i) - u_m(t,x_i))^2}{\sum_{i=1}^m u_m(t,x_i)^2} \right)^{1/2}.$$

We frequently calculate the order of convergence for the schemes proposed in the chapters, the following formula will be used:

$$OC = \frac{\log(\text{Error}_{h_1}) - \log(\text{Error}_{h_2})}{\log(h_1) - \log(h_2)}.$$

If $h_2 = \frac{h_1}{2}$, the above formula reduces to

$$OC = \frac{\log(\text{Error}_{h_1}) - \log(\text{Error}_{h_2})}{\log(2)}.$$

As noticed in Eq. (1.12) and will observe further in the chapters to come that the second

order convergence is obtained in L^2 norm. This is optimal order convergence which is proved in [17].

Some Advantages of Finite Element Method

Non-linear PDEs have also been solved and analyzed by several other methods, for instance, Finite difference method, Differential quadrature method, Adonian decomposition method, collocation method *etc.* The advantage of finite element method over other methods lies in the fact that this method is strongly consistent, which eases our labor to show only the convergence of the scheme, for, by the Lax-Richtmyer equivalence theorem, the stability is automatically implied. Another advantage is that the method can deal with complex domains easily by breaking it down to simpler triangles or rectangles. Also, the method gives solution at all points of the domain with the help of interpolation. Despite all these niceties there are some drawbacks too. The method can be applied to boundary value problems only. Also, the method is best fit for even order problems, since the weak formulation yields heterogeneous spaces for solution space and the test space for an odd ordered problem.

Chapter 2

Burgers′-Fisher Equation

In this chapter, we discuss existence, uniqueness; a priori error estimate and convergence of semi discrete and fully discrete solutions to Burgers'-Fisher equation. Existence and uniqueness of weak solution is proved in Sec. 2.3 by Galerkin finite element method for non-smooth initial data. A priori error estimates of semi-discrete solution are derived in $L^\infty(0,T;L^2(\Omega))$ norm and the convergence of semi-discrete solution is established in Sec. 2.4. Then, fully discretization is done with the help of Euler backward method. The non-linearity is removed by lagging it to previous time instant. Positivity of fully discrete solution is discussed in Sec. 2.5 and bounds on time step are discovered for which the solution remains positive if started with a positive initial solution. Some numerical examples are considered in Sec. 2.6 to demonstrate the effectiveness of the scheme.

2.1 Introduction

The Burgers'-Fisher equation is

$$u_t - u_{xx} + auu_x + bu(1-u) = 0,\ (t,x) \in (0,T) \times \Omega, \tag{2.1}$$

where $\Omega \subset \mathbb{R}$, a and b are advection and source/sink constants.

The equation describes a nonlinear parabolic mathematical model of various phenomena arising in different fields of science and engineering such as gas dynamics, heat conduction, nonlinear optics, chemical physics *etc.* It models velocity profile in fluid dynamics for viscous fluid [23], gas dynamics in an exhaust pipe [35] *etc.*

The Burgers'-Fisher equation takes into account the effects of non-linear advection, linear diffusion, and non-linear logistic reaction. The equation (2.1) is a combination of the Fishers' equation,

$$u_t - Du_{xx} = ku(1-u),$$

proposed in the context of population dynamics to describe the spatial spread of an advantageous allele [31] and the Burgers' equation

$$u_t - Du_{xx} + uu_x = 0,$$

introduced by Bateman and later studied by Burgers as a mathematical model of turbulence in 1948. Burgers' equation is one of the easiest model to understand the physical properties of phenomena such as sound and shock wave theory, wave processes in thermo-elastic medium, vorticity transportation, dispersion in porous media, mathematical modeling of turbulent fluid, hydrodynamic turbulence, elasticity, gas dynamics, heat conduction *etc.* [40, 54, 60, 87].

We supplement the problem (2.1) with the following initial and boundary conditions,

$$\begin{aligned} u(0,x) =& u_0(x) \text{ for } x \in \Omega, \\ u =& 0 \text{ on } (0,T) \times \partial\Omega, \end{aligned} \tag{2.2}$$

where the initial data $u_0(x)$ is considered non-smooth.

Recently, researchers have paid considerable attention to study solution of Burgers'-Fisher problem. There are many analytical as well as numerical solutions to the problem. For example, Adomian decomposition method (ADM) [49], homotopy perturbation method (HPM) [97], variation iteration method (VIM) [29], Exp-function method [78] *etc.* are some of the analytical methods which provide analytical solutions whereas Haar wavelet method [44], spectral collocation method [51], collocation method using radial basis [111], spectral domain decomposition approach [38], finite difference method [76], finite difference based pseudospectral approach [91] *etc.* are some of the numerical methods proving approximations to the solution of the problem.

Out of analytical methods, some of them give series solution using iterating polynomials which converge to the solution, some others use transformations which linearize the

non-linear problem and yet others utilize trial functions on iterating scheme to arrive at a solution. The methods of first kind suffer from the problem of complexity, that is, after a stage iterating polynomials become too complex to consider any further iterations. The second kind of methods suffer from the fact that each transformation loses some information. The accuracy of third-type methods depend upon the suitability of trial functions. Accuracy and simplicity are two critical issues for any solution. We want the solution to be accurate and seek to achieve it by a computationally efficient method. This is the motivation for the present work: to reduce complexity and to improve accuracy.

In some mathematical models, the property of non-negativity of solution is significant. For instance, if the model represents some population evolution or the chemical concentration of a reaction *etc.* Among all the above mentioned methods, finite difference method has the property of preserving non-negativity of solutions [100]. The finite difference method, though easy to comprehend and simple to implement, has some shortcomings. Other than the finite difference method, only the finite element method preserves this property of solution [29].

The Fishers' and Burgers' equations have been solved by the Galerkin finite element method [110, 133]. Further, the forced Fisher equation

$$u_t - u_{xx} - \lambda u(1-u) = (1-u)f(x),\ (t,x) \in (0,T) \times \Omega,$$

is also analyzed by the Galerkin method [42]. But, to the best of our knowledge, the Burgers'-Fisher equation has not been attempted by finite element method (FEM) so far. There are some advantages of FEM which tempts us to solve the problem by this method. Besides it being preserving positivity of solution, the method is strongly consistent and can handle complex domains. The method offers good accuracy as we will see in numerical examples where we compare the results with the earlier results.

2.2 Weak Formulation

The weak formulation to the problem (2.1) with initial and boundary conditions (2.2), is obtained by multiplying the equation (2.1) by some function $\phi \in H_0^1(\Omega)$ and then integrating w.r.t. space variable x over Ω. The use of integration by parts yields the following weak

formulation:

Find a $u(t,x) \in W(0,T;H(\Omega))$ such that

$$(u_t(t),\phi) + (u_x,\phi_x) + ((auu_x + bu(1-u)),\phi) = 0,\ t \in (0,T), \tag{2.3}$$

$$(u(0,x),\phi) = (u_0(x),\phi), \tag{2.4}$$

for all $\phi \in H_0^1(\Omega)$. We may recall the definition of $W(0,T;H(\Omega))$ given in 'Notations' as

$$W(0,T;H(\Omega)) = \left\{ f \in L^2(0,T;H_0^1(\Omega)) \ :\ f_t \in L^2(0,T;H^{-1}(\Omega)) \right\}.$$

2.3 Existence and Uniqueness of Weak Solution

Theorem 2.3.1. *If $u_0(x) \in L^2(\Omega),\ \Omega = (0,1)$, then the problem (2.3) with initial condition (2.4) has a unique solution in $W(0,T;H(\Omega))$.*

Proof. Proof of theorem is divided in the following parts,

(i) approximation of solution in a finite dimensional subspace V_m of $W(0,T;H(\Omega))$.

(ii) The approximate solution, say $u_m(t)$, obtained in part (i) is bounded in $L^2(0,T;H_0^1(\Omega))$ space.

(iii) Limit of the sequence $\{u_m(t)\}$ is a solution to the problem (2.3) and (2.4).

(iv) Uniqueness of the limit.

We prove these parts one by one.

(i) A finite dimensional subspace V_m of $W(0,T;H(\Omega))$ is chosen in a manner as pointed out in the previous chapter, which satisfies (1.7). Let the dimension of V_m is m. Suppose a basis for V_m is $\{\phi_1,\ \phi_2, ...,\ \phi_m\}$. For fixed m, let

$$u_m(t) = \sum_{k=1}^{m} c_k(t)\phi_k, \tag{2.5}$$

where $u_m(t) = u_m(t,.)$.

Let $g_m = \sum_{k=1}^{m} u_0^k \phi_k$, an L^2 projection of initial data u_0 onto the space V_m, $u_0^k = (u_0,\phi_k)$.

Now, we solve the following approximate problem,

Find $u_m \in V_m$ such that $\forall\ i = 1(1)m$,

$$(u_{m,t}(t), \phi_i) + (u_{m,x}(t), \phi_{i,x}) + (au_m(t)u_{m,x}(t) + bu_m(t)(1 - u_m(t)), \phi_i) = 0, \tag{2.6}$$

with $u_m(0) = g_m$.

The solution $u_m(t)$, given in (2.5), is called a Galerkin approximation of u.

Putting $u_m(t)$ from (2.5) into (2.6), we get a system of non-linear differential equations in $c_k(t)$, the solution for which exists by theory of differential equations [46].

(ii). In this part, we will show that the solution $u_m(t)$ of (2.6) is bounded in $L^2(0, T; H_0^1(\Omega))$,

Since the system (2.6) is true for every ϕ_i, hence it will hold for $u_m(t)$ as well, therefore,

$$(u_{m,t}(t), u_m(t)) + ||u_{m,x}(t)||^2_{L^2(\Omega)} + (au_m(t)u_{m,x}(t), u_m(t)) + (bu_m(t)(1 - u_m(t)), u_m(t)) = 0.$$

Using generalized Hölder inequality, we have

$$\frac{1}{2}\frac{d}{dt}||u_m(t)||^2_{L^2(\Omega)} + ||u_{m,x}(t)||^2_{L^2(\Omega)} \leq |a|||u_m(t)||_{L^4(\Omega)}||u_{m,x}(t)||_{L^2(\Omega)}||u_m(t)||_{L^4(\Omega)} + b||u_m(t)||^2_{L^2(\Omega)} + b||u_m(t)||^3_{L^3(\Omega)}. \tag{2.7}$$

If the basis functions $\{\phi_i' s\}$ are polynomials, we obtain $||u_{m,x}(t)||_{L^2(\Omega)} \leq K$ since Ω is bounded.

The embedding $H_0^1(\Omega) \hookrightarrow L^q(\Omega)$ for $q = 3, 4$ implies [42, 62]

$$||u_m(t)||_{L^q(\Omega)} \leq c||u_m||_1 \leq C||u_{m,x}||_{L^2(\Omega)},$$

for some constants c and C. We used the fact that the semi-norm and norm are equivalent on $H_0^1(\Omega)$ space.

Using these inequalities in (2.7), we get

$$\frac{d}{dt}||u_m(t)||^2_{L^2(\Omega)} + ||u_{m,x}(t)||^2_{L^2(\Omega)} \leq A(a, b, K) + |b|||u_m(t)||^2_{L^2(\Omega)}, \tag{2.8}$$

for some constant A depending upon $a,\ b$ and K only.

Integrating (2.8) in time and noting that $||u_{m,x}(t)||^2$ is non-negative,

$$||u_m(t)||^2_{L^2(\Omega)} \leq ||u_m(0)||^2_{L^2(\Omega)} + At + \int_0^t |b| ||u_m(s)||^2_{L^2(\Omega)} ds. \tag{2.9}$$

Applying Gronwall inequality to (2.9), we obtain

$$||u_m(t)||^2_{L^2(\Omega)} \leq (||u_m(0)||^2_{L^2(\Omega)} + At)\exp(|b|t).$$

Hence,

$$\sup_{t\in[0,T]} ||u_m(t)||^2_{L^2(\Omega)} \leq C(T), \quad \text{independent of } m.$$

Thus, $\{u_m\}_{m=1}^{\infty}$ is bounded in $L^\infty(0,T;L^2(\Omega))$.

Using (2.8), we see that $\{u_m\}_{m=1}^{\infty}$ is bounded in $L^2(0,T;H_0^1(\Omega))$.

(iii) As $\{u_m\}_{m=1}^{\infty}$ is bounded in $L^2(0,T;H_0^1(\Omega))$, which is a Hilbert space, hence we can extract a subsequence which is again denoted by u_m, without loss of generality, converging weakly in $L^2(0,T;H_0^1(\Omega))$ to $u \in L^2(0,T;H_0^1(\Omega))$ by property of weak convergence in Hilbert spaces.

Now, let $\psi(t) \in C_c^\infty[0,T]$ with $\psi(T) = 0$. Multiplying equation (2.6) by this time depending test function and integrating in time and using integration by parts, we obtain the following:

$$\begin{aligned} -(g_m,\phi_i)\psi(0) - \int_0^T (u_m(t), \psi_t(t)\phi_i)dt + \int_0^T (u_{m,x}(t), \psi(t)\phi_{i,x})dt \\ + \int_0^T (au_m(t)u_{m,x}(t) + bu_m(t)(1-u_m(t)), \psi(t)\phi_i)dt = 0. \end{aligned} \tag{2.10}$$

From the estimates calculated in part (ii), following can be established,

$$\begin{aligned} (g_m,\phi_i)\psi(0) \to (u_0,\phi_i)\psi(0), \ \text{(because } ||g_m|| \leq ||u_0||, \ \text{being } L^2 \text{ projection)} \\ \int_0^T (u_m(t), \psi_t(t)\phi_i)dt \to \int_0^T (u(t), \psi_t(t)\phi_i)dt, \\ \int_0^T (u_{m,x}(t), \psi(t)\phi_{i,x})dt \to \int_0^T (u_x(t), \psi(t)\phi_{i,x})dt, \\ \int_0^T (u_m(t), \psi(t)\phi_i)dt \to \int_0^T (u(t), \psi(t)\phi_i)dt. \end{aligned}$$

Next, if we could show the convergence for u_m^2 and $u_m u_{m,x}$, we will be done.

Making use of Hölder inequality and the Sobolev embedding theorem, we can write,

$$\begin{aligned}|\int_0^T (u_m^2(t) - u^2(t), \psi(t)\phi_i)dt| &\leq \int_0^T |\psi(t)| \int_\Omega |u_m - u||u_m + u||\phi_i| dxdt \\ &\leq \int_0^T |\psi(t)|||u_m(t) - u(t)||||u_m + u||_{L^4}||\phi_i||_{L^4} dt \\ &\leq C||\psi||_{L^\infty(0,T)}||\phi_i||_{H_0^1}||u_m - u||_{L^2(0,T;L^2(\Omega))}(||u_m||_{L^2(0,T;H_0^1)} + ||u||_{L^2(0,T;H_0^1)}). \quad (2.11)\end{aligned}$$

From this inequality, we get

$$\int_0^T (u_m^2(t), \psi(t)\phi_i)dt \to \int_0^T (u^2(t), \psi(t)\phi_i)dt.$$

Similarly, for $u_m u_{m,x}$,

$$\begin{aligned}|\int_0^T (u_m(t)u_{m,x}(t) - u(t)u_x(t), \psi(t)\phi_i)dt| &\leq \int_0^T |\psi(t)| \int_\Omega (|u_{m,x}(t)||u_m - u| \\ &\quad + |u||u_{m,x}(t) - u_x(t)|)|\phi_i| dxdt \\ &\leq \int_0^T |\psi(t)|(||u_m(t) - u(t)||||u_{m,x}(t)||_{L^4(\Omega)}||\phi_i||_{L^4(\Omega)} \\ &\quad + ||u||_{L^4(\Omega)}||u_{m,x}(t) - u_x(t)||||\phi_i||_{L^4(\Omega)}).\end{aligned}$$

Since $||u_{m,x}(t)||$ is bounded, therefore, $||u_{m,x}(t)||_{L^4}$ is bounded. Hence

$$\int_0^T (u_m(t)u_{m,x}(t), \psi(t)\phi_i)dt \to \int_0^T (u(t)u_x(t), \psi(t)\phi_i)dt.$$

Taking limit in (2.10) and noting the fact that (2.10) is true for every ϕ_i,

$$\begin{aligned}-(u_0, \phi)\psi(0) - \int_0^T (u(t), \psi_t(t)\phi)dt + \int_0^T (u_x(t), \psi(t)\phi_x)dt \\ + \int_0^T (au(t)u_x(t) + bu(t)(1 - u(t)), \psi(t)\phi)dt = 0. \quad (2.12)\end{aligned}$$

Since (2.12) is true for every $\psi \in C_c^\infty(0, T)$, hence u satisfies (2.3).

Now, we establish that u satisfies the initial condition as well. To that end, we multiply equation (2.3) by $\psi(t)$ and integrating by parts in t,

$$-(u(0),\phi)\psi(0)-\int_0^T(u(t),\psi_t(t)\phi)dt+\int_0^T(u_x(t),\psi(t)\phi_x)dt + \int_0^T(au(t)u_x(t)+bu(t)(1-u(t)),\psi(t)\phi)dt=0. \quad (2.13)$$

From (2.12) and (2.13), we have

$$(u_0-u(0),\phi)\psi(0)=0\ \forall\ \phi\in H_0^1(\Omega),\ \forall\ \psi\in C_c^\infty(0,T),$$

whence descends $u(0)=u_0$ *a.e.* in Ω. This completes the proof of existence of weak solution.

(iv) To prove the uniqueness, suppose there are two solutions u_1 and u_2 to the weak formulation (2.3) and (2.4). Then u_1-u_2 satisfies

$$((u_1-u_2)_t,\phi)+((u_1-u_2)_x,\phi_x) = -a(u_1u_{1,x}-u_2u_{2,x},\phi)-b(u_1(1-u_1)-u_2(1-u_2),\phi),\ \forall\ \phi\in H_0^1(\Omega).$$

Taking $\phi(.)=u_1(t,.)-u_2(t,.)$ and using the assumption on boundedness of $u_{1,x}$ and $u_{2,x}$,

$$\frac{d}{dt}||u_1-u_2||^2_{L^2(\Omega)}+||(u_1-u_2)_x||^2_{L^2(\Omega)}\leq K||u_1-u_2||^2_{L^2(\Omega)}+|b|||u_1-u_2||^3_{L^3(\Omega)}, \quad (2.14)$$

for some constant K depending solely on a and b.

Using the embedding $H^{1/2}(\Omega)\hookrightarrow L^3(\Omega)$ [42], we can write:

$$\begin{aligned} b||u_m(t)||^3_{L^3(\Omega)} &\leq b(c_1||u_m||_{H^{1/2}(\Omega)})^3 \\ &\leq b(c_2||u_m||^{1/2}_{L^2(\Omega)}||u_m||^{1/2}_{H_0^1(\Omega)})^3 \text{ (using interpolation between } L^2(\Omega)\ \&\ H_0^1(\Omega)) \\ &\leq b(c_3||u_m||^{3/2}_{L^2(\Omega)}||u_{m,x}||^{3/2}_{L^2(\Omega)}) \\ &\leq b\ \frac{c}{\epsilon}\ ||u_m(t)||^6_{L^2(\Omega)}+\epsilon||u_{m,x}(t)||^2_{L^2(\Omega)}. \end{aligned} \quad (2.15)$$

We used Young inequality for $p=4$ and $q=4/3$ to get the last inequality.

Using (2.15) in (2.14) for $\epsilon=1$, and integrating in time

$$||u_1(t)-u_2(t)||^2_{L^2(\Omega)}\leq ||u_1(0)-u_2(0)||^2_{L^2(\Omega)}$$

$$+\int_0^t K(1+|b|C_1||u_1(s)-u_2(s)||^4_{L^2(\Omega)})||u_1(s)-u_2(s)||^2_{L^2(\Omega)}ds.$$

Since both the solutions satisfy initial condition, therefore $||u_1(0)-u_2(0)||=0$. Using Gronwall inequality, we have $||u_1-u_2||^2_{L^2(\Omega)}\leq 0$ implying $u_1=u_2$ *a.e.* ∎

2.4 Semi-discretization of the Problem

We have established that the solution to the problem (2.3) exists uniquely under some assumptions. Moreover, the way to approximate this solution is also pointed out in the proof of the first part of the existence theorem. The approximate solution is called the Galerkin approximation and can be obtained from solving nonlinear ordinary differential equation (2.6) for $c_i's$. The error committed in such an approximation is important to demonstrate the efficiency of the method.

From (2.6), we have the following equation for semi-discrete Galerkin approximation u_m,

$$(u_{m,t}(t),\phi_m)+(u_{m,x}(t),\phi_{m,x})+(au_m(t)u_{m,x}(t),\phi_m)+(bu_m(t)(1-u_m(t)),\phi_m)=0, \quad (2.16)$$

for all $\phi_m\in V_m\subset H^1_0(\Omega)$ and $u_m(t)$ is as given in (2.5).

In (2.16), $u_{m,t}(t)$ stands for the derivative of $u_m(x,t)$ w.r.t. t evaluated at t.

2.4.1 A Priori Error Estimates

Theorem 2.4.1. *Let u satisfies (2.3)-(2.4) and $u(t),u_x(t)\in L^\infty(\Omega)$. Also, let $u_m(t)$ satisfies (2.6) and $u_m(t)\in L^\infty(\Omega)$. Then, for $u_0\in L^2(\Omega)$,*

$$||u-u_m||^2_{L^\infty(0,t;L^2(\Omega))}+\alpha||u-u_m||^2_{L^2(0,t;H^1_0(\Omega))}\leq A_1||u-U||^2(0)+A_2||(u-U)_t||^2_{L^2(0,t;L^2(\Omega))}$$
$$+A_3||u-U||^2_{L^2(0,t;H^1_0(\Omega))}+A_4||u-U||^2_{L^\infty(0,t;L^2(\Omega))}, \quad (2.17)$$

where U is some element in V_m of the form (2.5).

Note: u_m is a Galerkin approximation of u in V_m whereas U is some element of V_m of a particular form, *i.e.* (2.5). Therefore U may not be a solution to (2.3)-(2.4).

Proof. Since $u_m\in V_m$ and suppose U is another element in V_m, then $U-u_m\in V_m$. Taking

$\phi = U - u_m$ in (2.3) and $\phi_m = U - u_m$ in (2.16), then subtracting (2.16) from (2.3), we get

$$((u-u_m)_t, U-u_m) + ((u-u_m)_x, (U-u_m)_x) + (a(uu_x - u_m u_{m,x}) \\ + b(u(1-u) - u_m(1-u_m)), U-u_m) = 0.$$

Writing $U - u_m$ as $u - u_m + U - u$,

$$\Big((u-u_m)_t, u-u_m\Big) + \Big((u-u_m)_x, (u-u_m)_x\Big) = \Big((u-u_m)_t, u-U\Big) \\ + \Big((u-u_m)_x, (u-U)_x\Big) - a\Big(uu_x - u_m u_{m,x}, u-u_m\Big) + a\Big(uu_x - u_m u_{m,x}, u-U\Big) \\ - b\Big(u(1-u) - u_m(1-u_m), u-u_m\Big) + b\Big(u(1-u) - u_m(1-u_m), u-U)\Big). \quad (2.18)$$

To avoid confusion, we take up term by term simplification of (2.18).

$$\Big((u-u_m)_t, u-u_m\Big) = \frac{1}{2}\frac{d}{dt}||u-u_m||^2.$$
$$\Big((u-u_m)_x, (u-u_m)_x\Big) = ||(u-u_m)_x||^2.$$

Since $u \in H_0^1(\Omega)$ and $u_m \in V_m \subset H_0^1(\Omega)$. Since, semi-norm and norm are equivalent in H_0^1 space, therefore,

$$||(u-u_m)_x||^2 \geq \alpha ||u-u_m||^2_{H_0^1(\Omega)}.$$

The Cauchy-Schwartz inequality and the Young inequality for $\epsilon = \alpha/c$ give,

$$\Big((u-u_m)_x, (u-U)_x\Big) \leq ||(u-u_m)_x||||(u-U)_x|| \leq c||u-u_m||_{H_0^1(\Omega)}||u-U||_{H_0^1(\Omega)} \\ \leq \frac{\alpha}{2}||u-u_m||^2_{H_0^1(\Omega)} + C||u-U||^2_{H_0^1(\Omega)},$$

where $C = \frac{c^2}{2\alpha}$.

$$a\Big(uu_x - u_m u_{m,x}, u-u_m\Big) \leq |a|||uu_x - u_m u_{m,x}||||u-u_m|| \\ \leq \epsilon||uu_x - u_m u_{m,x}||^2 + C_1(a)||u-u_m||^2 \\ \leq \epsilon(||u-u_m|||u_x|| + ||u_m||||u_x - u_{m,x}||) + C_1(a)||u-u_m||^2.$$

The constant C_1 depends on a alone. Assumptions ensure that the quantity in parenthesis is bounded. Similarly,

$$\begin{aligned}
a(uu_x - u_m u_{m,x}, u-U) &\leq \epsilon||uu_x - u_m u_{m,x}||^2 + C_2(a)||u-U||^2,\\
b\Big(u(1-u) - u_m(1-u_m), u-u_m\Big) &\leq \epsilon||u(1-u) - u_m(1-u_m)||^2 + C_3(b)||u-u_m||^2,\\
b\Big(u(1-u) - u_m(1-u_m), u-U)\Big) &\leq \epsilon||u(1-u) - u_m(1-u_m)||^2 + C_4(b)||u-U||^2.
\end{aligned}$$

These simplifications reduce the equation (2.18) into the following form,

$$\begin{aligned}
\frac{d}{dt}||u-u_m||^2 + \alpha||u-u_m||^2_{H_0^1(\Omega)} \leq ((u-u_m)_t, u-U) + c||u-u_m||^2 \\
+ c_1||u-U||^2 + c_2||u-U||^2_{H_0^1(\Omega)}, \quad (2.19)
\end{aligned}$$

where constants c and c_1 depend solely on a and b.
Multiplying (2.19) by integrating factor e^{-ct} and integrating in time, we get

$$\begin{aligned}
&e^{-ct}||u-u_m||^2(t) - ||u-u_m||^2(0) + \alpha\int_0^t e^{-cs}||u-u_m||^2_{H_0^1(\Omega)}ds\\
&\leq \int_0^t ((u-u_m)_t, e^{-cs}(u-U))ds + \int_0^t c_1 e^{-cs}||u-U||^2 ds + \int_0^t c_2 e^{-cs}||u-U||^2_{H_0^1(\Omega)}ds,
\end{aligned} \quad (2.20)$$

for $t \in (0,T)$ *a.e.* Now, applying integration by parts to the first integral on the right of the above inequality,

$$\begin{aligned}
\int_0^t ((u-u_m)_t, e^{-cs}(u-U))ds &= e^{-ct}(u-U, u-u_m) - (u-U, u-u_m)(0)\\
&\quad - \int_0^t e^{-cs}(u-u_m, (u-U)_t)ds + \int_0^t ce^{-cs}(u-u_m, u-U)ds\\
&\leq \epsilon\Big\{||u-u_m||^2(t) + ||u-u_m||^2(0) + ||u-u_m||^2_{L^2(0,t;L^2(\Omega))}\Big\}\\
+ C'\Big\{||u-U||^2_{L^2(0,t;L^2(\Omega))} &+ ||(u-U)_{,t}||^2_{L^2(0,t;L^2(\Omega))} + ||u-U||^2(t) + ||u-U||^2(0)\Big\}. \quad (2.21)
\end{aligned}$$

Using estimate (2.21) in (2.20) and observing the fact that $||u-u_m||^2(0) \leq ||u-U||^2(0)$, u_m being Galerkin approximation and $||u-U||^2_{L^2(0,t;L^2(\Omega))} \leq ||u-U||^2_{L^2(0,t;H_0^1(\Omega))}$, we get the estimate (2.17). ∎

2.4.2 Convergence Analysis of Semi-discrete Solution

Theorem 2.4.2. *Let u satisfies (2.3)-(2.4) and u_m satisfies (2.6). Under the assumptions of theorem (2.4.1), semi-discrete solution u_m converges to the weak solution u as V_m fills the space $W(0,T;H(\Omega))$.*

Proof. Suppose the interpolant of $u(t)$ in V_m is denoted by $I_h u(t)$ for each t. Then, from theory of finite elements [95, 113],

$$||u - I_h u|| + h||u - I_h u||_1 \leq Ch^2|u|_2.$$

Since (2.17) is true for every $U \in V_m$, therefore, putting $U = I_h u(t)$, we get
for $t \in [0,T]$

$$||u-u_m||^2 + \alpha \int_0^t ||u-u_m||^2_{H_0^1} ds \leq A_1 h^4 |u(0)|^2_{H^2(\Omega)} + A_2 h^4 \int_0^t \left|\frac{\partial u}{\partial t}\right|^2_{H^2(\Omega)} ds + A_3 h^2 \int_0^t |u|_{H^2(\Omega)} ds + A_4 h^4 |u|^2_{H^2(\Omega)}(t). \quad (2.22)$$

As we see from (2.22), $h \to 0$ gives $u_m(t) \to u(t)$ for each $t \in [0,T]$. ∎

2.5 Fully Discretization of the Problem

The problem (2.6) is called the semi-discrete problem because the time is still a continuous variable. In this section, we discretize the time variable.
Suppose N represents the number of instants when we want to record our solution. Let $\Delta t = T/N$, the time step, then the homogeneous discretization for time is $0 < t_1 < ... < t_{N-1} < T$, where $t_k = k\Delta t$.
Using Euler's backward method to discretize the time derivative and lagging nonlinearity to the previous level of time, we have the following fully discrete problem:

$$\left(\frac{u_m^k - u_m^{k-1}}{\Delta t}, \phi_m\right) + (u_{m,x}^k, \phi_{m,x}) + (a u_m^{k-1} u_{m,x}^k + b u_m^k (1 - u_m^{k-1}), \phi_m) = 0, \ \forall \phi_m \in V_m \quad (2.23)$$

where $u_m^k = u_m(x, t_k)$. The semi-discrete solution at $t = t_k$ is $u(x, t_k)$ or u^k. From (2.3), u^k satisfies the following equation,

$$(u_t^k, \phi) + (u_x^k, \phi_x) + (au^k u_x^k + bu^k(1 - u^k), \phi) = 0, \ \forall \ \phi \in H_0^1(\Omega). \tag{2.24}$$

2.5.1 Convergence Analysis of Fully Discrete Solution

We will use the following lemma to prove the convergence of fully discrete solution,

Lemma: If $u_{tt} \in L^2(0, T; L^2(\Omega))$, then

$$\left|\left| u_t^k - \frac{u^k - u^{k-1}}{\Delta t} \right|\right|^2 \leq \frac{\Delta t}{3} \int_{t_{k-1}}^{t_k} ||u_{tt}||^2 dt. \tag{2.25}$$

Proof. See [101]. ∎

Theorem 2.5.1. *Suppose* $|a| \leq 1$. *If* u^k *is a solution of (2.24),* $u(t)$, $u_x(t) \in L^\infty(\Omega)$ *and* $u_{tt} \in L^2(0, T; L^2(\Omega))$. *Moreover, let* u_m^k *is a solution of (2.23) and* $||u_m^k||_{L^\infty(\Omega)} \leq 1$, *then*

$$||u^N - u_m^N||^2 \leq C\Bigg(h^4 |u(t)|_2^2 + \Delta t(F_2 + F_4)h^4 \sum_{k=1}^{N} |u^k|_2^2 + \Delta t F_6 h^2 \sum_{k=1}^{N} |u^k|_2^2 + (\Delta t)^2 F_3 \int_0^T ||u_t||^2 dt + F_8 \frac{(\Delta t)^2}{3} \int_0^T ||u_{tt}||^2 dt + F_9 h^4 \int_0^T |u_t^k|_2^2 dt \Bigg),$$

where $u^N(.) = u(t^N, .)$, $u_m^N(.) = u_m(t^N, .)$ *and* $C, F_2, F_3, F_4, F_6, F_8, F_9$ *are some positive fixed quantities independent of* h *and* Δt.

Proof. To estimate the error $u^N - u_m^N$, it is written in following manner,

$$u^N - u_m^N = u^N - U^N + U^N - u_m^N = e_I^N + e_D^N, \tag{2.26}$$

where e_I and e_D represent interpolation and discretization errors respectively.
It is clear that $e_D \in V_m$, therefore taking $\phi = e_D^k$ in (2.23) and (2.24), and subtracting the two, we have

$$(u_t^k - \frac{u_m^k - u_m^{k-1}}{\Delta t}, e_D^k) + (u_x^k - u_{m,x}^k, e_{D,x}^k) + a(u^k u_x^k - u_m^{k-1} u_{m,x}^k, e_D^k) + b(u^k(1 - u^k) - u_m^k(1 - u_m^{k-1}), e_D^k) = 0. \tag{2.27}$$

Next, we take up term by term simplification of (2.27).

First term yields,

$$\left(u_t^k - \frac{u_m^k - u_m^{k-1}}{\Delta t}, e_D^k\right) = \left(u_t^k - \frac{u^k - u^{k-1}}{\Delta t}, e_D^k\right) + \left(\frac{e_I^k - e_I^{k-1} + e_D^k - e_D^{k-1}}{\Delta t}, e_D^k\right).$$

Second term can be written as,

$$(u_x^k - u_{m,x}^k, e_{D,x}^k) = (e_{I,x}^k + e_{D,x}^k, e_{D,x}^k).$$

Adding and subtracting $u^{k-1}u_x^k$ and $u_m^{k-1}u_x^k$, third term can be written as,

$$a(u^k u_x^k - u_m^{k-1}u_{m,x}^k, e_D^k) = a((u^k - u^{k-1})u_x^k, e_D^k) + a((u^{k-1} - u_m^{k-1})u_x^k, e_D^k) + (au_m^{k-1}(e_{I,x}^k + e_{D,x}^k), e_D^k).$$

Fourth term is written as,

$$b(u^k(1-u^k) - u_m^k(1-u_m^{k-1}), e_D^k) = b((e_I^k + e_D^k)(1-u^{k-1}), e_D^k) - b(u_m^k(e_I^{k-1} + e_D^{k-1}), e_D^k) - b(u^k(u^k - u^{k-1}), e_D^k). \quad (2.28)$$

Using these values in (2.27), we have

$$\begin{aligned}(e_D^k - e_D^{k-1}, e_D^k) + \Delta t(e_{D,x}^k, e_{D,x}^k) &= -\Delta t\left(u_t - \frac{u^k - u^{k-1}}{\Delta t}, e_D^k\right) - \Delta t(e_{I,x}^k, e_{D,x}^k) \\ &-(e_I^k - e_I^{k-1}, e_D^k) - a\Delta t(u_x^k(u^k - u^{k-1}), e_D^k) - a\Delta t(u_x^k(u^{k-1} - u_m^{k-1}), e_D^k) \\ &-a\Delta t(u_m^{k-1}(e_{I,x}^k + e_{D,x}^k), e_D^k) - b\Delta t((e_I^k + e_D^k)(1-u^{k-1}), e_D^k) \\ &+b\Delta t(u_m^k(e_I^{k-1} + e_D^{k-1}), e_D^k) + b\Delta t(u^k(u^k - u^{k-1}), e_D^k). \quad (2.29)\end{aligned}$$

We again simplify the terms of this inequality one by one. Young inequality and Cauchy Schwartz inequality imply,

$$\begin{aligned}(e_D^k - e_D^{k-1}, e_D^k) = ||e_D^k||^2 - (e_D^{k-1}, e_D^k) &\geq ||e_D^k||^2 - ||e_D^{k-1}||||e_D^k|| \\ &\geq \frac{1}{2}(||e_D^k||^2 - ||e_D^{k-1}||^2).\end{aligned}$$

Utilizing (2.25) with Cauchy-Schwartz inequality, we see

$$\left(u_t - \frac{u^k - u^{k-1}}{\Delta t}, e_D^k\right) \leq \frac{\Delta t}{6}\int_{t_{k-1}}^{t_k} ||u_{tt}||^2 dt + \frac{1}{2}||e_D^k||^2.$$

The Cauchy Schwartz inequality and the Young inequality for $\epsilon = 5/2$ yield,

$$|(e_{I,x}^k, e_{D,x}^k)| \leq ||e_{I,x}^k||||e_{D,x}^k|| \leq \frac{5}{4}||e_{I,x}^k||^2 + \frac{1}{5}||e_{D,x}^k||^2.$$

From [101], using Cauchy-Schwartz inequality and Young inequality for $\epsilon = \Delta t$, we have

$$|(e_I^k - e_I^{k-1}, e_D^k)| \leq \Delta t||e_D^k||^2 + \frac{1}{4}\int_{t_{k-1}}^{t_k} ||e_{I,t}^k||^2 dt.$$

Again taking recourse to Young inequality, we simplify the term $(u_x^k(u^k - u^{k-1}), e_D^k)$ as

$$\begin{aligned}
a\Delta t(u_x^k(u^k - u^{k-1}), e_D^k) &\leq |a|\Delta t\int_\Omega u_x^k(u^k - u^{k-1})e_D^k dx \\
&\leq |a|\Delta t||u_x^k||_{L^\infty(\Omega)}||u^k - u^{k-1}||||e_D^k|| \text{ (Cauchy Schwartz inequality)} \\
&\leq \frac{|a|}{2}\Delta t||u_x^k||_{L^\infty(\Omega)}(||u^k - u^{k-1}||^2 + ||e_D^k||^2) \text{ (for } \epsilon = 1) \\
&\leq \frac{|a|}{2}\Delta t||u_x^k||_{L^\infty(\Omega)}\left(\Delta t\int_{t_{k-1}}^{t_k} ||u_t||^2 dt + ||e_D^k||^2\right).
\end{aligned}$$

Proceeding in similar fashion for other terms,

$$\begin{aligned}
a\Delta t(u_x^k(u^{k-1} - u_m^{k-1}), e_D^k) &\leq \frac{|a|}{2}\Delta t||u_x^k||_{L^\infty(\Omega)}(||u^{k-1} - u_m^{k-1}||^2 + ||e_D^k||^2) \\
&\leq \frac{|a|}{2}\Delta t||u_x^k||_{L^\infty(\Omega)}(||u^{k-1} - U^{k-1} + U^{k-1} - u_m^{k-1}||^2 + ||e_D^k||^2) \\
&\leq \frac{|a|}{2}\Delta t||u_x^k||_{L^\infty(\Omega)}(||e_I^{k-1}||^2 + ||e_D^{k-1}||^2 + ||e_D^k||^2).
\end{aligned}$$

Using Young inequality for $\epsilon = 7/2$ and the triangle inequality yield,

$$a\Delta t(u_m^{k-1}(e_{I,x}^k + e_{D,x}^k), e_D^k) \leq |a|\Delta t||u_m^{k-1}||_{L^\infty(\Omega)}\left(\frac{1}{2}||e_{I,x}^k||^2 + \frac{1}{5}||e_{D,x}^k||^2 + \frac{7}{4}||e_D^k||^2\right).$$

Similarly, the following inequalities follow,

$$b\Delta t((e_I^k + e_D^k)(1 - u^{k-1}), e_D^k) \leq |b|\Delta t.\max\{1, ||u^{k-1}||_{L^\infty(\Omega)}\}(||e_D^k||^2 + \frac{1}{2}||e_I^k||^2),$$

$$b\Delta t(u_m^k(e_I^{k-1}+e_D^{k-1}),e_D^k)\leq\frac{|b|}{2}\Delta t||u_m^k||_{L^\infty(\Omega)}(||e_D^{k-1}||^2+||e_I^{k-1}||^2+||e_D^k||^2),$$
$$b\Delta t(u^k(u^k-u^{k-1}),e_D^k)\leq|b|\Delta t||u^k||_{L^\infty(\Omega)}\bigg(\Delta t\int_{t_{k-1}}^{t_k}||u_t||^2dt+||e_D^k||^2\bigg).$$

The choices of specific $\epsilon's$ in Young inequality are made so that the cancellation of some terms could be possible.

Using all these inequalities in (2.29), we have

$$||e_D^k||^2-||e_D^{k-1}||^2+\Delta tF_1^k||e_{D,x}^k||^2\leq\Delta tF_2^k||e_D^k||^2+\Delta tF_3^k||e_D^{k-1}||^2+\Delta t^2F_4^k\int_{t_{k-1}}^{t_k}||u_t||^2dt$$
$$+\Delta tF_5^k||e_I^{k-1}||^2+\Delta tF_6^k||e_I^k||^2+\Delta tF_7^k||e_{I,x}^k||^2+\frac{\Delta t^2}{6}\int_{t_{k-1}}^{t_k}||u_{tt}||^2dt+\frac{1}{2}\int_{t_{k-1}}^{t_k}||e_{I,t}^k||^2dt,\quad(2.30)$$

where $F_1^k=\frac{8}{5}-\frac{2}{5}|a|||u_m^{k-1}||$,
$F_2^k=3+|a|\bigg(2||u_x^k||_{L^\infty(\Omega)}+\frac{7}{2}||u_m^{k-1}||_{L^\infty(\Omega)}\bigg)+|b|(||u_m^k||_{L^\infty}+2||u^k||_{L^\infty}+2\max\{1,||u^{k-1}||_{L^\infty}\})$,
$F_3^k=|a|||u_x^k||_{L^\infty}+|b|||u^k||_{L^\infty}$, $F_4^k=F_5^k=|a|||u_x^k||_{L^\infty}+2|b|||u^k||_{L^\infty}$, $F_6^k=|b|\max\{1,||u_{L^\infty}^{k-1}\}$
$F_7^k=\frac{5}{2}+|a|||u_m^{k-1}||_{L^\infty}$.

Under the assumptions on $|a|$ and u_m^{k-1}, we conclude $F_1^k\geq1$.

Now, summing (2.30) over $k=1(1)N$, and representing supremum of F_i^k by F_i, we obtain

$$||e_D^N||^2+\Delta t\sum_{k=1}^N||e_{D,x}^k||^2\leq\Delta t(F_2+F_3)\sum_{k=1}^N||e_D^k||^2+(\Delta t)^2F_4\int_0^T||u_t||^2dt$$
$$+\Delta t(F_5+F_6)\sum_{k=1}^N||e_I^k||^2+\Delta tF_7\sum_{k=1}^N||e_{I,x}^k||^2+\frac{(\Delta t)^2}{6}\int_0^T||u_{tt}||^2dt+\frac{1}{2}\int_0^T||e_{I,t}^k||^2dt.\quad(2.31)$$

Taking Δt small enough to make sure that $\Delta t(F_2+F_4)<1$ and applying discrete form of Gronwall inequality to (2.31), we have

$$||e_D^N||^2+\Delta t\sum_{k=1}^N||e_{D,x}^k||^2\leq K\bigg((\Delta t)^2F_4\int_0^T||u_t||^2dt+\Delta t(F_5+F_6)\sum_{k=1}^N||e_I^k||^2$$
$$+\Delta tF_7\sum_{k=1}^N||e_{I,x}^k||^2+\frac{(\Delta t)^2}{6}\int_0^T||u_{tt}||^2dt+\frac{1}{2}\int_0^T||e_{I,t}^k||^2dt\bigg),\quad(2.32)$$

where $K=\exp\bigg(\frac{T(F_2+F_3)}{1-\Delta t(F_2+F_3)}\bigg)$.

From the theory of finite element interpolation [113],

$$||e_I^k||+h||e_{I,x}^k||\leq h^2|u^k|_2. \tag{2.33}$$

From (2.26), (2.32) and (2.33), and using the triangle inequality, we obtain the error of full discretization, which can be written as,

$$\begin{aligned}||u^N-u_m^N||^2 &\leq ||e_D^N||^2+||e_I^N||^2\\ &\leq C\bigg(h^4|u|_2^2+(\Delta t)^2F_4\int_0^T||u_t||^2dt+\Delta t(F_5+F_6)h^4\sum_{k=1}^N|u^k|_2^2+\Delta tF_7h^2\sum_{k=1}^N|u^k|_2^2\\ &\qquad+\frac{(\Delta t)^2}{6}\int_0^T||u_{tt}^k||^2dt+\frac{1}{2}h^4\int_0^T|u_t^k|_2^2dt\bigg),\end{aligned} \tag{2.34}$$

where C is some constant independent of h and Δt.
From (2.34), it follows that as $h\to 0, \Delta t\to 0$, $u_m^N\to u^N$, that is, for any time T, the fully discrete solution u_m^N converges to the weak solution at that time. ■

2.5.2 Positivity of the Approximate Solution

In this sub-section, we investigate the positivity of solution to (2.23). The domain is discretized uniformly in time and space. The time step is $\Delta t>0$ and space step length is h. For a generic element $e_i=(x_i,x_{i+1})$,

$$u_m^k(x)=\sum_{j\in\{i,i+1\}}c_j^k\phi_j(x),\ x\in e_i, \tag{2.35}$$

where linear basis $\phi_i's$ are given by

$$\phi_i(x)=\frac{x_{i+1}-x}{h},\ \phi_{i+1}(x)=\frac{x-x_i}{h},\ x\in e_i,$$

$h=x_{i+1}-x_i$.

Theorem 2.5.2. *For a uniform discretization of the domain $[0,T]\times\Omega$ with respect t and x, the sufficient condition on Δt for positivity of u_m^k, the fully discrete solution, is given by:*

$$-\frac{3}{h^2}+\frac{a}{2h}(2c_1^{k-1}+c_2^{k-1})+b\Big(\frac{3c_1^{k-1}+c_2^{k-1}}{4}-1\Big)<\frac{1}{\Delta t}\leq$$

$$\frac{6}{h^2} - \frac{a}{h}(2c_1^{k-1} + c_2^{k-1}) + b\Big(\frac{c_1^{k-1} + c_2^{k-1}}{2} - 1\Big),$$

where c_1, c_2 *are the values of* u_m^k *at node points of* e_i.

Proof. From (2.23) and (2.35), we have

$$\Big(\sum_{j=i}^{i+1} c_{j,t}^k \phi_j, \phi_l\Big) + \Big(\sum_{j=i}^{i+1} c_j^k \phi_{j,x}, \phi_{l,x}\Big) + a\Big(\sum_{j=i}^{i+1} c_j^{k-1}\phi_j \sum_{j=i}^{i+1} c_j^k \phi_{j,x}, \phi_l\Big) + b\Big(\sum_{j=i}^{i+1} c_j^k \phi_j, \phi_l\Big) - b\Big(\sum_{j=i}^{i+1} c_j^{k-1}\phi_j \sum_{j=i}^{i+1} c_j^k \phi_j, \phi_l\Big) = 0,\ l = i, i+1.$$

We get the following system from above,

$$Ac'(t^k) + (B + aC + b(A - D))c(t^k) = 0, \tag{2.36}$$

where matrices A, B, C and D are given by

$$A = \begin{bmatrix} h/3 & h/6 \\ h/6 & h/3 \end{bmatrix}, \qquad B = \begin{bmatrix} 1/h & -1/h \\ -1/h & 1/h \end{bmatrix}, \tag{2.37}$$

$$C = \frac{1}{6}\begin{bmatrix} -(2c_i^{k-1} + c_{i+1}^{k-1}) & 2c_i^{k-1} + c_{i+1}^{k-1} \\ -(c_i^{k-1} + 2c_{i+1}^{k-1}) & c_i^{k-1} + 2c_{i+1}^{k-1} \end{bmatrix}, \qquad D = \frac{h}{12}\begin{bmatrix} 3c_i^{k-1} + c_{i+1}^{k-1} & c_i^{k-1} + c_{i+1}^{k-1} \\ c_i^{k-1} + c_{i+1}^{k-1} & c_i^{k-1} + 3c_{i+1}^{k-1} \end{bmatrix}, \tag{2.38}$$

and $c(t)$ is an unknown vector. Discretizing (2.36) by Euler backward difference scheme in time, we see the following system,

$$\mathcal{A}c^k = \frac{A}{\Delta t}c^{k-1}, \text{ for } \mathcal{A} = \frac{A}{\Delta t} + B + aC + b(A - D). \tag{2.39}$$

We observe that A has positive entries. Then, for $c^{k-1} \geq 0$, the right hand side of (2.39) is non-negative. A sufficient condition for c^k to be non-negative is that the matrix $\mathcal{A}$ is an M-matrix [101]. M-matrix is a matrix whose diagonal entries are positive and off-diagonal entries are non-positive. The reason to show $\mathcal{A}$ is M-matrix lies in the fact that M-matrices have inverse matrices with every entry positive.

We have

$$\mathcal{A}_{11} = \frac{h}{3\Delta t} + \frac{1}{h} - \frac{a}{6}(2c_1^{k-1} + c_2^{k-1}) + \frac{bh}{3} - \frac{bh}{12}(3c_1^{k-1} + c_2^{k-1}). \tag{2.40}$$

Similarly, we can write an expression for any $\mathcal{A}_{ii}$, keeping assembly of diagonal elements in mind. $\mathcal{A}_{11} > 0$ implies

$$\frac{1}{\Delta t} > -\frac{3}{h^2} + \frac{a}{2h}(2c_1^{k-1} + c_2^{k-1}) + b\Big(\frac{3c_1^{k-1} + c_2^{k-1}}{4} - 1\Big). \tag{2.41}$$

Further,

$$\mathcal{A}_{12} = \frac{h}{6\Delta t} - \frac{1}{h} + \frac{a}{6}(2c_1^{k-1} + c_2^{k-1}) + \frac{bh}{6} - \frac{bh}{12}(c_1^{k-1} + c_2^{k-1}),$$

for $\mathcal{A}_{12} \leq 0$,

$$\frac{1}{\Delta t} \leq \frac{6}{h^2} - \frac{a}{h}(2c_1^{k-1} + c_2^{k-1}) + b\Big(\frac{c_1^{k-1} + c_2^{k-1}}{2} - 1\Big). \tag{2.42}$$

The matrix $\mathcal{A}$ is not symmetric, due to non-symmetry of matrix C, therefore, $\mathcal{A}_{21}$ should also be looked into. But, we find $\mathcal{A}_{12} \leq 0$ implies $\mathcal{A}_{21} \leq 0$.
Combining (2.41) and (2.42), we have the result. ∎

2.6 Numerical Examples

In order to check the accuracy and efficiency of the proposed scheme (2.23), we have considered the problem (2.1) over the domain $[0, T] \times [0, 1]$ with following initial and boundary conditions,

$$\begin{aligned} u(0, x) = u_0(x) &= \frac{1}{2} + \frac{1}{2}\tanh\Big(-\frac{ax}{4}\Big), \\ u(t, 0) &= \frac{1}{2} + \frac{1}{2}\tanh\Big(\frac{a}{4}\Big\{\frac{a}{2} - \frac{2b}{a}\Big\}t\Big), \\ u(t, 1) &= \frac{1}{2} + \frac{1}{2}\tanh\Big(-\frac{a}{4}\Big[1 - \Big\{\frac{a}{2} - \frac{2b}{a}\Big\}t\Big]\Big). \end{aligned}$$

The exact solution of (2.1) for these initial and boundary conditions, is given by $u(t, x) = \frac{1}{2} + \frac{1}{2}\tanh(\frac{-a}{4}\{x - (\frac{a}{2} - \frac{2b}{a})t\})$ [122].

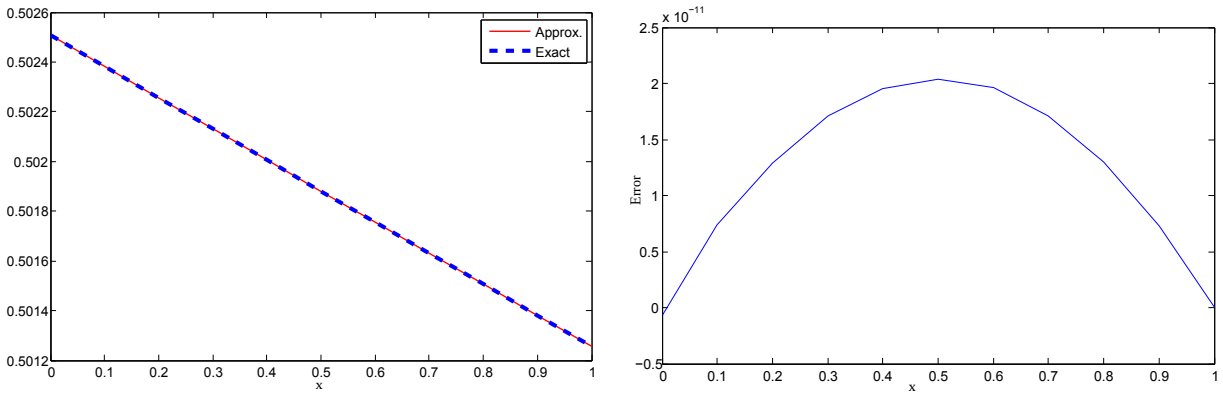

(a) Comparision of FEM and Exact solutions *(b) L^2 Error*

Figure 2.1: *For parameters $a = 0.01, b = -0.01$ at time $T = 1$ (Example 1)*

In order to find numerical solution, the element matrices given in (2.37)-(2.38) are assembled. And the proposed scheme is applied to find the solution upto the desired time level. We take the space parameter $h = 0.1$ and time step $\Delta t = 10^{-5}$ for all examples.

Example 1: Taking advection coefficient $a = 0.01$, source coefficient $b = -0.01$, the approximate solution is computed and compared with the exact solution in Table 2.1. Table 2.1 gives solution as well as absolute error at grid points for the time $T = 1$ and $T = 50$. Fig. 2.1a compares approximate solution with exact solution and Fig. 2.1b depicts error at time $T = 1$.

Table 2.1: *Computation of solution and absolute error for $a = 0.01, b = -0.01$*

	T=1			T=50		
x	Exact	Approx	Error	Exact	Approx	Error
0.10	0.5023812320	0.5023812320	7.42×10^{-12}	0.6226355677	0.6226355442	2.35×10^{-8}
0.20	0.5022562346	0.5022562346	1.29×10^{-11}	0.6225180803	0.6225180567	2.35×10^{-8}
0.30	0.5021312370	0.5021312371	1.71×10^{-11}	0.6224005784	0.6224005549	2.35×10^{-8}
0.40	0.5020062392	0.5020062392	1.96×10^{-11}	0.6222830622	0.6222830387	2.35×10^{-8}
0.50	0.5018812411	0.5018812411	2.04×10^{-11}	0.6221655316	0.6221655080	2.35×10^{-8}
0.60	0.5017562427	0.5017562427	1.96×10^{-11}	0.6220479866	0.6220479631	2.35×10^{-8}
0.70	0.5016312442	0.5016312442	1.71×10^{-11}	0.6219304273	0.6219304037	2.35×10^{-8}
0.80	0.5015062454	0.5015062454	1.30×10^{-11}	0.6218128536	0.6218128301	2.36×10^{-8}
0.90	0.5013812464	0.5013812464	7.27×10^{-12}	0.6216952657	0.6216952421	2.36×10^{-8}

Example 2: In this Example, results are computed for $a = 0.001, 0.01$ and $b = -0.001, -0.01$ at different times. The Table 2.2 compares absolute errors of the present scheme with VIM [88] and ADM [88] schemes at different times. It is observed that though the errors are of same order for small times but for large times the present scheme performs better and maintains accuracy to a far greater extent.

Table 2.2: *Absolute Error Comparison of proposed scheme with VIM and ADM*

		$a = 0.0001, b = -0.0001$			$a = 0.01, b = -0.01$		
x	T	FEM	VIM [88]	ADM [88]	FEM	VIM [88]	ADM [88]
0.1	1	9.79×10^{-14}	1.77×10^{-14}	1.77×10^{-14}	7.42×10^{-12}	1.78×10^{-8}	1.78×10^{-8}
0.5		7.62×10^{-14}	5.21×10^{-15}	5.21×10^{-15}	2.04×10^{-11}	5.29×10^{-9}	5.29×10^{-9}
0.9		1.45×10^{-14}	7.29×10^{-15}	7.29×10^{-15}	7.27×10^{-12}	7.28×10^{-9}	7.28×10^{-9}
0.1	10	3.21×10^{-14}	2.05×10^{-11}	2.05×10^{-11}	6.06×10^{-12}	2.07×10^{-5}	2.07×10^{-5}
0.5		1.74×10^{-14}	1.93×10^{-11}	1.93×10^{-11}	1.83×10^{-11}	1.94×10^{-5}	1.94×10^{-5}
0.9		1.71×10^{-14}	1.80×10^{-11}	1.80×10^{-11}	6.26×10^{-12}	1.81×10^{-5}	1.81×10^{-5}
0.1	50	2.50×10^{-10}	2.60×10^{-9}	2.60×10^{-9}	2.35×10^{-8}	0.002522	0.002522
0.5		2.50×10^{-10}	2.57×10^{-9}	2.60×10^{-9}	2.35×10^{-8}	0.002522	0.002522
0.9		2.50×10^{-10}	2.53×10^{-9}	2.53×10^{-9}	2.36×10^{-8}	0.002522	0.002522

Example 3: In this Example, we compare absolute error of the present scheme with the Exp-function method [78] for different set of values of a, b : $a = 0.001, b = -0.001$; $a = 0.1, b = -0.1$ and $a = 0.5, b = -0.5$. The comparison is presented in Table 2.3.

Example 4: This Example compares the present scheme results with HAM [10] for $a = -1, b = -1$ at times $T = 0.5$, $T = 0.7$ and $T = 1$ in Table 2.4.

Example 5: In this Example, we compare the present scheme results with that of results by compact finite difference scheme (CFD6) [102] for $a = 0.001, b = -0.001$. at different times in Table 2.5.

Example 6: This example validates the theory developed in sub-section 2.5.2 for the bounds of Δt. If $h = 0.1$, $a = 0.01$ and $b = -0.01$, then we have from the condition (2.42), $\Delta t \geq 0.0016$. The implication of this threshold on Δt is that for all $\Delta t > 0.0016$, the matrix $\mathcal{A}$ will have positive inverse, which ensures the positivity of solution. However, the condition is only sufficient and smaller $\Delta t's$ than the threshold limit can also offer positive solution as we saw in the aforementioned examples where we took smaller value of Δt. It

can be easily checked for smaller Δt, say $\Delta t = 0.001$ the inverse of $\mathcal{A}$ has some of entries negative, for example $\mathcal{A}(2,1) = -0.07735$.

Table 2.3: *Absolute Error Comparison of present scheme with Exp-Function method at time $T = 0.1$*

	$a = 0.001, b = -0.001$		$a = 0.1, b = -0.1$		$a = 0.5, b = -0.5$	
x	FEM	Exp-Fun [78]	FEM	Exp-Fun [78]	FEM	Exp-Fun [78]
0.0	1.40×10^{-13}	2.23×10^{-8}	4.75×10^{-13}	8.01×10^{-8}	2.67×10^{-13}	1.67×10^{-6}
0.1	3.66×10^{-10}	1.98×10^{-8}	3.83×10^{-8}	7.00×10^{-8}	3.02×10^{-7}	1.16×10^{-6}
0.2	6.97×10^{-10}	1.70×10^{-8}	7.29×10^{-8}	5.98×10^{-8}	5.61×10^{-7}	7.77×10^{-7}
0.3	9.60×10^{-10}	1.39×10^{-8}	1.00×10^{-7}	4.97×10^{-8}	7.62×10^{-7}	4.84×10^{-7}
0.4	1.12×10^{-9}	1.04×10^{-8}	1.18×10^{-7}	3.95×10^{-8}	8.92×10^{-7}	2.67×10^{-7}
0.5	1.18×10^{-9}	6.54×10^{-9}	1.24×10^{-7}	2.95×10^{-8}	9.43×10^{-7}	1.12×10^{-7}
0.6	1.12×10^{-9}	2.35×10^{-9}	1.18×10^{-7}	1.97×10^{-8}	9.10×10^{-8}	6.85×10^{-9}
0.7	9.60×10^{-10}	2.18×10^{-9}	1.01×10^{-7}	1.02×10^{-8}	7.92×10^{-7}	5.97×10^{-8}
0.8	6.97×10^{-10}	7.06×10^{-9}	7.39×10^{-8}	9.79×10^{-10}	5.94×10^{-7}	9.57×10^{-8}
0.9	3.66×10^{-10}	1.22×10^{-8}	3.92×10^{-8}	7.78×10^{-9}	3.26×10^{-7}	1.07×10^{-7}
1.0	1.40×10^{-14}	1.78×10^{-8}	1.66×10^{-16}	1.60×10^{-8}	8.32×10^{-16}	9.90×10^{-8}

Table 2.4: *Absolute Error Comparison of proposed scheme with HAM*

		T=0.001		T=0.005		T=0.010	
x	(a, b)	FEM	HAM [10]	FEM	HAM [10]	FEM	HAM [10]
0.1	$(-1, -1)$	1.91×10^{-6}	9.32×10^{-6}	7.08×10^{-7}	8.90×10^{-5}	4.99×10^{-7}	9.09×10^{-4}
0.5		4.72×10^{-7}	4.73×10^{-6}	1.69×10^{-6}	5.44×10^{-5}	1.08×10^{-6}	5.03×10^{-4}
0.9		1.72×10^{-6}	1.32×10^{-6}	5.11×10^{-7}	1.90×10^{-5}	3.54×10^{-7}	3.09×10^{-4}

Table 2.5: *Absolute Error Comparison of proposed scheme with CFD6*

		T=0.001		T=0.005		T=0.010	
x	(a, b)	FEM	CFD6 [102]	FEM	CFD6 [102]	FEM	CFD6 [102]
0.1	$(0.001, -0.001)$	1.21×10^{-9}	1.01×10^{-7}	1.69×10^{-9}	4.38×10^{-7}	1.28×10^{-9}	7.53×10^{-7}
0.5		2.28×10^{-12}	1.04×10^{-7}	2.49×10^{-9}	5.21×10^{-7}	2.50×10^{-9}	1.04×10^{-6}
0.9		1.20×10^{-10}	1.01×10^{-7}	1.69×10^{-9}	4.38×10^{-7}	1.28×10^{-9}	7.53×10^{-7}

Chapter 3

Coupled Reaction Diffusion Models

In this chapter, we establish the existence and uniqueness of weak solutions to the coupled reaction-diffusion models using Banach fixed point theorem (Sec. 3.3). The Galerkin finite element method is used for the approximation of solutions, and an a priori error estimate is derived for such approximations in Sec. 3.4. A scheme is proposed by combining the C-N and the P-C methods for the time discretization in Sec. 3.5. Some numerical examples are considered to illustrate the accuracy and efficiency of the proposed scheme in Sec. 3.6. It is found that the scheme is second-order convergent. In addition, nonuniform grids are used in some examples to enhance the accuracy of the scheme.

3.1 Introduction

The coupled reaction-diffusion models frequently arise in the field of chemistry, biology, sociology, physics, geology, ecology, *etc.* [41, 94]. These models are naturally applied in chemistry, for example, the Brusselator model, Gray-Scott model *etc.* However, such models can also describe dynamical processes of non-chemical nature, for instance, the predator-prey model. In 1952, in his pioneering work on morphogenesis, Turing [116] first proposed that the reaction-diffusion systems may be used to study the replicating patterns such as stripes, spots, dappling, *etc.*, seen on the skin of many animals like zebras, lions, cats, and so on. In [116], Turing explained that the involvement of diffusion, under some circumstances, could lead to pattern forming instability, called 'Turing instability'.

A general one dimensional two species (chemicals) coupled reaction-diffusion model may be

defined as:

$$u_t - d_u u_{xx} = f(u,v),\ (t,x) \in (0,T] \times \Omega, \tag{3.1}$$

$$v_t - d_v v_{xx} = g(u,v),\ (t,x) \in (0,T] \times \Omega, \tag{3.2}$$

where d_u and d_v are the diffusion coefficients for u and v respectively. The most general forms of f and g for these models are as follows:

$$f(u,v) = a_1 + a_2 u + a_3 v - m_1 uv - m_2 u^2 v - m_3 uv^2,$$
$$g(u,v) = b_1 + b_2 u + b_3 v + m_1 uv + m_2 u^2 v + m_3 uv^2.$$

Some well-known forms of this model, such as the Gray-Scott model, Brusselator model, Schnakenberg model, prey-predator model, *etc.*, have gained much attention from the research community due to their important applications to biology and chemistry. These models have been studied at length in literature [53, 55, 57, 68].

A more general form of the model (3.1)-(3.2) is solved by Xiao et al. [124]; however, some important questions of existence, uniqueness and error bounds *etc.* are not discussed. The main focus of Xiao et al. [124] was to develop one step and multi-step finite element schemes for delayed predator-prey competition reaction-diffusion systems. The existence and uniqueness for a more general model is discussed by Almeida et al. [2] for non-local diffusion — but only for linear reaction.

The special cases such as the Gray-Scott model, Brusselator model, Schnakenberg model *etc.* of the system (1.1)-(1.2) lack the element of generality in themselves. For instance, Gray-Scott, Brusselator and Schnakenberg models take $g(u,v) = -\beta v + uv^2, \beta u - u^2 v$ and $\beta - u^2 v$, respectively. But, none of these models consider the case where v has a positive net birth rate (birth-death), because in this case, g will have some formula like $g(u,v) = \beta v - u^m v^n$, for some $m, n \geq 1$. Therefore, an attempt is made in this chapter to study the system in generality.

Moreover, these systems possess high order non-linearity, which makes it difficult to find analytical solutions of such systems. Therefore, efforts have been made to propose numerical schemes to approximate solutions accurately. Some of the important schemes developed so far include finite difference schemes [34], implicit-explicit time-stepping schemes [77],

positive finite volume methods [36], discontinuous Galerkin methods [128], finite volume spectral element methods [105], differential quadrature methods [55], variational multiscale element-free Galerkin and local discontinuous Galerkin methods [24] and meshless local Petrov-Galerkin methods [48], to name to a few.

The present scheme differs from the other variants of the finite element methods in the sense that the classical Galerkin method with the C-N and P-C techniques is considered. The proposed scheme is fast, easy and accurate, which is established by comparing the results by the proposed scheme with the earlier ones.

For numerical simulations, we consider a linear model with an exact solution to check the competence of the proposed approach by calculating L^2, L^∞ errors and order of convergence. Furthermore, two well-known nonlinear models — the Gray-Scott and Brusselator models, are simulated to capture their pattern formations.

3.2 Weak Formulation

The weak formulation to the problem (3.1)-(3.2) with initial conditions $u(0,x) = u_0(x),\ v(0,x) = v_0(x)$, is obtained by multiplying the equations (3.1) and (3.2) by some function (called test function) $\phi \in H^1(\Omega)$ and then integrating them w.r.t. space variable x over Ω. Using integration by parts together with homogeneous Neumann boundary conditions, we define the weak solution of our problem as follows:

We say that the functions (u, v) such that

$$u,\ v \in L^2(0,T;L^8(\Omega) \cap H^1(\Omega)) \text{ with } u',\ v' \in L^2(0,T;L^8(\Omega)) \tag{3.3}$$

is a weak solution of (3.1)-(3.2) if

$$(u',\phi) + d_u(u_x,\phi_x) = (f(u,v),\phi), \tag{3.4}$$

$$(v',\phi) + d_v(v_x,\phi_x) = (g(u,v),\phi), \tag{3.5}$$

hold for every $\phi \in H^1(\Omega)$, and

$$u(0,x) = u_0(x),\ v(0,x) = v_0(x). \tag{3.6}$$

Here, u' represents the derivative of u with respect to t.

Theorem 3.2.1. *Suppose $u \in L^2(0,T;X)$ with $u' \in L^2(0,T;X)$. Then $u \in C([0,T];X)$ and*

$$\max_{0\leq t\leq T} ||u(t)||_X \leq K(||u||_{L^2(0,T;X)} + ||u'||_{L^2(0,T;X)}).$$

Proof. See [30], Chapter 5, Section 5.9. ∎

Taking $X = L^8(\Omega) \cap H^1(\Omega)$, we conclude from the Theorem 3.2.1 that $u, v \in C([0,T]; L^8(\Omega) \cap H^1(\Omega))$, and hence Eq. (3.6) makes sense. The space $C([0,T]; L^8(\Omega) \cap H^1(\Omega))$ is our solution space, let us call it $\mathcal{S}$.

Note: To clarify the use of space $L^8(\Omega)$ in the above formulation, we note that in earlier chapters $\Omega \subset \mathbb{R}$ and in $\mathbb{R}$, H^1 functions are continuous which makes the non-linear function $f(u)$ integrable; however, in 2D, we need to ensure the function $f(u)$ is integrable. In this case, the highest order non-linearity in the formulation is cubic, that is u^2v, where u is the first chemical, v is the second chemical. To make $u^2v\phi$ integrable in the weak formulation, where ϕ is a test function, we take $u(t), v(t) \in L^8(\Omega)$. In such a space, $u^2(t)$ belongs to $L^4(\Omega)$, by generalized Hölder inequality and $v(t) \in L^4(\Omega)$, since Ω is bounded, hence of finite measure. Therefore, the product $u^2(t)v(t)$ belongs to L^2, again by generalized Hölder inequality. Since ϕ comes from $H^1(\Omega)$ space which is contained in $L^2(\Omega)$, hence $\int_\Omega u^2(t)v(t)\phi dx$ exists by Hölder inequality. It may be pointed out that we may take examples of 1D, but this theory extends to 2D and applies for 1D as well.

3.3 Existence and Uniqueness of Weak Solution

In this section, we establish the existence and uniqueness of the weak solutions to the weak problem (3.4)-(3.5). Existence of semi-linear and quasi-linear systems has been discussed in literature by many techniques. For instance, Amann [5] showed the existence of solution to such systems by the semi-group technique. More details related to this technique may be found in Pazy [93]. Another technique is due to Friedman [32], where a series of a priori estimates on unknown function are derived. Contrary to these works, this study attempts to minimize the effort by applying Banach fixed point theorem.

Theorem 3.3.1. *Let $u_0(x)$, $v_0(x) \in H^1(\Omega)$ and u, v satisfy (3.3)-(3.5). If u and v are*

bounded functions in Ω*, then the coupled system of equations* (3.1)-(3.2) *has a unique solution.*

Proof. The proof of existence of the solution follows from Banach fixed point theorem as demonstrated in [30] for the semilinear case. To apply the theory to the present case, we put our problem in the following form:

$$\frac{d}{dt}\mathcal{X} - \Delta\mathcal{X} = F(\mathcal{X}),$$

where $\mathcal{S}\times\mathcal{S} \ni \mathcal{X} = \begin{pmatrix} u \\ v \end{pmatrix}$ and $\mathbb{R}^2 \ni F(\mathcal{X}) = \begin{pmatrix} f(\mathcal{X}) \\ g(\mathcal{X}) \end{pmatrix}$.
Now, we show that $F(.)$ is Lipschitz continuous. We find that

$$|F(\mathcal{X}_1) - F(\mathcal{X}_2)| = \sqrt{(f(u_1,v_1) - f(u_2,v_2))^2 + (g(u_1,v_1) - g(u_2,v_2))^2}. \tag{3.7}$$

Direct calculation shows that,

$$\begin{aligned} f(u_1,v_1) - f(u_2,v_2) &= (u_1-u_2)\{a_2 - m_1v_2 - m_2v_1(u_1+u_2) - m_3v_2^2\} \\ &\quad + (v_1-v_2)\{a_3 - m_1u_1 - m_2u_2^2 - m_3u_1(v_1+v_2)\} \\ &= \xi_1(u_1-u_2) + \xi_2(v_1-v_2), \end{aligned} \tag{3.8}$$

$$\begin{aligned} g(u_1,v_1) - g(u_2,v_2) &= (u_1-u_2)\{b_2 + m_1v_2 + m_2v_2(u_1+u_2) + m_3v_2^2\} \\ &\quad + (v_1-v_2)\{b_3 + m_1u_1 + m_2u_1^2 + m_3u_1(v_1+v_2)\} \\ &= \xi_3(u_1-u_2) + \xi_4(v_1-v_2), \end{aligned} \tag{3.9}$$

where $\xi_1,\ \xi_2,\ \xi_3$ and ξ_4 are some non-constants which may depend on $u_1,\ u_2$ and $v_1,\ v_2$. For a realistic model, ξ_1 and ξ_2 have the same sign, since a_2 and a_3 are unlikely to have the opposite signs simultaneously. For example, for an auto-catalytic population, $a_2 > 0$, and then a_3 will be zero in this case, since the mutual effect of v on u is captured in m_1, m_2, m_3. Therefore, applying $(a+b)^2 \le 2(a^2+b^2)$, we find

$$(f(u_1,v_1) - f(u_2,v_2))^2 \le 2\xi_1^2(u_1-u_2)^2 + 2\xi_2^2(v_1-v_2)^2.$$

Similarly, ξ_3 and ξ_4 have the same sign, and hence

$$(g(u_1, v_1) - g(u_2, v_2))^2 \leq 2\xi_3^2(u_1 - u_2)^2 + 2\xi_4^2(v_1 - v_2)^2.$$

From Eq. (3.7), we obtain,

$$|F(\mathcal{X}_1) - F(\mathcal{X}_2)| \leq \sqrt{2(\xi_1^2 + \xi_3^2)(u_1 - u_2)^2 + 2(\xi_2^2 + \xi_4^2)(v_1 - v_2)^2}.$$

Whence, $|F(\mathcal{X}_1) - F(\mathcal{X}_2)| \leq 2\sqrt{\xi_1^2 + \xi_3^2}\sqrt{(u_1 - u_2)^2 + (v_1 - v_2)^2} = 2\sqrt{\xi_1^2 + \xi_3^2}|\mathcal{X}_1 - \mathcal{X}_2|^2$, if $\xi_2^2 + \xi_4^2 \leq \xi_1^2 + \xi_3^2$,
or $|F(\mathcal{X}_1) - F(\mathcal{X}_2)| \leq 2\sqrt{\xi_2^2 + \xi_4^2}\sqrt{(u_1 - u_2)^2 + (v_1 - v_2)^2} = 2\sqrt{\xi_2^2 + \xi_4^2}|\mathcal{X}_1 - \mathcal{X}_2|^2$, if $\xi_1^2 + \xi_3^2 \leq \xi_2^2 + \xi_4^2$.
Since u and v are assumed bounded, therefore, $\xi_1^2 + \xi_2^2 + \xi_3^2 + \xi_4^2 \leq K$, for some K. This renders $F(.)$ Lipschitz continuous.
Since $\mathcal{S}$ is a Banach space. Appealing to a result of [30], Chapter 9, page 503, we are through.
Uniqueness: Suppose there exist two solutions (u_1, v_1) and (u_2, v_2) of (3.4)-(3.5), where $u_1 \neq u_2$ and/or $v_1 \neq v_2$, then

$$(u_1', \phi) + d_u(u_{1,x}, \phi_x) = (f(u_1, v_1), \phi), \tag{3.10}$$

$$(v_1', \phi) + d_v(v_{1,x}, \phi_x) = (g(u_1, v_1), \phi), \tag{3.11}$$

for every $\phi \in H^1(\Omega)$ and

$$(u_2', \phi) + d_u(u_{2,x}, \phi_x) = (f(u_2, v_2), \phi), \tag{3.12}$$

$$(v_2', \phi) + d_v(v_{2,x}, \phi_x) = (g(u_2, v_2), \phi), \tag{3.13}$$

for every $\phi \in H^1(\Omega)$.
Subtracting (3.12) from (3.10) and (3.13) from (3.11), we have

$$((u_1 - u_2)', \phi) + d_u((u_1 - u_2)_x, \phi_x) = (f(u_1, v_1) - f(u_2, v_2), \phi), \ \forall \phi \in H^1(\Omega), \tag{3.14}$$

$$((v_1 - v_2)', \phi) + d_v((v_1 - v_2)_x, \phi_x) = (g(u_1, v_1) - g(u_2, v_2), \phi), \ \forall \phi \in H^1(\Omega). \tag{3.15}$$

Under the assumption of boundedness of the solutions, we get from equations (3.8) and (3.9) that $|f(u_1, v_1) - f(u_2, v_2)| \leq K_1|u_1 - u_2| + K_2|v_1 - v_2|$ and $|g(u_1, v_1) - g(u_2, v_2)| \leq K_3|u_1 - u_2| + K_4|v_1 - v_2|$. Taking $\phi = u_1 - u_2$ in (3.14) and $\phi = v_1 - v_2$ in (3.15), we obtain

$$\frac{d}{dt}||u_1 - u_2||^2 \leq K_1||u_1 - u_2||^2 + K_2||(u_1 - u_2)(v_1 - v_2)||_{L^1(\Omega)},$$
$$\frac{d}{dt}||v_1 - v_2||^2 \leq K_3||v_1 - v_2||^2 + K_4||(u_1 - u_2)(v_1 - v_2)||_{L^1(\Omega)}.$$

Using Young inequality $ab \leq (a^2 + b^2)/2$, and taking K to be the maximum of the constants K_1, K_2, K_3 and K_4, we have,

$$\frac{d}{dt}(||u_1 - u_2||^2 + ||v_1 - v_2||^2) \leq K(||u_1 - u_2||^2 + ||v_1 - v_2||^2),$$
$$\frac{d}{dt}\{e^{-Kt}(||u_1 - u_2||^2 + ||v_1 - v_2||^2)\} \leq 0.$$

Integrating from 0 to t, we get $||u_1(t) - u_2(t)||^2 + ||v_1(t) - v_2(t)||^2 \leq e^{Kt}(||u_1(0) - u_2(0)||^2 + ||v_1(0) - v_2(0)||^2)$. Since $u_1(0) = u_2(0)$ and $v_1(0) = v_2(0)$, implying $u_1(t) = u_2(t)$ and $v_1(t) = v_2(t)$ a.e. ∎

3.4 A Priori Error Estimates and Convergence

The process of finite element approximation starts by the selection of a finite dimensional subspace V_m of the solution space $\mathcal{S}$, followed by the selection of a basis for the finite dimensional space. Subsequently, we approximate the solution by solving the system of equations, which are non-linear in our case. In this process, some error is committed. We derive an a priori error estimate for such error in this section. Furthermore, the a priori estimate allows us to understand the order by which the approximation converges to the solution. A priori error estimates are available for linear, semi-linear and even quasi-linear problems [113]. However, such results are not achieved for the coupled systems, which this study attempts to prove. We find that the second order convergence for quasi-linear systems is also valid for nonlinear coupled systems.

Consider a partition of Ω as (x_i, x_{i+1}), $i = 1, ..., m-1$ with the discretization parameter $h = \max_{1 \leq i \leq m-1}(x_{i+1} - x_i)$. The subspace V_m, characterized by h, satisfies (1.7). A Lagrange basis of linear continuous Lagrange polynomials $\{\phi_i\}_{i=1}^m$ for V_m is chosen, where $\phi_i(x) = 1$

if $x = x_i$ and $\phi_i(x) = 0$ for $x = x_j,\ j \neq i$. If u_m and v_m denote the approximations of u and v in V_m, we intend to find out the semi-discrete errors $||u_m(t) - u(t)||$ and $||v_m(t) - v(t)||$. Towards that end, we write $u_m(t) - u(t) = (u_m(t) - U(t)) + (U(t) - u(t)) = \theta(t) + \rho(t)$, where $U(t)$ is the elliptic projection of $u(t)$ onto V_m defined by (1.11).
The error estimates for $\rho(t)$ are available to us from literature, as noted in (1.12).
Therefore, we need to find error estimates only for $\theta(t)$. To accomplish this, we calculate

$$\begin{aligned}(\theta(t)_t, \phi) + d_u(\theta(t)_x, \phi_x) &= (u_m(t)_t, \phi) + d_u(u_m(t)_x, \phi_x) - (U(t)_t, \phi) - d_u(U(t)_x, \phi_x)\\ &= (f(u_m(t), v_m(t)), \phi) - (u_t + \rho_t, \phi) - d_u(u_x, \phi_x),\ \forall\ \phi \in V_m\\ &= (f(u_m(t), v_m(t)), \phi) - (f(u(t), v(t)), \phi) - (\rho_t, \phi),\end{aligned}$$

using (1.11). Taking $\phi = \theta(t)$, we have

$$\begin{aligned}\frac{1}{2}\frac{d}{dt}||\theta(t)||^2 + d_u||\theta(t)_x||^2 &\leq ||f(u_m(t), v_m(t)) - f(u(t), v(t))||||\theta(t)|| + ||\rho_t||||\theta(t)||\\ &\leq K(||u_m(t) - u(t)|| + ||v_m(t) - v(t)||)||\theta|| + ||\rho_t||||\theta(t)|| \qquad (3.16)\\ &\leq K(||\theta|| + ||\rho|| + ||\rho_t||)||\theta||. \qquad (3.17)\end{aligned}$$

It is assumed in (3.16) that $u(t)$ is bounded. Moreover, this assumption leads to the boundedness of $u_m(t)$ as well. Next, in (3.17), the norm $||v_m(t) - v(t)||$ has been dropped because of its similar nature to $||u_m(t) - u(t)||$. Therefore,

$$\begin{aligned}\frac{d}{dt}||\theta(t)|| &\leq K(||\theta|| + ||\rho|| + ||\rho_t||),\\ \frac{d}{dt}\left(e^{-Kt}||\theta(t)||\right) &\leq K(||\rho|| + ||\rho_t||). \qquad (3.18)\end{aligned}$$

Integrating (3.18) w.r.t. t from 0 to t,

$$\begin{aligned}||\theta(t)|| &\leq e^{Kt}||\theta(0)|| + Ke^{Kt}\int_0^t (||\rho|| + ||\rho_t||)ds,\\ ||\theta(t)|| &\leq K_1||\theta(0)|| + K_2\int_0^t (||\rho|| + ||\rho_t||)ds,\end{aligned}$$

where $t \in (0, T]$ and the constants K_1 and K_2 depend on T.

Theorem 3.4.1. *Under appropriate assumptions on u and ρ defined as above, we have*

$$||\rho(t)||+||\rho_t(t)||\leq K(u)h^2, \text{ for } t \in [0,T]. \tag{3.19}$$

Proof. See [113], Chapter 13. ∎

Based on the smoothness available on $u_0(x)$, we see $||\theta(0)||\leq Kh^2$. And therefore, $||\theta(t)||\leq Kh^2$.

3.5 Fully Discretization

So far, we have discretized space variable only. In this section, we discretize time variable too using C-N scheme. Following from the previous section, $u_m,\ v_m$ are the approximations of $u,\ v$ in V_m, having the Lagrange basis $\{\phi_i\}_{i=1}^m$ as described earlier, then

$$u_m = \sum_{i=1}^{m} c_i(t)\phi_i(x), \tag{3.20}$$

$$v_m = \sum_{i=1}^{m} d_i(t)\phi_i(x), \tag{3.21}$$

for some unknown vectors $c = (c_i)_{i=1}^m$ and $d = (d_i)_{i=1}^m$. (u_m, v_m) of Eqs. (3.20)-(3.21) satisfy (3.4)-(3.5). Therefore,

$$\sum_{i=1}^{m}(c_i'(t)\phi_i(x),\phi_j(x)) + d_u\sum_{i=1}^{m}(c_i(t)\phi_{i,x},\phi_{j,x}) = \Big(f\Big(\sum_{i=1}^{m}c_i(t)\phi_i(x),\sum_{i=1}^{m}d_i(t)\phi_i(x)\Big),\phi_j\Big),$$
$$\sum_{i=1}^{m}(d_i'(t)\phi_i(x),\phi_j(x)) + d_v\sum_{i=1}^{m}(d_i(t)\phi_{i,x},\phi_{j,x}) = \Big(g\Big(\sum_{i=1}^{m}c_i(t)\phi_i(x),\sum_{i=1}^{m}d_i(t)\phi_i(x)\Big),\phi_j\Big),$$

for every $1 \leq j \leq m$. The above systems can be written in the following matrix form:

$$Ac' + d_uBc = p(c(t),d(t)), \tag{3.22}$$

$$Ad' + d_vBd = q(c(t),d(t)), \tag{3.23}$$

where p and q are the vectors involving unknown vectors c and d. For non-uniform grids, the above matrices A, B are to be assembled from the element matrices A^e and B^e, which

are given by,

$$A^e = \begin{bmatrix} h_i/3 & h_i/6 \\ h_i/6 & h_i/3 \end{bmatrix},\ B^e = \begin{bmatrix} 1/h_i & -1/h_i \\ -1/h_i & 1/h_i \end{bmatrix}, \tag{3.24}$$

where $h_i = x_{i+1} - x_i$, $i = 1, 2, ..., m-1$.

Matrices A, B are assembled diagonally from the element matrices A^e, B^e. To make the assembly process more clear, we give the assembled matrix A here,

$$A = \begin{bmatrix} h_1/3 & h_1/6 & 0 & \dots & 0 \\ h_1/6 & h_1/3 + h_2/3 & h_2/6 & \dots & 0 \\ 0 & h_2/6 & h_2/3 + h_3/3 & \dots & 0 \\ \vdots & \vdots & \vdots & \ddots & \vdots \\ 0 & 0 & 0 & h_m/6 & h_m/3 \end{bmatrix}.$$

The exact forms of matrices p and q are described in the next section, where we consider examples. Discretizing (3.22) and (3.23) by C-N scheme at time level $t^{k-\frac{1}{2}}$, we get:

$$A\Big(\frac{c^k - c^{k-1}}{\Delta t}\Big) + d_u B\Big(\frac{c^k + c^{k-1}}{2}\Big) = p(c(t^{k-\frac{1}{2}}), d(t^{k-\frac{1}{2}})), \tag{3.25}$$

$$A\Big(\frac{d^k - d^{k-1}}{\Delta t}\Big) + d_v B\Big(\frac{d^k + d^{k-1}}{2}\Big) = q(c(t^{k-\frac{1}{2}}), d(t^{k-\frac{1}{2}})), \tag{3.26}$$

where c^k and d^k denote $c(t^k)$ and $d(t^k)$ respectively. Subjected to further discussion, we point out that $c(t^{k-\frac{1}{2}})$ and $d(t^{k-\frac{1}{2}})$ inside the matrices p and q, are to be reduced to the known terms c^{k-1}, c^{k-2} and d^{k-1}, d^{k-2} respectively. Since, p and q are non-linear in c and d, we apply P-C method for such reductions. The algorithm is precisely discussed in the upcoming section sub-headed as 'Gray-Scott Model'.

3.6 Numerical Demonstrations and Discussions

3.6.1 Coupled Linear Model

Starting with a simple linear model, we consider the following example:

$$u_t - d_u u_{xx} = -\beta u + v,$$

$$v_t - d_v v_{xx} = -\gamma v.$$

For $d_u = d_v$, the system has the following exact solution [130],

$$u = \{e^{-(\beta+d_u)t} + e^{-(\gamma+d_u)t}\}\cos(x),\ v = (\beta-\gamma)e^{-(\gamma+d_u)t}\cos(x).$$

Taking initial conditions from the exact solution, we test the proposed scheme for accuracy, convergence and computational cost (CPU time).

We observe from the Table 3.1 that the present scheme is fast, accurate and offers consistent second order convergence (Fig. 3.3). In Tables 3.2 and 3.3, we compare the FEM results with [20, 28, 57, 85] for different parameters. FEM results are better and the method is computationally efficient.

Table 3.1: *Comparision of L^2, L^∞ errors in P, their orders of convergence and CPU Times (in Seconds), Parameters: $\Omega = [0,1],\ T = 1,\ \beta = 1,\ \gamma = 1,\ d_u = d_v = 1,\ h = \frac{1}{m},\ \Delta t = \frac{h}{6\pi}$*

	Nonlinear Galerkin method [129]					Present scheme with uniform grid				
m	L_2	Order	L_∞	Order	CPU	L_2	Order	L_∞	Order	CPU
10	2.719e-2	-	1.749e-2	-	0.09	2.016e-5	-	2.774e-5	-	0.0049
20	1.237e-3	4.46	1.176e-3	3.89	0.17	5.045e-6	1.998	6.944e-6	1.998	0.0111
40	2.228e-4	2.47	3.064e-4	1.94	0.37	1.258e-6	2.004	1.735e-6	2.001	0.0332
80	5.408e-5	2.04	1.065e-4	1.52	0.73	3.141e-7	2.002	4.331e-7	2.002	0.142
160	1.145e-5	2.24	3.210e-5	1.73	2.74	7.849e-8	2.001	1.082e-7	2.001	0.711

Table 3.2: *Comparison of L^∞ Errors of different methods. Parameters: $\Omega = [0,1]$, $h = \frac{1}{m}$, $m = 100$, $\Delta t = \frac{h}{6\pi}$, $d_u = d_v = 1$, $\beta = 0.1$, $\gamma = 0.01$.*

	ECSCM[28]	CN-MG[20]		IIF2[20]		BS-DQM[85]	DQM[57]		Present	
T	m=512	m=512	(Sec)	m=512	(Sec)	m=200	m=100	(Sec)	m=100	(Sec)
0.04	1.10e-4	1.09e-4	1.02	2.73e-1	0.065	2.29e-5	2.02e-5	0.94	5.485e-7	0.013
0.02	2.84e-5	2.67e-5	0.57	6.40e-2	0.033	3.66e-6	2.07e-5	0.42	2.947e-7	0.0089
0.01	7.91e-6	6.30e-6	0.32	1.20e-2	0.017	4.47e-6	2.09e-6	0.24	1.503e-7	0.0057
0.005	2.80e-6	1.70e-6	0.16	1.10e-3	0.009	4.90e-6	2.10e-6	0.12	7.711e-8	0.0045

Table 3.3: *Comparison of L^∞ Errors of different methods. Parameters: $\Omega = [0, 1]$, $h = \frac{1}{m}$, $m = 100$, $\Delta t = 0.01h$, $d_u = d_v = 0.001$, $\beta = 100.0$, $\gamma = 1.0$.*

	ECSCM[28]	CN-MG[20]		IIF2[20]		BS-DQM[85]	DQM[57]		Present	
T	m=512	m=512	(Sec)	m=512	(Sec)	m=200	m=100	(Sec)	m=100	(Sec)
0.04	4.87e-3	4.87e-3	0.25	4.89e-3	1.63	2.90e-5	2.79e-5	1.34	6.255e-7	0.053
0.02	1.21e-3	1.22e-3	0.16	1.21e-3	0.81	2.91e-5	1.45e-4	0.68	2.393e-6	0.028
0.01	3.04e-4	3.04e-4	0.10	3.03e-4	0.41	3.79e-5	2.77e-4	0.33	3.523e-6	0.015
0.005	7.08e-4	7.60e-5	0.06	7.58e-5	0.21	6.18e-5	6.16e-5	0.16	3.015e-6	0.0099

3.6.2 Gray Scott model

The Gray-Scott model [41] illustrates an irreversible chemical reaction of two reagents and two products. One of the product is a reagent itself, while the other is an inert product that does not take part in further reaction processes and must be taken out of locale. The mechanism is represented by $P + 2Q \to 3Q$ and $Q \to I$, where P, Q are chemical species and I is an inert product. The proportion of consumption of P and Q is noteworthy. Representing the concentrations of chemicals P and Q by u and v respectively, the non-dimensional form of the model is given by the following system:

$$u_t - d_u u_{xx} = \alpha - \alpha u - uv^2, \tag{3.27}$$

$$v_t - d_v v_{xx} = uv^2 - \beta v. \tag{3.28}$$

It is assumed that the chemical P is fed from an infinite capacity reservoir at a constant rate α and is extracted at the rate αu. P is consumed in a ratio of one to two, with Q. This justifies the appearance of $-uv^2$ in (3.27). Q is produced in $P + 2Q \to 3Q$ and is lost in $Q \to I$, with a rate β, proportional to its concentration.

Converting the equations (3.27)-(3.28) into weak form and then applying the C-N scheme, we obtain the following matrix form:

$$\Big(\frac{A}{\Delta t} + d_u\frac{B}{2} + \alpha\frac{A}{2} + \frac{C(d)}{2}\Big)c^k = \Big(\frac{A}{\Delta t} - d_u\frac{B}{2} - \alpha\frac{A}{2} - \frac{C(d)}{2}\Big)c^{k-1} + \alpha p,$$

$$\Big(\frac{A}{\Delta t} + d_v\frac{B}{2} + \beta\frac{A}{2}\Big)d^k = \Big(\frac{A}{\Delta t} - d_v\frac{B}{2} - \beta\frac{A}{2}\Big)d^{k-1} + q(c, d),$$

where A, B are assembled from A^e, B^e which are given in (3.24), p is assembled from the element vector $p^e = [h_i/2,\ h_i/2]'$, C is assembled from the following element matrix,

$$C^e = \frac{h_i}{60} \begin{bmatrix} 12(d_i^{k-1/2})^2 + 2(d_{i+1}^{k-1/2})^2 + 6d_i^{k-1/2}d_{i+1}^{k-1/2} & 3(d_i^{k-1/2})^2 + 3(d_{i+1}^{k-1/2})^2 + 4d_i^{k-1/2}d_{i+1}^{k-1/2} \\ 3(d_i^{k-1/2})^2 + 3(d_{i+1}^{k-1/2})^2 + 4d_i^{k-1/2}d_{i+1}^{k-1/2} & 2(d_i^{k-1/2})^2 + 12(d_{i+1}^{k-1/2})^2 + 6d_i^{k-1/2}d_{i+1}^{k-1/2} \end{bmatrix},$$

and q is assembled from the element vector q^e, given by:

$$\frac{h_i}{60} \begin{bmatrix} \{12(d_i^{k-1/2})^2 + 2(d_{i+1}^{k-1/2})^2 + 6d_i^{k-1/2}d_{i+1}^{k-1/2}\}c_i^{k-1/2} \\ \{3(d_i^{k-1/2})^2 + 3(d_{i+1}^{k-1/2})^2 + 4d_i^{k-1/2}d_{i+1}^{k-1/2}\}c_i^{k-1/2} \\ \qquad + \{3(d_i^{k-1/2})^2 + 3(d_{i+1}^{k-1/2})^2 + 4d_i^{k-1/2}d_{i+1}^{k-1/2}\}c_{i+1}^{k-1/2} \\ \qquad + \{2(d_i^{k-1/2})^2 + 12(d_{i+1}^{k-1/2})^2 + 6d_i^{k-1/2}d_{i+1}^{k-1/2}\}c_{i+1}^{k-1/2} \end{bmatrix},$$

where $c_i^{k-1/2}$ denote the value of unknown c at node x_i for time $t^{k-1/2}$. As, the matrix C and the vector q contain the unknowns c and d and are nonlinear nature, we apply P-C method in an appropriate way. The steps of the algorithm are as follows:

i. we have c^0, d^0 from the initial solution,

ii. find $d^{1,p}$, indicating d^1 predicted, by replacing $d^{1/2}$ with d^0 and $c^{1/2}$ with c^0,

iii. find $c^{1,p}$ by replacing $d^{1/2}$ with $\frac{d^0+d^{1,p}}{2}$,

iv. find d^1 by replacing $d^{1/2}$ with $\frac{d^0+d^{1,p}}{2}$ and $c^{1/2}$ with $\frac{c^0+c^{1,p}}{2}$,

v. find c^1 by replacing $d^{1/2}$ with $\frac{d^0+d^1}{2}$,

vi. find d^2 by replacing $d^{3/2}$ with $\frac{3}{2}d^1 - \frac{1}{2}d^0$ and $c^{3/2}$ with $\frac{3}{2}c^1 - \frac{1}{2}c^0$,

vii. find c^2 by replacing $d^{3/2}$ with $\frac{d^1+d^2}{2}$,

repeating the steps *vi.* and *vii.* for d and c, we can find c and d to any level of time.

Demonstration:

A pulse in one dimensional space may loosely be defined as an interval of high v and low u. Outside of such an interval u is near one and v is near zero (Fig. 3.1). Therefore, we see that the variation in a pulse is limited to a short interval, where a proper observation

is needed and for the rest of interval, we may relax our attention. Secondly, since we want to observe the splitting of pulse, we can not reduce the domain Ω considerably. A way out of this situation is found by using the non-uniform grids (Fig. 3.2).

For the nonuniform grids, the method of geometric progression is used. Therefore, a typical grid pattern for $\Omega = [0, 1]$, which is dense at the end $x = 0$ will be generated as $x = [0, fd * cumsum(r^{0:m-1})]$, where $fd = \frac{r-1}{r^m-1}$, the first difference, r is some number near 0.9, chosen according to our requirement of mesh, *i.e.* $r = 0.99$ will give more uniform mesh than what $r = 0.90$ will give.

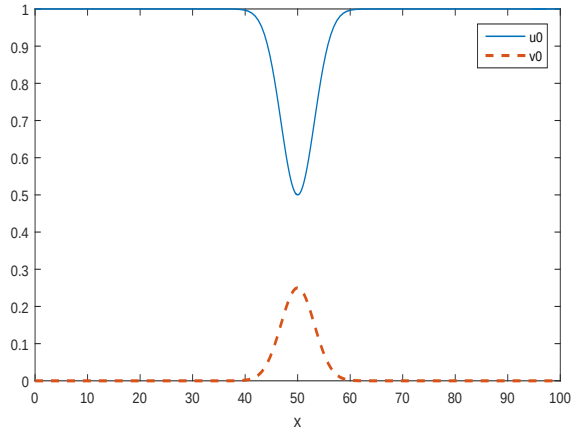

Figure 3.1: *Initial values of species u and v.*

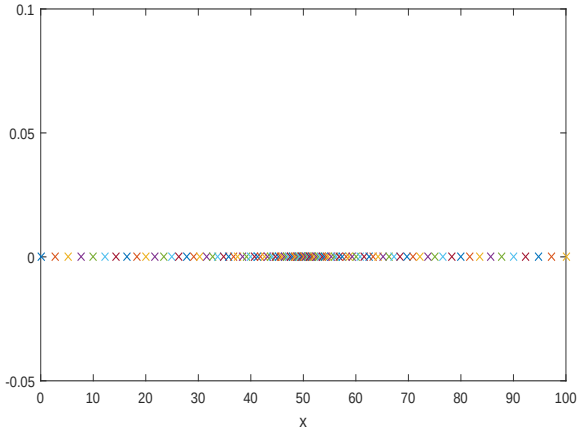

Figure 3.2: *The nonuniform grid for x.*

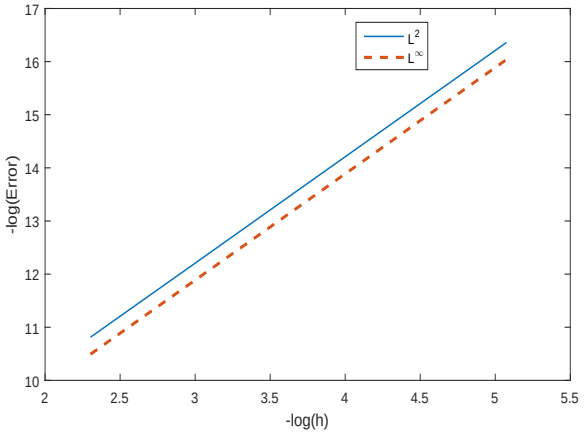

Figure 3.3: *The L^2 and L^∞ orders of convergence.*

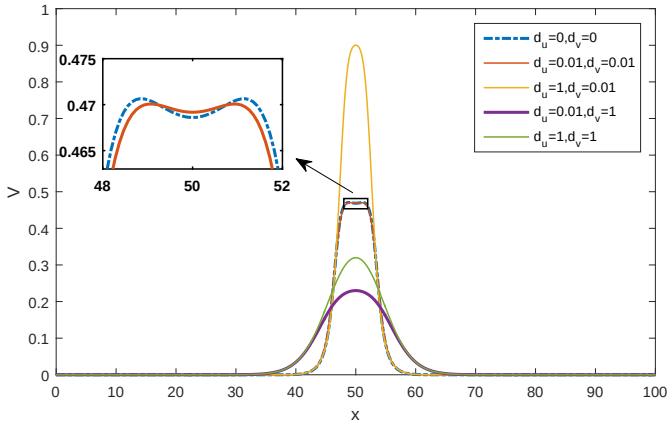

Figure 3.4: *Pulse state at $T = 12$ for different d_u's and d_v's.*

Taking the initial solution $u_0(x) = 1 - \frac{1}{2}\sin(\frac{\pi x}{100})^{100}$ and $v_0(x) = \frac{1}{4}\sin(\frac{\pi x}{100})^{100}$ (Fig. 3.1), we apply the above algorithm to obtain the results at different times in the domain $\Omega = [0, 100]$.

Due to the feed from P, chemical Q increases in the beginning. But increase in Q requires more P, and if P becomes insufficient to sustain a high Q, the middle of Q quickly caves in, meaning pulse splitting occurs and the two pulses now move apart from the center. In this new location, the presence of enough P causes Q to increase once again and the process repeats (Fig 3.5).

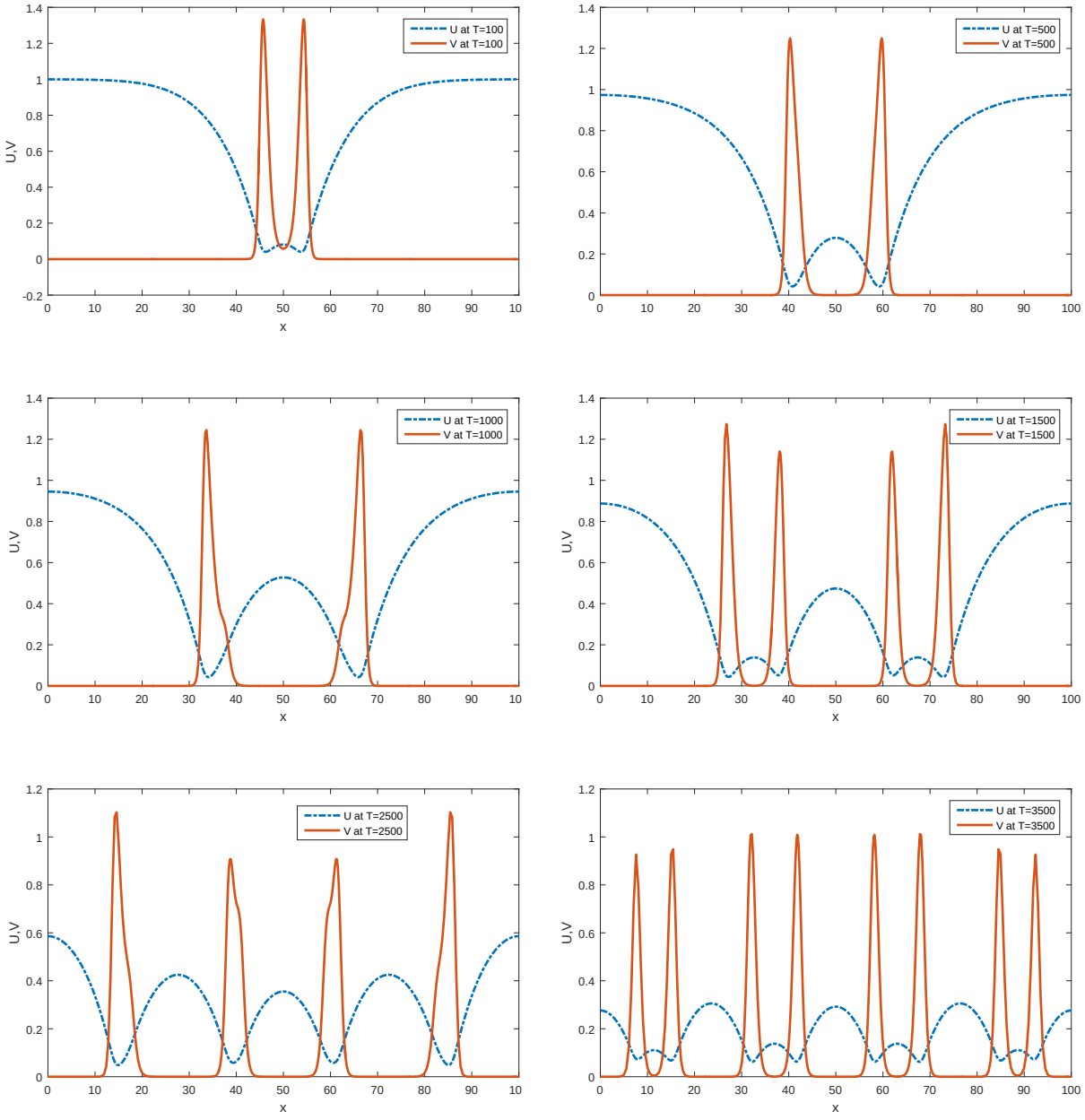

Figure 3.5: *The Gray Scott solution u, v for $d_u = 1$, $d_v = 0.01$, $\alpha = 0.01$,$\beta = 0.05$.*

The factor $uv - \beta$ is crucial for the growth of Q. Pulse splitting occurs when this factor becomes negative (Figs. 3.6 and 3.7). With this in mind, we note that parameter β affects

the processes of splitting. The smaller β quickens the splitting process and the larger β delays it (Fig. 3.8b). The effect of variation in α is the opposite but lesser than β's. This is due to the fact that α represents the rate of replenishment of P from the source, whereas the extraction rate is αu. Therefore, a net positive infusion of P occurs (Fig. 3.8a).

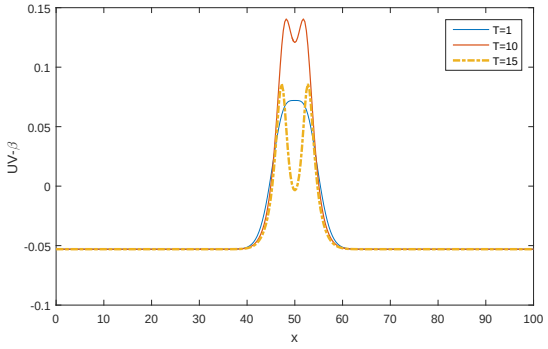

Figure 3.6: *Variation of $uv-\beta$ for different times taking $m = 200$, $d_u = 1$, $d_v = 0.01$, $\alpha = 0.01$,$\beta = 0.053$.*

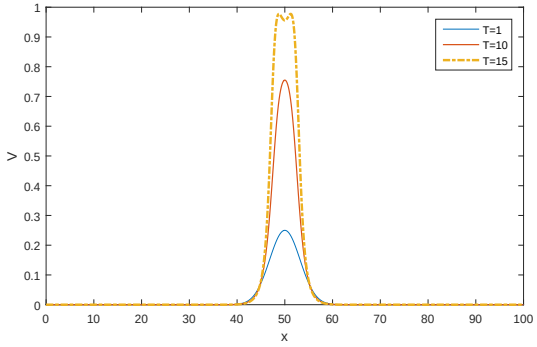

Figure 3.7: *Splitting of pulse (Q) at different times taking $m = 200$, $d_u = 1$, $d_v = 0.01$, $\alpha = 0.01$,$\beta = 0.053$.*

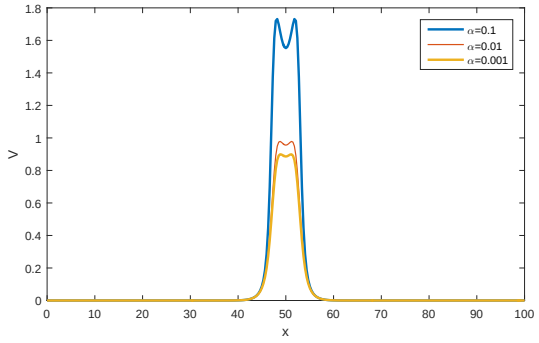

(a) *with respect to α, taking $\beta = 0.53$.*

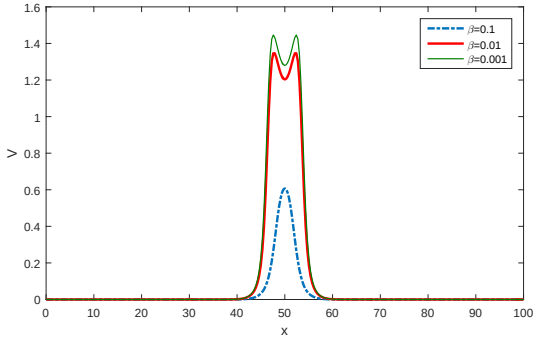

(b) *with respect to β, taking $\alpha = 0.01$*

Figure 3.8: *Effect of α and β on pulse splitting (V), taking $d_u = 1$, $d_v = 0.01$, $T = 15$, $m = 200$.*

Further, the diffusivity also affects the pulse splitting. If there is no diffusion of either chemical, then the process of splitting occurs much sooner than if there was a diffusion of chemicals. Because if there is no diffusion, the flux gradients will be sharper since the chemical P cannot move to fill in at the positions of high Q, therefore, caving in starts quickly (Fig. 3.4).

The benefits of non-uniform grid are briefly highlighted. In Table 3.4, CPU times (in seconds) for different data sets at several times are compared to show that the time taken

in uniform and non-uniform grids is almost the same, but the accuracy is far better in the case of non-uniform grids (Figs. 3.9a and 3.9b). If we treat the solution for $m = 800$ as the exact solution, then the error in the solution for $m = 400$ is negligible in case of non-uniform grids (Fig. 3.9a) whereas the error is considerable in the case of uniform grids (Fig. 3.9b).

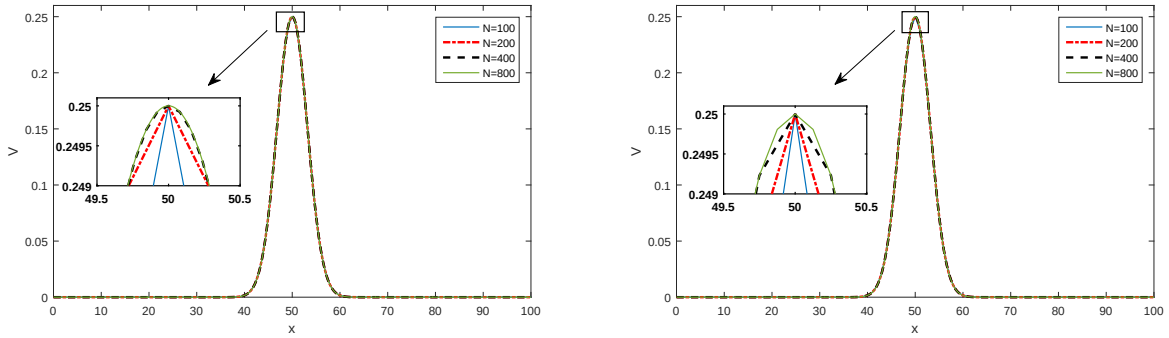

(a) *Non-uniform grid* ***(b)*** *Uniform grid*

Figure 3.9: *Q for different number of nodes under uniform grid taking* $d_u = 1$, $d_v = 0.01$, $\alpha = 0.01$,$\beta = 0.053$, $T = 1$.

In Figures 3.10a and 3.10b, peaks are plotted against t for two domains $\Omega = [0, 100]$ and $\Omega = [0, 200]$ respectively. It is observed that a large domain can sustain a large number of peaks.

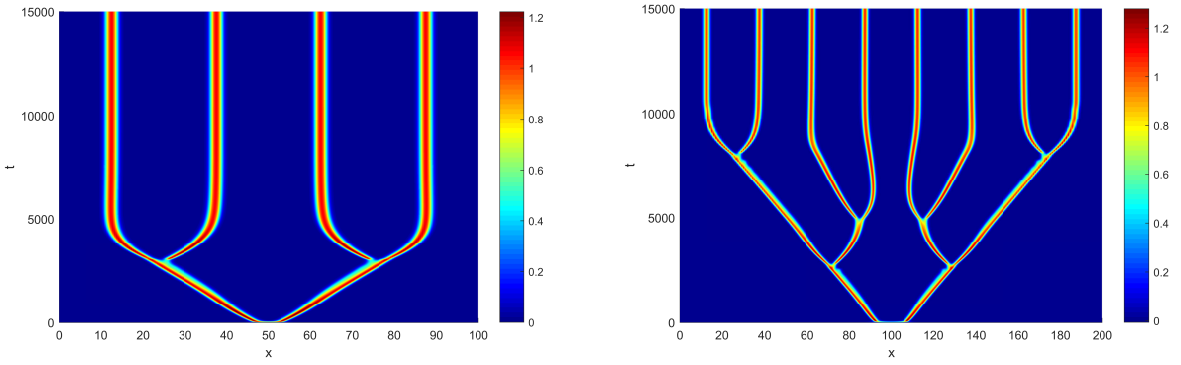

(a) $\Omega = [0, 100]$ ***(b)*** $\Omega = [0, 200]$

Figure 3.10: *Peak splitting of Gray Scott solution* v *in* Ω *taking* $d_u = 1$, $d_v = 0.01$, $\alpha = 0.01$,$\beta = 0.06$.

3.6.3 Brusselator Model

The Brusselator model represents a sequence of four irreversible chemical reactions viz. $S_1 \to P$, $S_2 + P \to Q + S_3$, $2P + Q \to 3P$ and $P \to S_4$. It is assumed that the chemicals S_1 and S_2 are available in abundance and the changes in their concentrations remain insignificant throughout the course of the experiment. Representing the concentrations of P and Q by u and v respectively, we have the following governing equations for the mechanism of these reactions

$$u_t - d_u u_{xx} = \alpha + u^2 v - \beta u - u,$$
$$v_t - d_v v_{xx} = -u^2 v + \beta u,$$

where $\alpha,\ \beta$ are some reaction parameters.

Following the scheme as pointed out in the previous example, we work out the matrix form of this system.

In contrast to the Gray-Scott model, the constraint on supply of either chemical in this model is non-existent. Therefore, the pulse splitting phenomenon observed in the Gray-Scott model is unavailable. However, an interesting phenomenon of oscillations of $u,\ v$ near the equilibrium point is observed. $(\alpha, \frac{\beta}{\alpha})$ is the equilibrium point for the system if $\beta < \alpha^2 + 1$ holds. The condition $\beta < \alpha^2 + 1$ is crucial for oscillations. If it holds, the system attain equilibrium. If the condition does not meet, the oscillations occur about $(\alpha, \frac{\beta}{\alpha})$ (Figs. 3.11a and 3.11b). In this model, another important observation is regarding diffusivity. In the Gray-Scott model, the diffusivity played a significant role for splitting; however, here the diffusivity has little effect on the equilibrium because of the abundant availability of chemicals. Figs. 3.12a and 3.12b plot the relative movement of chemicals $P,\ Q$ with respect to each other before reaching equilibrium.

Table 3.4: *Comparision of CPU times (Sec.) for uniform and non-uniform grids*

Grid type	$\alpha = 0.01,\ \beta = 0.053,\ d_u = 1,\ d_v = 0.01$				$\alpha = 0.01,\ \beta = 100.0,\ d_u = 1,\ d_v = 0.01$			
	$T = 1$	$T = 10$	$T = 50$	$T = 100$	$T = 1$	$T = 10$	$T = 50$	$T = 100$
Uniform	0.0335	0.184	0.847	1.680	0.0336	0.183	0.848	1.670
Non-uniform	0.0374	0.189	0.858	1.694	0.0373	0.189	0.856	1.684

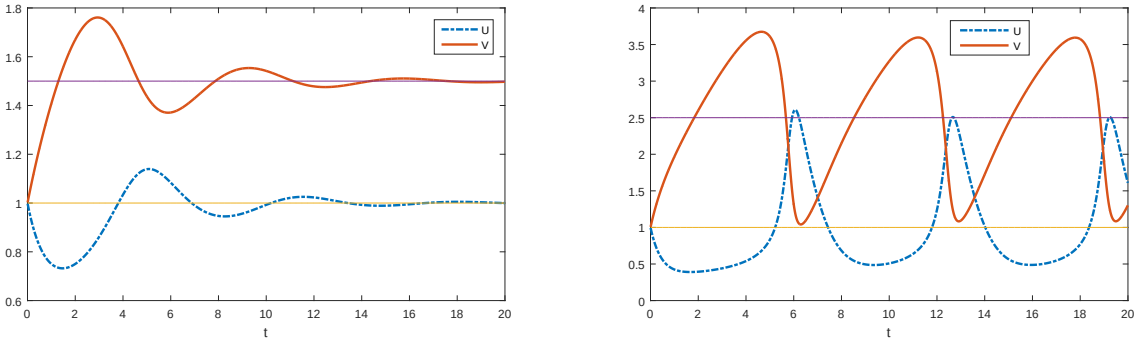

(a) $\beta = 1.5$ ***(b)*** $\beta = 2.5$

Figure 3.11: *Variation of* u, v *with time in* $\Omega = [0, 1]$ *taking* $U_0 = 1, V_0 = 1, d_u = 1$, $d_v = 1$, $\alpha = 1$.

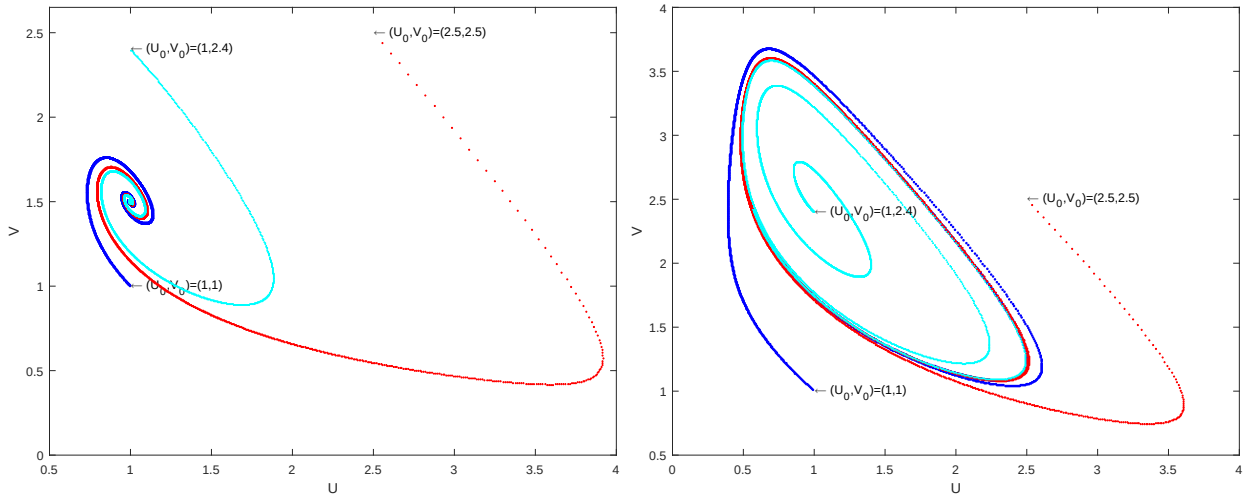

(a) $\beta = 1.5$ ***(b)*** $\beta = 2.5$

Figure 3.12: u *vs.* v *for time* $t \in [0, 20]$, $\Omega = [0, 1]$ *taking* $d_u = 1$, $d_v = 1$, $\alpha = 1$ *for different initial solution* U_0, V_0.

Chapter 4

Brusselator Model

In this chapter, we approximate solution to the Brusselator model when cross-diffusion is present. Since this model is a coupled reaction diffusion model for which the existence and uniqueness has been discussed in the previous chapter, therefore, we would not repeat that part. Instead, we would like to discuss the stability issues regarding the model since stability is particularly important for this model, which has been studied earlier for without cross-diffusion cases. Thus, we extend the stability analysis to the cross-diffusion cases in this chapter in Sec. 4.4. A priori error estimate for the approximation is presented in Sec. 4.3, though a priori error for coupled systems has been discussed in the previous chapter but a different approach is adopted here. Next, using C-N method with P-C scheme for discretization of time, we propose an algorithm for numerical simulation of the solution in Sec. 4.5. Lastly, some numerical examples are considered in Sec. 4.5 to illustrate the efficiency and accuracy of the method and to plot the Turing patterns of the model.

4.1 Introduction

The phenomenon of chemical oscillations like iodine clock reaction, Belousov Zhabotinsky(BZ) reaction *etc.* is remarkable and fascinating. If one of chemicals has visible color, then after crossing a certain concentration threshold, the color of chemical composition abruptly changes. The first homogeneous isothermal chemical oscillation was observed by William C. Bray in 1921 [16]. However, it was contested and refuted at the time, for a misunderstanding that it is against the second law of thermodynamics, which says that the entropy of any isolated system must increase. The entropy of any system at equilibrium

is considered the maximum. Therefore, if oscillations were to occur, entropy can not be always increasing. Later, the lacunae in this argument was found and it was observed that the oscillating system never passes through its equilibrium state. We take up this issue further in numerical simulations section. Later, chemical oscillations were studied in detail and several oscillating reactions were discovered. For instance, Lotka-Volterra model which is a oscillating population model of prey (yeast) and predator (paramecia), Bray reaction, Briggs Rauscher reaction, BZ reaction and its many variants. A crucial element in these oscillating reactions is involvement of process of auto-catalysis. Auto-catalysis process occurs when a chemical changes its concentration by itself. In such reactions some reagents are also products in the reaction.

Brusselator model is also an oscillating auto-catalytic model, which was proposed by Prigogine and Lefever in 1968. The model is a series of chemical reactions [94],

$$P \xrightarrow{a} X,\ Q + X \xrightarrow{b} Y + R,\ 2X + Y \xrightarrow{\lambda_1} 3X,\ X \xrightarrow{\lambda_2} S \tag{4.1}$$

where $P,\ Q,\ R,\ S,\ X,\ Y$ represent some chemicals. The numbers written over arrows represent the rate of that reaction. We may observe that the chemicals $X,\ Y$ are reagents as well as products, that is, these chemicals are auto-catalytic and play a major role in oscillation of the reaction. Therefore, these chemicals are our main objects of study. An illustration of the Brusselator model is the BZ reaction which is composed of several reactions, but the essence of these intermediate reactions can be summarized in the following processes,

(a) reduction of bromate to bromine, the bromide ion acts as the reducing agent

$$BrO_3^- + 5Br^- + 6H^+ \rightarrow 3Br_2 + 3H_2O, \tag{4.2}$$

(b) when the concentration of the bromide ion Br^- becomes low, cerium catalyst gets converted to its oxidized form. This is a consequence of auto-catalysis.

$$BrO_3^- + 3H^+ + 2Ce(III) + HBrO_2 \rightarrow 2Ce(IV) + 2HBrO_2 + H_2O. \tag{4.3}$$

Sharp color change is witnessed.

(c) Third process includes

$$Ce(IV) + CHBr(COOH)_2 \rightarrow Ce(III) + Br^- + other\ products. \tag{4.4}$$

(4.3) is auto-catalyzed by BrO_3^- and strongly inhibited by Br^- ions [61]. As reaction (4.3) takes place $Ce(IV)$ is produced, which pushes more production of Br^- from reaction (4.4) and that causes slowing down of reaction (4.3). This slow down of (4.3) results in reduction of Br^- production and when Br^- becomes low, reaction (4.3) again gets activated. The whole process of auto-catalysis results in chemical oscillations.

Taking concentrations of chemicals $P,\ Q,\ R,\ S$ fixed throughout the reaction process and assuming that u and v represent the concentrations of the chemicals X and Y respectively, we may write equations of the rate of change of u, v as

$$u_t = a - bu + \lambda_1 u^2 v - \lambda_2 u, \tag{4.5}$$

$$v_t = bu - \lambda_1 u^2 v. \tag{4.6}$$

We see here that there is no diffusion involved in these equations. The equilibrium point for the equations (4.5)-(4.6) can be obtained by setting $u_t = 0 = v_t$, which comes out to be $\left(\frac{a}{\lambda_2}, \frac{b\lambda_2}{a\lambda_1}\right)$. Eigenvalue analysis reveals that for $\lambda_1 = 1 = \lambda_2$, if $b < 1 + a^2$, the equilibrium point is stable and unstable otherwise. If the diffusion of these auto-catalytic chemicals be allowed then stable equilibrium may become unstable. This diffusion induced instability is called the *Turing instability*.

In this chapter, we see how diffusion and cross-diffusion affects stability of equilibrium point. The system under consideration is the following,

$$u_t - (d_{11}\Delta u + d_{12}\Delta v) = a - bu + \lambda_1 u^2 v - \lambda_2 u, \tag{4.7}$$

$$v_t - (d_{21}\Delta u + d_{22}\Delta v) = bu - \lambda_1 u^2 v, \tag{4.8}$$

$$\frac{\partial u}{\partial \boldsymbol{n}} = 0 = \frac{\partial v}{\partial \boldsymbol{n}}, \tag{4.9}$$

$$u(\boldsymbol{x}, 0) = u_0(\boldsymbol{x}),\ v(\boldsymbol{x}, 0) = v_0(\boldsymbol{x}), \tag{4.10}$$

where d_{11} and d_{22} denote the diffusion coefficients for the chemical X and Y respectively; d_{12} is the cross-diffusion coefficient of chemical X in the presence of chemical Y and sim-

ilarly d_{21} represents the cross-diffusion coefficient of chemical Y due to the presence of chemical X; a, b, λ_1 and λ_2 are the rate of chemical reactions describing Brusselator model as depicted in Eq. (4.1).

The term "Brusselator" was coined by Tyson [118], combining Brussels and oscillator. Prigogine and Lefever belonged to Brussels school. Though some qualitative analysis was done for the model in 1970's, but the first approximate solution was given by Adomian in terms of a series of Adomian polynomials using decomposition method in 1995 taking only initial solution [1]. This was followed by Twizell proposing a second order finite difference scheme to approximate the solution for given homogenous Neumann conditions in a rectangular domain [117]. Ang extended this result to arbitrary domain by boundary element method [6]. Twizell argued that the behavior of reaction terms in the model are important for numerical treatment. Preying upon this idea, Kang analyzed when these reaction terms are bounded and when they are not [61]. This model has also been discussed and simulated by several other techniques such as finite difference scheme [26], meshfree technique developed by collocation method using radial basis functions [119], variational multiscale element free Galerkin (VMEFG) and local discontinuous Galerkin (LDG) methods [24] *etc.* Differential quadrature method with polynomial basis was applied in [83] for approximation of the solution, this was improved further by using modified cubic B-splines in [53]. Recently, Alqahtani [3] extended the discussion using modified trigonometric B-splines and studied different types of patterns of the model. Lin et al. introduced cross-diffusion in the inhomogeneous Brusselator model and applied finite volume element method to approximate the solution and to depict beautiful pattern formation [72].

In this regard, we see that the stability analysis has very limited literature that too for diffusion only. Further, cross-diffusion is recently introduced. We try to discuss these topics in this chapter. Since the system under consideration is a coupled system and is similar to the system discussed in the previous Chapter, the existence may be referred to that Chapter.

4.2 Weak Formulation

The weak formulation to the problem (4.7)-(4.8) with boundary and initial conditions (4.9)-(4.10), is obtained by multiplying the equations (4.7) and (4.8) by some function (called test function) $\phi \in H^1(\Omega)$ and then integrating w.r.t. space variable x over Ω. The use of

integration by parts together with homogeneous Neumann boundary condition (4.9) yield the following weak formulation:
We say that functions (u, v) such that

$$u,\ v \in L^2(0,T;H^1(\Omega)) \text{ with } u',\ v' \in L^2(0,T;L^2(\Omega))$$

is a weak solution of (4.7)-(4.10) if

$$(u',\phi) + d_{11}(\nabla u, \nabla\phi) + d_{12}(\nabla v, \nabla\phi) = (f(u,v),\phi),\ \forall\phi \in H^1(\Omega), \tag{4.11}$$

$$(v',\phi) + d_{21}(\nabla u, \nabla\phi) + d_{22}(\nabla v, \nabla\phi) = (g(u,v),\phi),\ \forall\phi \in H^1(\Omega), \tag{4.12}$$

where

$$f(u,v) = a - bu + \lambda_1 u^2 v - \lambda_2 u, \text{and } g(u,v) = bu - \lambda_1 u^2 v, \tag{4.13}$$

and

$$u(0,x) = u_0(x),\ v(0,x) = v_0(x). \tag{4.14}$$

Here, u' represents derivative of u with respect to t.

Theorem 4.2.1. *Suppose $u \in L^2(0,T;X)$ with $u' \in L^2(0,T;X)$. Then $u \in C([0,T];X)$ and*

$$\max_{0\le t\le T} ||u(t)||_X \le K(||u||_{L^2(0,T;X)} + ||u'||_{L^2(0,T;X)}),$$

for some positive constant K.

Proof. See [30], Chapter 5. ∎

Taking $X = L^2(\Omega)$, by Theorem 4.2.1, we see Eq. (4.14) makes sense.

4.3 A Priori Error Estimate

We find from Theorem 4.2.1 that $C([0,T];L^2(\Omega))$ is our solution space, let us call it $\mathcal{S}$, which is infinite dimensional space since all polynomials are members of it. We intend to approximate the solution $(u,v) \in \mathcal{S}\times\mathcal{S}$ in a finite dimensional space. Therefore, we take a subspace V_m, say, of $\mathcal{S}$. V_m satisfies (1.7).
Suppose u_m and v_m are the approximations of u and v in V_m, then u_m and v_m satisfy

(4.11)-(4.12). Since V_m is a finite dimensional space, we can choose a basis for it. Choosing the Lagrange hat functions $\{\phi_i\}_{i=1}^m$as basis functions, we may write u_m and v_m as,

$$u_m(t) = \sum_{i=1}^{m} c_i(t)\phi_i,\ v_m(t) = \sum_{i=1}^{m} d_i(t)\phi_i,$$

where $c_i(t)$ and $d_i(t)$ are unknown vectors. Since u_m and v_m satisfy (4.11)-(4.12), we have,

$$\sum_{i=1}^{N}(\phi_i,\phi_j)\frac{d}{dt}c_i(t) + d_{11}\sum_{i=1}^{N}(\nabla\phi_i,\nabla\phi_j)c_i(t) + d_{12}\sum_{i=1}^{N}(\nabla\phi_i,\nabla\phi_j)d_i(t) = \left(f\left(\sum_{i=1}^{N}c_i(t)\phi_i, \sum_{i=k}^{N}d_k(t)\phi_k\right),\phi_j\right), \tag{4.15}$$

$$\sum_{i=1}^{N}(\phi_i,\phi_j)\frac{d}{dt}d_i(t) + d_{21}\sum_{i=1}^{N}(\nabla\phi_i,\nabla\phi_j)c_i(t) + d_{22}\sum_{i=1}^{N}(\nabla\phi_i,\nabla\phi_j)d_i(t) = \left(g\left(\sum_{i=1}^{N}c_i(t)\phi_i, \sum_{i=k}^{N}d_k(t)\phi_k\right),\phi_j\right). \tag{4.16}$$

Clearly, Eqs. (4.15)-(4.16) are first order ordinary differential equations. From (4.13), we see that if u and v are bounded, f and g can be rendered Lipschitz continuous. Therefore, the functions u_m and v_m exist [46].

Theorem 4.3.1. *Suppose u, v are the solutions of (4.11)-(4.12). Let u_m, v_m denote the Galerkin approximations of u, v. Further assume that $||u(t)||_{L^\infty} < K_1, ||u'(t)||_{L^\infty} < K_2, ||u'_m(t)||_{L^\infty} < K_3, ||v(t)||_{L^\infty} < K_4, ||v'(t)||_{L^\infty} < K_5, ||v'_m(t)||_{L^\infty} < K_6$, and the Lipschitz constants for f and g are $\mathscr{L}_1$ and $\mathscr{L}_2$, that is,*

$$|f(u,v) - f(U,V)| \leq \mathscr{L}_1(|u-U| + |v-V|),$$
$$|g(u,v) - g(U,V)| \leq \mathscr{L}_2(|u-U| + |v-V|).$$

Then,

$$||u(t)-u_m(t)||^2 + ||v(t)-v_m(t)||^2 \leq K_c\left(||u(0)-u_m(0)||^2 + ||v(0)-v_m(0)||^2\right) + K_u(a,b,\lambda_1,\lambda_2,T,$$
$$\mathscr{L}_1,\mathscr{L}_2)h^2(1+h^2)\int_0^T ||u(s)||_2^2 ds + K_v(a,b,\lambda_1,\lambda_2,T,\mathscr{L}_1,\mathscr{L}_2)h^2(1+h^2)\int_0^T ||v(s)||_2^2 ds,$$

where K_u and K_v are some positive constants depending only on T and the parameters of

the model.

Proof. u_m and v_m satisfy the following equations,

$$(u_m', \phi_m) + d_{11}(\nabla u_m, \nabla \phi_m) + d_{12}(\nabla v_m, \nabla \phi_m) = (f(u_m, v_m), \phi_m), \ \forall \phi_m \in V_m, \tag{4.17}$$

$$(v_m', \phi_m) + d_{21}(\nabla u_m, \nabla \phi_m) + d_{22}(\nabla v_m, \nabla \phi_m) = (g(u_m, v_m), \phi_m), \ \forall \phi_m \in V_m. \tag{4.18}$$

Since V_m is contained in $\mathcal{S}$, we may take ϕ in (4.11) as ϕ_m, similarly in (4.12). Now subtracting (4.17) from (4.11) and (4.18) from (4.12), we get

$$\begin{aligned}((u-u_m)', \phi_m) + d_{11}(\nabla(u-u_m), \nabla\phi_m) + d_{12}(\nabla(v-v_m), \nabla\phi_m)& \\ = (f(u,v) - f(u_m, v_m), \phi_m),& \qquad (4.19)\\ ((v-v_m)', \phi_m) + d_{21}(\nabla(u-u_m), \nabla\phi_m) + d_{22}(\nabla(v-v_m), \nabla\phi_m)& \\ = (g(u,v) - g(u_m, v_m), \phi_m).& \qquad (4.20)\end{aligned}$$

Suppose U, V are some other elements in V_m, which may not be solutions of (4.11), (4.12) respectively. Then, taking $\phi_m = U - u_m$ in (4.19) and $\phi_m = V - v_m$ in (4.20). Further, writing $U - u_m$ as $(u - u_m) + (U - u)$ and using Cauchy-Schwartz inequality, we obtain,

$$\begin{aligned}\frac{1}{2}\frac{d}{dt}||u-u_m||^2 + d_{11}||\nabla(u-u_m)||^2 \leq\ & ||u'-u_m'||||U-u|| + d_{11}||\nabla(u-u_m)||||\nabla(U-u)|| \\ & + d_{12}||\nabla(v-v_m)||||\nabla(u-u_m)|| + d_{12}||\nabla(v-v_m)||||\nabla(U-u)|| + \mathscr{L}_1(||u-u_m||^2 \\ & + ||v-v_m||||u-u_m|| + ||u-u_m||||U-u|| + ||v-v_m||||U-u||). \qquad (4.21)\end{aligned}$$

Similarly, writing $V - v_m$ as $(v - v_m) + (V - v)$, we get

$$\begin{aligned}\frac{1}{2}\frac{d}{dt}||v-v_m||^2 + d_{22}||\nabla(v-v_m)||^2 \leq\ & ||v'-v_m'||||V-v|| + d_{21}||\nabla(u-u_m)||||\nabla(v-v_m)|| \\ & + d_{21}||\nabla(u-u_m)||||\nabla(v-V)|| + d_{22}||\nabla(v-v_m)||||\nabla(V-v)|| + \mathscr{L}_2(||u-u_m||||v-v_m|| \\ & + ||v-v_m|||^2 + ||u-u_m||||V-v|| + ||v-v_m||||V-v||). \qquad (4.22)\end{aligned}$$

Adding (4.21) and (4.22), and using Young inequality, we get

$$\frac{1}{2}\frac{d}{dt}(||u-u_m||^2 + ||v-v_m||^2) + d_{11}||\nabla(u-u_m)||^2 + d_{22}||\nabla(v-v_m)||^2$$

$$\leq ||u'-u'_m||||U-u||+||v'-v'_m||||V-v||+\Big[\mathscr{L}_1\Big(1+\frac{\epsilon_7}{2}+\frac{1}{2\epsilon_8}\Big)$$
$$+\mathscr{L}_2\Big(1+\frac{\epsilon_{10}}{2}+\frac{1}{2\epsilon_{11}}\Big)\Big]||u-u_m||^2+\Big(\frac{d_{11}}{2\epsilon_1}+\frac{d_{12}\epsilon_2}{2}+\frac{d_{21}\epsilon_3}{2}+\frac{d_{21}}{2\epsilon_5}\Big)||\nabla(u-u_m)||^2$$
$$+\Big[\mathscr{L}_1\Big(\frac{1}{2\epsilon_7}+\frac{1}{2\epsilon_9}\Big)+\mathscr{L}_2\Big(\frac{1}{2\epsilon_{10}}+\frac{1}{2\epsilon_{12}}\Big)\Big]||v-v_m||^2+\Big(\frac{d_{12}}{2\epsilon_2}+\frac{d_{21}}{2\epsilon_3}+\frac{d_{22}}{2\epsilon_4}+\frac{d_{12}}{2\epsilon_6}\Big)||\nabla(v-v_m)||^2$$
$$+\Big[\mathscr{L}_1\Big(\frac{\epsilon_8}{2}+\frac{\epsilon_9}{2}\Big)+\mathscr{L}_2\Big(\frac{\epsilon_{11}}{2}+\frac{\epsilon_{12}}{2}\Big)\Big]||U-u||^2+\Big(\frac{d_{11}\epsilon_1}{2}+\frac{d_{12}\epsilon_6}{2}\Big)||\nabla(U-u)||^2$$
$$+\Big[\mathscr{L}_1\Big(\frac{\epsilon_3}{2}+\frac{\epsilon_7}{2}\Big)+\mathscr{L}_2\Big(\frac{\epsilon_5}{2}+\frac{\epsilon_{10}}{2}\Big)\Big]||V-v||^2+\Big(\frac{\epsilon_4 d_{22}}{2}+\frac{\epsilon_5 d_{21}}{2}\Big)||\nabla(V-v)||^2. \quad (4.23)$$

Now a term by term treatment yields, $||u'-u'_m||||U-u||\leq (K_2+K_3)||U-u||$ and $||v'-v'_m||||V-v||\leq (K_5+K_6)||V-v||$. Making appropriate choices for $\epsilon's$, the terms $d_{11}||\nabla(u-u_m)||$ and $d_{22}||\nabla(v-v_m)||$ cancel out from both the sides of (4.23). Further, suppose of maximum of coefficients of $||u-u_m||^2$ and $||v-v_m||$ is K_m. And lastly, U and V are elements from V_m, therefore, we may take them as interpolants of u and v respectively. From literature [113], we have the following error estimates for these choices of U, V

$$||U-u||+h||\nabla(U-u)||\leq Kh^2||u||_2,$$

for $u\in H^2$. Similarly for V.

Using all this information in (4.23), we have the following highly simplified form of (4.23),

$$\frac{d}{dt}\left(e^{-K_m t}||u-u_m||^2+||v-v_m||^2\right)\leq K_u h^2(1+h^2)||u||_2+K_v h^2(1+h^2)||v||_2.$$

Integrating from 0 to T, we obtain the desired estimate. ∎

4.4 Stability Analysis

To study the stability of system (4.7)-(4.9), we apply the concept of linear analysis [67]. The linearized system can be put in the form $\mathcal{U}_t=(\boldsymbol{D}+\boldsymbol{A})\mathcal{U}$, that is

$$\begin{pmatrix} u_t \\ v_t \end{pmatrix}=\left(\begin{pmatrix} d_{11}\Delta & d_{12}\Delta \\ d_{21}\Delta & d_{22}\Delta \end{pmatrix}+\begin{pmatrix} f_u & f_v \\ g_u & g_v \end{pmatrix}_{(u_0,v_0)}\right)\begin{pmatrix} u \\ v \end{pmatrix},$$

where (u_0, v_0) is the equilibrium point of diffusionless system (4.7)-(4.8), given by $\left(\frac{a}{\lambda_2}, \frac{b\lambda_2}{a\lambda_1}\right)$. To find out eigenvalues of the above system, we consider the following trial solution,

$$\mathcal{U}(t, \boldsymbol{x}) \propto e^{\lambda(k)t} e^{i\boldsymbol{k}.\boldsymbol{x}},$$

where $k^2 = \boldsymbol{k}.\boldsymbol{k}$ represents the modulus of the wave vector. This yields the following characteristic equation,

$$\begin{vmatrix} f_u - d_{11}k^2 - \lambda & f_v - d_{12}k^2 \\ g_u - d_{21}k^2 & g_v - d_{22}k^2 - \lambda \end{vmatrix} = 0,$$

which can be simplified as

$$\lambda^2 + a_1\lambda + a_2 = 0, \tag{4.24}$$

where $a_1 = (d_{11} + d_{22})k^2 - f_u - g_v$ and $a_2 = (d_{11}d_{22} - d_{12}d_{21})k^4 - (g_v d_{11} + f_u d_{22} - f_v d_{21} - g_u d_{12})k^2 + f_u g_v - f_v g_u$. Note that $f_u,\ f_v,\ g_u,\ g_v$ are all evaluated at (u_0, v_0). There will be two roots of equation (4.24), say $\lambda_1,\ \lambda_2$. If $\max\{\lambda_1,\ \lambda_2\} < 0$ or real parts of the roots $Re(\lambda_i) < 0$, $i = 1, 2$, we have the stable equilibrium point. Therefore, we see the onset of instability will occur at $\lambda = 0$, whence $a_2 = 0$, that is for those k's such that

$$(d_{11}d_{22} - d_{12}d_{21})k^4 - (g_v d_{11} + f_u d_{22} - f_v d_{21} - g_u d_{12})k^2 + f_u g_v - f_v g_u = 0. \tag{4.25}$$

To get a unique wave number for onset of instability, we must have the discriminant of equation (4.25) zero, hence

$$(g_v d_{11} + f_u d_{22} - f_v d_{21} - g_u d_{12})^2 = 4(d_{11}d_{22} - d_{12}d_{21})(f_u g_v - f_v g_u). \tag{4.26}$$

The roots of Eq. (4.25) are given by $-\frac{B}{2A} \pm \frac{\sqrt{D}}{2A}$, where $A,\ B$ are coefficients of k^4 and k^2 respectively in Eq. (4.25) and D represents the discriminant of it, which is zero by Eq. (4.26), therefore

$$k^2 = \frac{g_v d_{11} + f_u d_{22} - f_v d_{21} - g_u d_{12}}{2(d_{11}d_{22} - d_{12}d_{21})}. \tag{4.27}$$

Since, $f_u = 2\lambda_1 uv - b - \lambda_2$, $f_v = \lambda_1 u^2$, $g_u = b - 2\lambda_1 uv$ and $g_v = -\lambda_1 u^2$. At the point of equilibrium, these values will be $f_u = b - \lambda_2$, $f_v = a^2\frac{\lambda_1}{\lambda_2^2}$, $g_u = -b$ and $g_v = -a^2\frac{\lambda_1}{\lambda_2^2}$. Using

these values in (4.27) and making use of (4.26), we have $k^2 = \frac{a\sqrt{\lambda_1/\lambda_2}}{\sqrt{d_{11}d_{22}-d_{12}d_{21}}}$. Clearly, if $d_{12} = 0 = d_{21}$, then $k^2 = \frac{a\sqrt{\lambda_1/\lambda_2}}{\sqrt{d_{11}d_{22}}}$ which is lesser than the former. Therefore, the wave number increases when the cross-diffusion is present.

4.5 Numerical Demonstrations and Discussions

Taking $\lambda_1 = 1 = \lambda_2$, the two-dimensional Brusselator model under consideration is:

$$u_t - d_{11}\Delta u - d_{12}\Delta v = a - (b+1)u + u^2 v, \tag{4.28}$$

$$v_t - d_{21}\Delta u - d_{22}\Delta v = bu - u^2 v, \tag{4.29}$$

with initial conditions (4.10) and homogeneous Neumann boundary conditions (4.9), $(x, y) \in \Omega,\ t \in [0, T]$. The weak formulation of this model is given by:

$$(u_t, \phi) + d_{11}(\nabla u, \nabla\phi) + d_{12}(\nabla v, \nabla\phi) = (a, \phi) - (b+1)(u, \phi) + (u^2 v, \phi),$$
$$(v_t, \phi) + d_{21}(\nabla u, \nabla\phi) + d_{22}(\nabla v, \nabla\phi) = b(u, \phi) - (u^2 v, \phi),\ \forall\ \phi \in H^1(\Omega).$$

Taking a Lagrange basis of linear continuous polynomials, we find the solution in finite dimensional space. To do that, we convert this weak formulation into matrix form,

$$Ac' + d_{11}Bc + d_{12}Bd = aD - (b+1)Ac + p(c, d),$$
$$Ad' + d_{21}Bc + d_{22}Bd = bAc - Q(c)d.$$

Applying Crank-Nicolson method at $t = t^{k-\frac{1}{2}}$, we get

$$\left(\frac{A}{dt} + d_{11}\frac{B}{2} + (b+1)\frac{A}{2}\right)c^k = \left(\frac{A}{dt} - d_{11}\frac{B}{2} - (b+1)\frac{A}{2}\right)c^{k-1} + aD - d_{12}Bd^{k-1/2} + f,$$
$$\left(\frac{A}{dt} + d_{22}\frac{B}{2} + \frac{E(c)}{2}\right)d^k = \left(\frac{A}{dt} - d_{22}\frac{B}{2} - \frac{E(c)}{2}\right)d^{k-1} + (bA - d_{21}A)c^{k-1/2},$$

where matrices A, B and others can be calculated by inner product method as pointed out in earlier chapters.

To resolve the problem of non-linearity involved in f and E, predictor corrector method is used. The following algorithm is proposed,

(i) find c^p by replacing $c^{1/2}$, $d^{1/2}$ with c^0, d^0, to be obtained from the initial profile,

(ii) find d^p by replacing $c^{1/2}$ with $\frac{c^0+c^p}{2}$,

(iii) find c^1 by replacing $c^{1/2}$, $d^{1/2}$ with $\frac{c^0+c^p}{2}$, $\frac{d^0+d^p}{2}$ respectively,

(iv) find d^1 by replacing $c^{1/2}$ with $\frac{c^0+c^1}{2}$,

(v) find c^2 by replacing $c^{3/2}$, $d^{3/2}$ with $\frac{3c^1-c^0}{2}$, $\frac{3d^1-d^0}{2}$ respectively,

(vi) find d^2 by replacing $c^{3/2}$ with $\frac{c^1+c^2}{2}$,

repeating steps (v) and (vi), we reach to any time level.

Example 1.

As a first example, we take the model (4.28)-(4.29) without cross diffusion and with following initial profiles [82]

$$u_0(x, y) = 0.5 + y,$$
$$v_0(x, y) = 1.0 + 5x,$$

with $a = 1,\ b = 3.4$ and $d_{11} = 0.002 = d_{22},\ d_{12} = 0 = d_{21}$. Clearly, $b > 1 + a^2$, hence convergence does not occur and oscillations are seen in Fig. 4.1, 4.7 and Table 4.1. We may observe that the solutions u and v show a periodic repetition after every six seconds (t=6). This may be seen from Fig 4.1. The particular choices of d_{11} and d_{22} are to make the 3D demonstration of $u,\ v$ pleasing to eye, otherwise, low or high diffusivity causes the flux gradients to become sharper or flatter. Fig. 4.2 plots solution u versus v at point points $(0.3, 0.7)$ and $(0.6, 0.4)$. The figure shows that the solution pair (u, v) never passes through equilibrium point $(a, b/a)$. Clearly, when u is a; b is far away from b/a. This is the reason why oscillations are permitted as no law of thermodynamics stands violated. Had the solution pair passed through the equilibrium point, the entropy of the system could not have an always increasing nature thereby making a case for violation of second law thermodynamics.

Example 2.

Taking same initial profiles as in previous example, we change a and b to make this time the condition of stability true. Therefore, we take $a = 2,\ b = 1$ and $d_{11} = 0.002 = d_{22},\ d_{12} = 0 = d_{21}$. Clearly, $b < 1 + a^2$, hence the solution converges to the equilibrium point $(2, 0.5)$ which may be seen in Figure 4.4 and Table 4.2.

Example 3.

In this example, we consider the Brusselator model (4.28)-(4.29) with initial conditions,

$$u_0(x, y) = \frac{1}{2}x^2 + \frac{1}{3}y^3,$$
$$v_0(x, y) = \frac{1}{2}y^2 + \frac{1}{3}x^3.$$

Taking parameters $a = 1$, $b = \frac{1}{2}$ and $d_{11} = 0.002 = d_{22},\ d_{12} = 0 = d_{21}$, we see the condition of convergence is met, hence convergence is possible, which is evident in Fig. 4.5 and Table 4.3.

Example 4.

For $a = 0,\ b = 1$, $d_{11} = \frac{1}{4} = d_{22},\ d_{12} = 0 = d_{21}$, an exact solution to (4.28)-(4.29) is given by [53]

$$u(x, y, t) = e^{-x-y-\frac{1}{2}t},$$
$$v(x, y, t) = e^{x+y+\frac{1}{2}t}.$$

Taking initial profile from the exact solution, we test the accuracy and rate of convergence of the proposed scheme. The result are plotted in Fig. 4.6 and are tabulated in Tables 4.4-4.6. Figure 4.6 and Table 4.4 show that the solution converges to the equilibrium point $(0, \infty)$. Fig. 4.3 shows the second order convergence for L^∞ error as well as for relative error. Tables 4.5 and 4.6 compare L^∞ and relative errors respectively for u, v with the collocation method having multiquadric (MQ) radial basis function and thin plate spline (TPS) radial basis functions [119]. The results by the proposed scheme are better than TPS. Moreover, the rate of convergence of MQ is very slow, whereas the proposed scheme

gives a consistent second order convergence.

Example 5.

In this example, we have considered cross-diffusion Brusselator model with $a = 6$, $b = 1$, $d_{11} = 0.4$, $d_{12} = 24$, $d_{21} = 0.02$, $d_{22} = 2$ and a randomized initial profile [72]:

$$u_0(x, y) = 5.8 + \frac{1}{3}\text{rand}(x),$$
$$v_0(x, y) = 0.13 + \frac{1}{10}\text{rand}(x).$$

Through this example we demonstrate that the cross-diffusion driven patterns predominate the initial patterns and therefore even starting with some random initial structure the final patterns that emerge are intermix of spots and stripes.

The approximations u_m and v_m are plotted in Fig. 4.8. Evidently, the randomness in the initial solution settles down and an equilibrium pattern appears. These patterns are very similar to the patterns obtained in earlier works [24].

Table 4.1: *Approximate solution u, v at different points. Parameters:* $\Omega = [0, 1] \times [0, 1]$, $h = \frac{1}{64}$, $\Delta t = 0.008$, $a = 1$, $b = 3.4$, $d_{11} = 0.002 = d_{22}, d_{21} = 0 = d_{12}$.

$(x, y) \rightarrow$	(0.2,0.3)		(0.6,0.6)		(0.7,0.4)	
$t \downarrow$	u	v	u	v	u	v
1	0.3170	3.0156	0.8439	3.2690	3.2312	1.4597
2	0.3005	3.7299	0.6672	3.5402	1.6068	1.7114
3	0.3262	4.3949	0.4303	4.1423	0.5870	2.7854
5	0.4682	5.4855	0.4270	5.2682	0.3355	4.2497
7	1.8689	1.5311	3.6852	0.9001	0.4368	5.3233
9	0.3413	3.5219	0.4902	2.9096	2.7502	1.1383
$\downarrow$	$\downarrow$	$\downarrow$	$\downarrow$	$\downarrow$	$\downarrow$	$\downarrow$
∞	-	-	-	-	-	-

Table 4.2: *Approximate solution u, v at different points. Parameters: $\Omega = [0,1] \times [0,1]$, $h = \frac{1}{64}$, $\Delta t = 0.008$, $a = 2$, $b = 1$, $d_1 = 0.002 = d_2$.*

$(x, y) \rightarrow$	(0.2,0.3)		(0.6,0.6)		(0.7,0.4)	
$t \downarrow$	u	v	u	v	u	v
1	2.4995	0.4558	2.9387	0.3283	3.5450	0.2723
2	2.1761	0.4490	2.2880	0.4230	2.4995	0.3849
3	2.0449	0.4840	2.0760	0.4743	2.1413	0.4564
5	2.0019	0.4992	2.0034	0.4986	2.0071	0.4971
7	2.0001	0.5000	2.0001	0.5000	2.0002	0.4999
9	2.0000	0.5000	2.0000	0.5000	2.0000	0.5000
$\downarrow$	$\downarrow$	$\downarrow$	$\downarrow$	$\downarrow$	$\downarrow$	$\downarrow$
∞	2.0	0.5	2.0	0.5	2.0	0.5

Table 4.3: *Approximate solution u, v at different points. Parameters: $\Omega = [0,1] \times [0,1]$, $h = \frac{1}{64}$, $\Delta t = 0.008$, $a = 1$, $b = 0.5$, $d_1 = 0.002 = d_2$.*

$(x, y) \rightarrow$	(0.2,0.3)		(0.6,0.6)		(0.7,0.4)	
$t \downarrow$	u	v	u	v	u	v
1	0.5390	0.2020	0.5895	0.3567	0.6149	0.3370
2	0.7135	0.3954	0.7688	0.4943	0.7740	0.4817
3	0.8305	0.5068	0.8883	0.5449	0.8864	0.5386
5	0.9788	0.5284	0.9998	0.5179	0.9974	0.5184
7	1.0065	0.5026	1.0057	0.4995	1.0056	0.4999
9	1.0017	0.4989	1.0006	0.4991	1.0007	0.4991
$\downarrow$	$\downarrow$	$\downarrow$	$\downarrow$	$\downarrow$	$\downarrow$	$\downarrow$
∞	1.0	0.5	1.0	0.5	1.0	0.5

Table 4.4: *Approximate solution u, v at different points. Parameters:* $\Omega = [0,1] \times [0,1]$, $h = \frac{1}{64}$, $\Delta t = 0.008$, $a = 0$, $b = 1$, $d_1 = 0.002 = d_2$

$(x, y) \rightarrow$	(0.2,0.3)		(0.6,0.6)		(0.7,0.4)	
$t \downarrow$	u	v	u	v	u	v
1	0.3689	2.7741	0.2243	4.5509	0.2240	4.5364
2	0.2234	4.5162	0.1356	7.4320	0.1355	7.4229
3	0.1354	7.4101	0.0822	12.2086	0.0821	12.2031
5	0.0498	20.0932	0.0302	33.1250	0.0302	33.1230
7	0.0183	54.6009	0.0111	90.0205	0.0111	90.0198
9	0.0067	148.4139	0.0041	244.6926	0.0041	244.6925
$\downarrow$	$\downarrow$	$\downarrow$	$\downarrow$	$\downarrow$	$\downarrow$	$\downarrow$
∞	0	∞	0	∞	0	∞

Table 4.5: *Comparision of L^∞ errors with collocation method. Parameters:* $\Omega = [0,1] \times [0,1]$, $T = 2$, $a = 0$, $b = 1$, $d_{11} = \frac{1}{4} = d_{22}$, $d_{12} = 0 = d_{21}$

Present Method							MQ [119]		TPS [119]	
m	h	Δt	u	v	m	Δt	u	v	u	v
81	0.125	0.001	8.34e-5	1.50e-3	100	0.001	5.20e-6	2.86e-7	7.64e-5	3.68e-3
289	0.0625	0.005	2.11e-5	3.74e-4	400	0.005	2.64e-6	1.45e-7	2.35e-5	1.28e-3
1089	0.03125	0.01	3.86e-6	9.13e-5	900	0.01	1.81e-6	7.94e-7	9.03e-6	5.95e-4

Table 4.6: *Comparision of relative errors u^r with collocation method. Parameters:* $\Omega = [0,1] \times [0,1]$, $T = 2$, $a = 0$, $b = 1$, $d_{11} = \frac{1}{4} = d_{22}$, $d_{21} = 0 = d_{12}$

Present Method							MQ [119]		TPS [119]	
m	h	Δt	u	v	N	Δt	u	v	u	v
81	0.125	0.001	2.53e-4	8.16e-5	100	0.001	9.89e-6	9.53e-6	2.98e-4	2.29e-4
289	0.0625	0.005	6.75e-5	2.22e-5	400	0.005	4.49e-6	4.41e-6	2.12e-5	2.04e-5
1089	0.03125	0.01	1.28e-5	5.65e-6	900	0.01	2.85e-6	2.61e-6	6.89e-6	6.95e-6

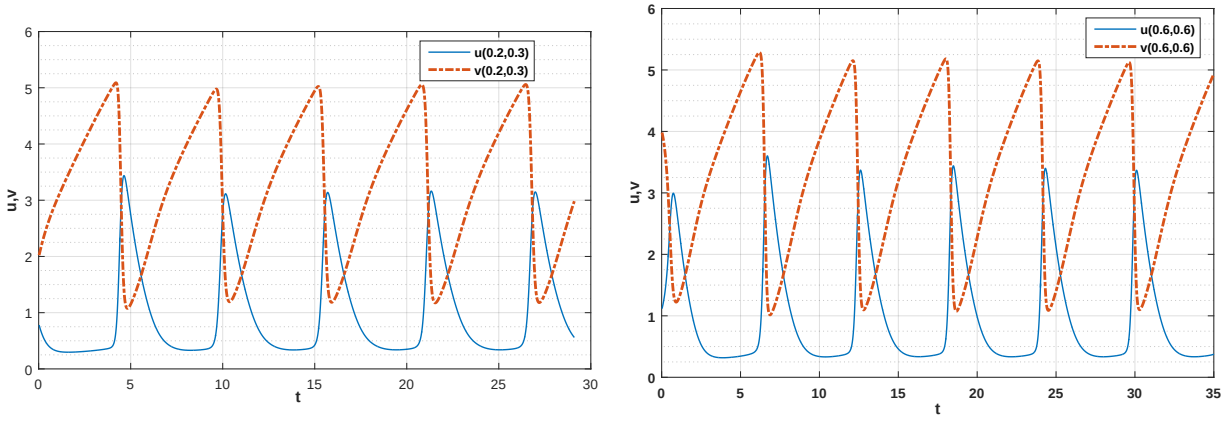

Figure 4.1: *Convergence of approximate solution* u, v *at* $(x, y) = (0.2, 0.3)$ *(left),* $(x, y) = (0.6, 0.6)$ *(right)*

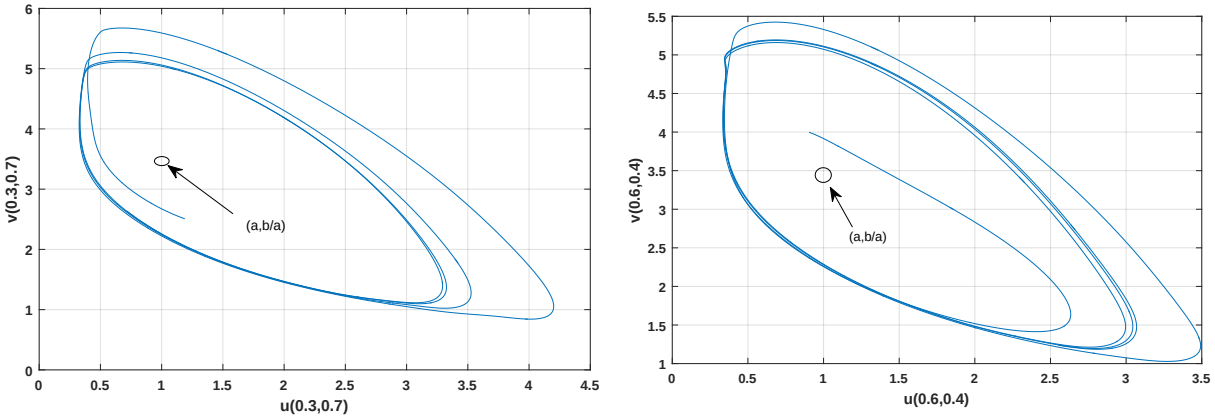

Figure 4.2: *u versus v at* $(x, y) = (0.3, 0.7)$ *(left),* $(x, y) = (0.6, 0.4)$ *(right)*

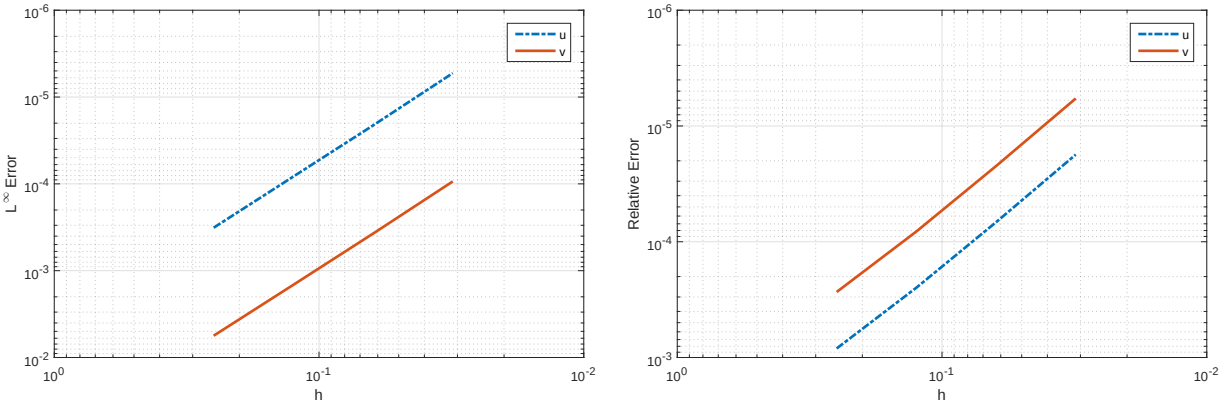

Figure 4.3: *Order of convergence of approximate solution* u, v *of* L^{∞} *error (left), relative error (right)*

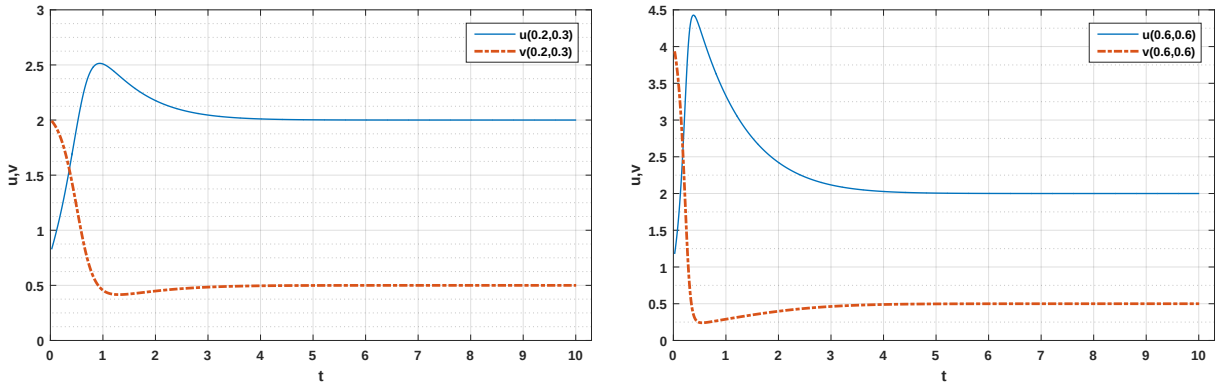

Figure 4.4: *Convergence of approximate solution* u, v *at* $(x, y) = (0.2, 0.3)$ *(left),* $(x, y) = (0.6, 0.6)$ *(right)*

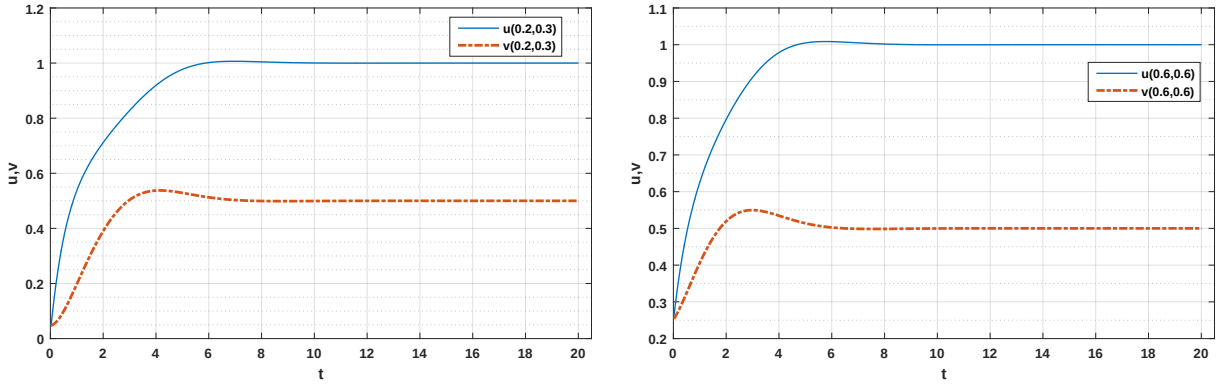

Figure 4.5: *Convergence of approximate solution* u, v *at* $(x, y) = (0.2, 0.3)$ *(left),* (b) $(x, y) = (0.6, 0.6)$ *(right)*

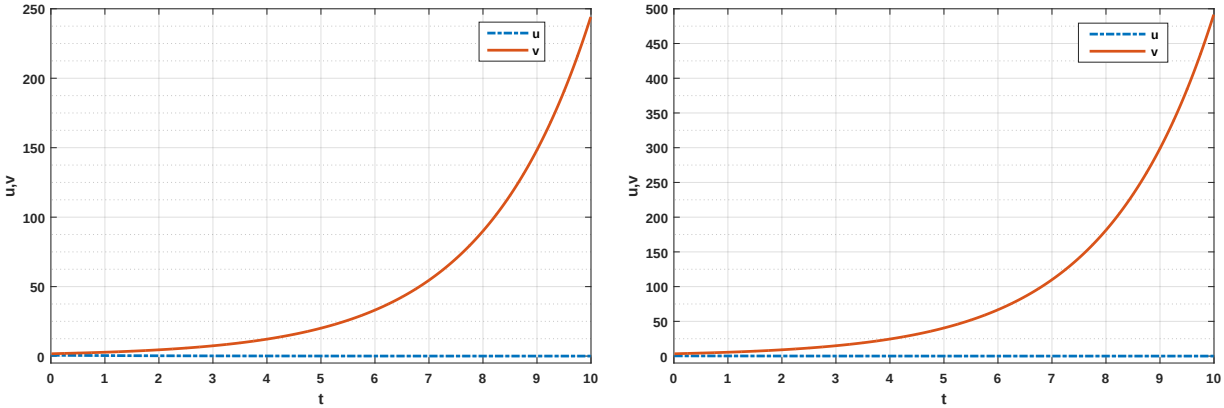

Figure 4.6: *Convergence of approximate solution* u, v *at* $(x, y) = (0.2, 0.3)$ *(left),* $(x, y) = (0.6, 0.6)$ *(right)*

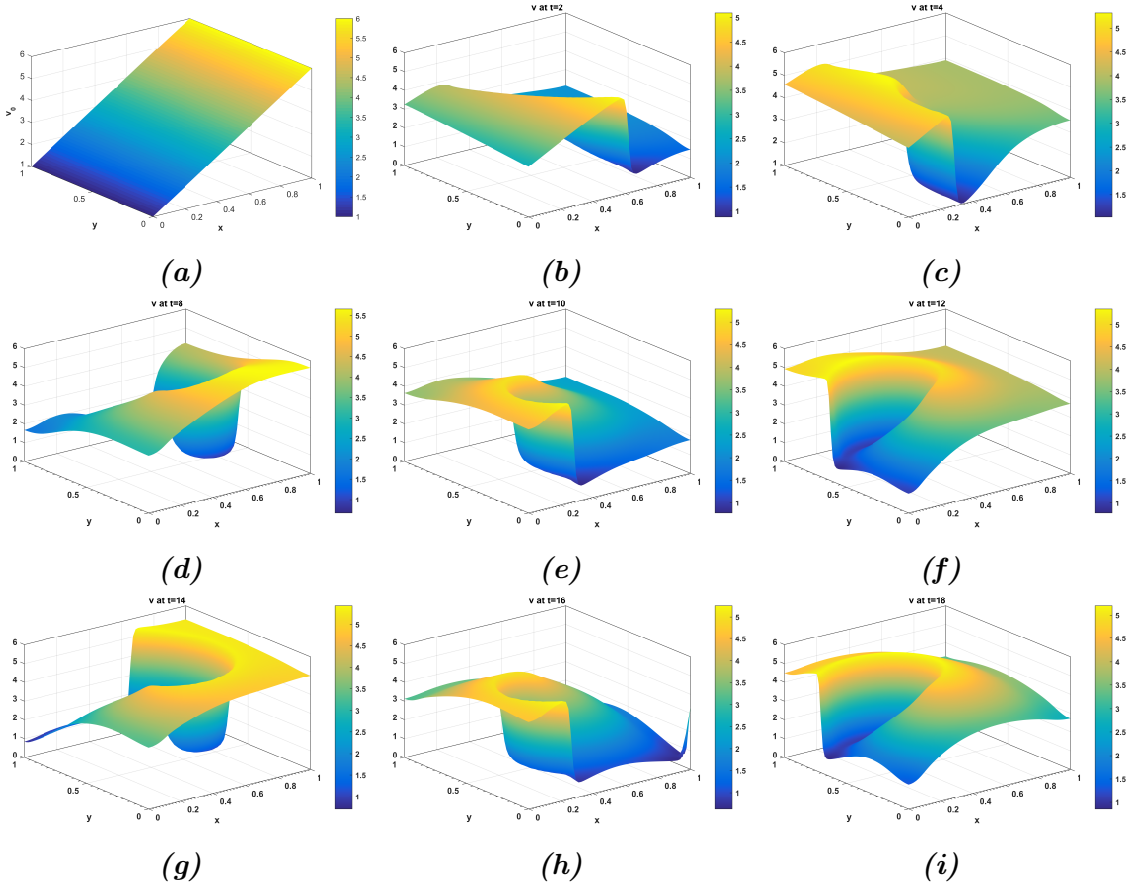

Figure 4.7: *Approximations v at different times for Example 1. Parameters:* $a = 1$, $b = 3.4$, $d_{11} = 0.002 = d_{22}$, $d_{12} = 0 = d_{21}$, $\Omega = [0,1] \times [0,1]$, $\Delta t = 0.008$, $h = 1/64$

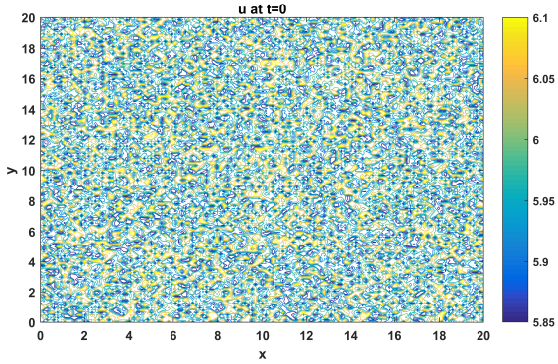

(a)

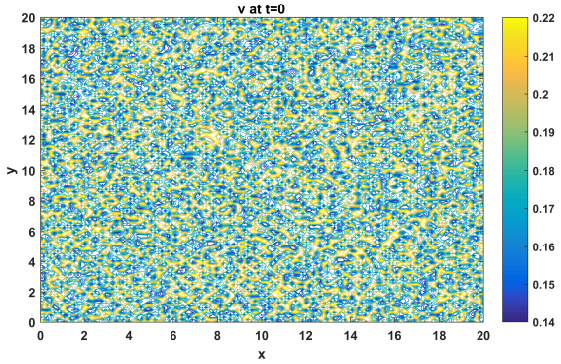

(b)

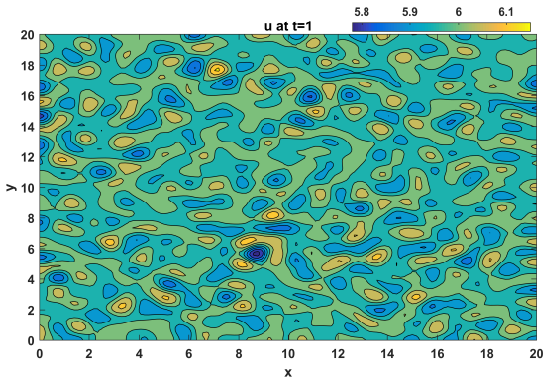

(c)

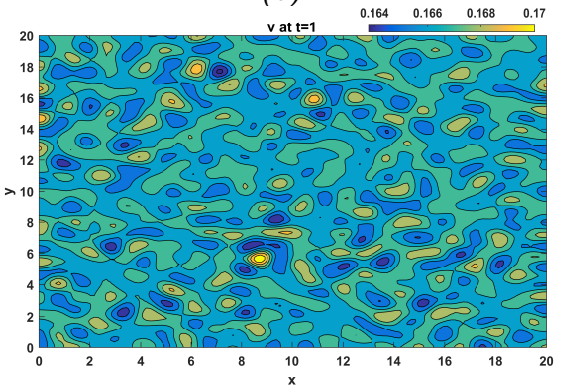

(d)

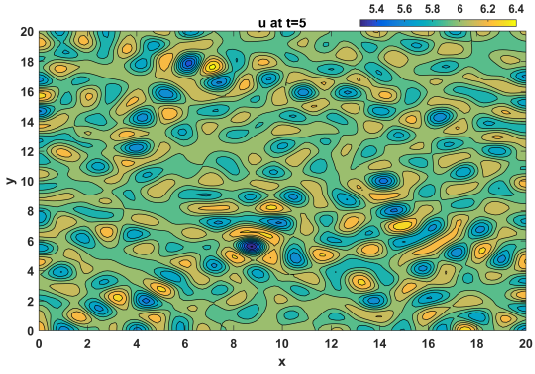

(e)

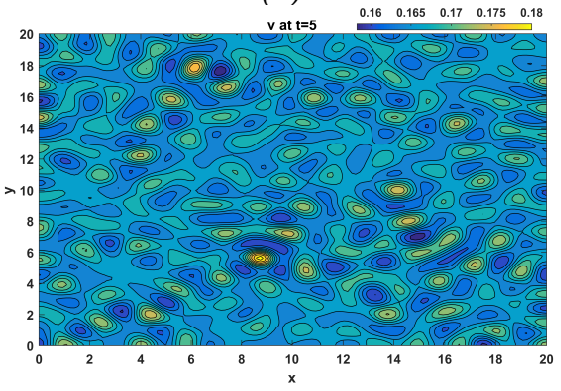

(f)

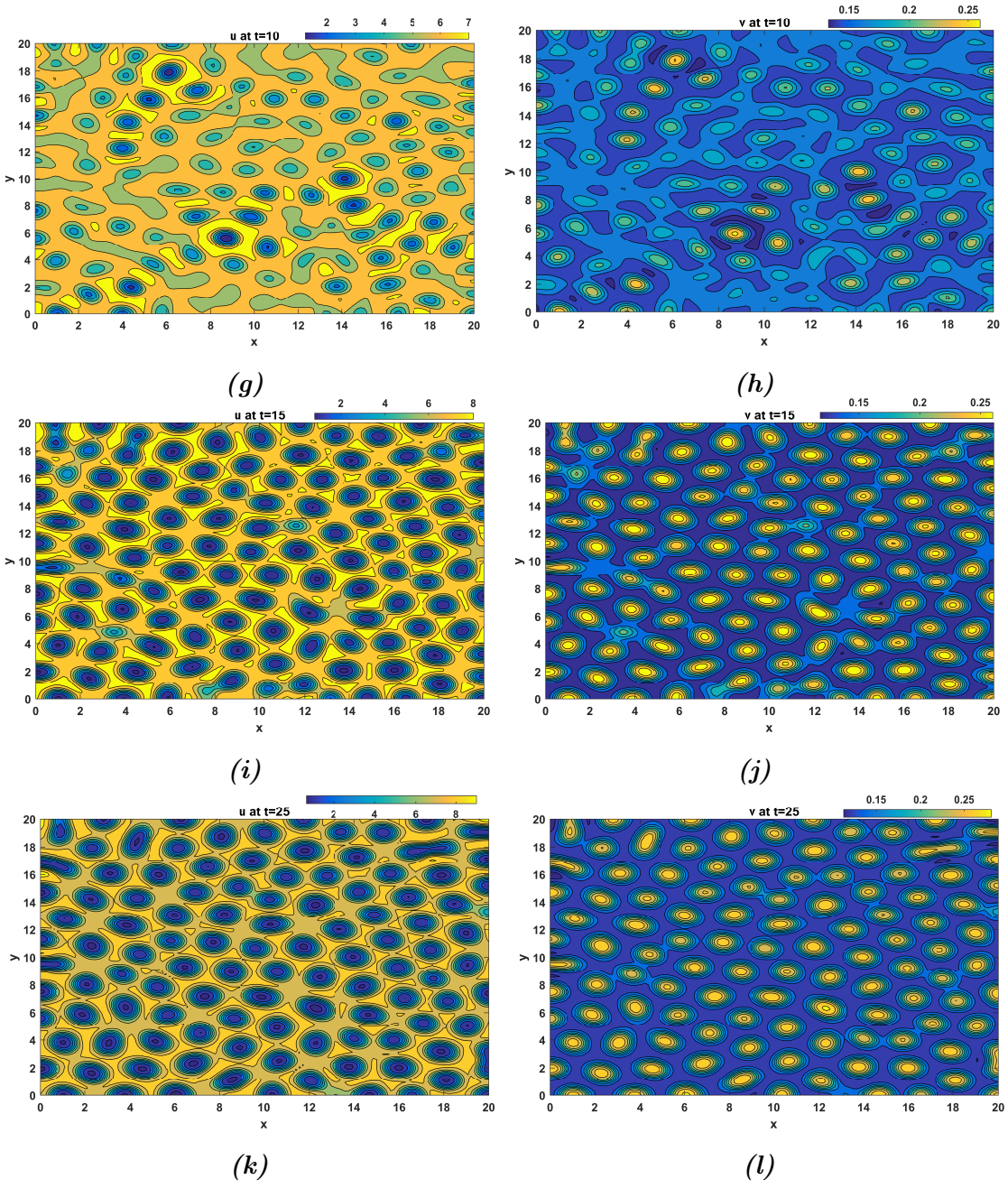

Figure 4.8: *The approximations u (left) and v (right) at different times for Example 5, Parameters: $a = 6$, $b = 1$, $d_{11} = 0.4$, $d_{12} = 24$, $d_{21} = 0.02$, $d_{22} = 2$, $\Delta t = 0.005$, $h = 1/128$.*

Chapter 5

Schrödinger Equation

In this chapter, we study some soliton-type analytical solutions of Schrödinger equation, with their numerical treatment by Galerkin finite element method. Since the equation yields a coupled system of reaction diffusion model (RDM) on separating real and imaginary parts and the analytical questions relating to existence and uniqueness *etc.* of RDM has already been discussed at length in the earlier chapters, therefore, we would not discuss such issues here. Instead, we focus on soliton solution of the equation which is particularly important for the equation. Thus, some analytical solutions to the equation are obtained for different values of parameters in Sec. 5.2, thereafter the problem of truncating infinite domain to finite interval is taken up in Sec. 5.3 and truncation approximations are worked out for finding out appropriate intervals so that information is not lost while reducing the domain. The benefit of domain truncation is that we do not need to introduce artificial boundary conditions to find out numerical approximations. To verify theoretical results, numerical simulations are performed by Galerkin finite element method in Sec. 5.4. C-N method is used for the time discretization and non-linearity is resolved using P-C method, which is second order accurate and computationally efficient.

5.1 Introduction

Just as Newton's second law of motion is important to predict the path taken by a physical system under some given initial conditions, so is important the Schrödinger equation to quantum theory of matter to study the changes over time of a physical system possessing quantum effects such as wave-particle duality. It was named after Erwin Schrdinger, who

derived the equation in 1925 and published it in general form in 1926 [103]. One example of this equation has wide ranging applications and hence has attracted much attention from the mathematical research community. The example possesses cubic non-linearity and is given by the following equation, for an open subset Ω of $\mathbb{R}$,

$$\frac{1}{i}\frac{\partial u}{\partial t} - \frac{\partial^2 u}{\partial x^2} + \nu|u|^2 u = 0, \ (t,x) \in (0,T] \times \Omega, \tag{5.1}$$

where $i = \sqrt{-1}$, ν is some real parameter and the complex function $u(t,x)$ governs the evolution of slowly varying waves in a stable dispersive physical system with little dissipation, for example waves in deep water [90]. The Eq. (5.1) is supplemented with sufficiently smooth initial condition $u(0,x) = u_0(x)$ and boundary conditions $u(t,x) = 0$ on $\partial\Omega$.

This equation has applications in optical pulses, plasma physics, water waves, particle-in-a-box, harmonic oscillator, hydrogen atom, rigid rotator and bimolecular dynamics *etc.* [7, 90]. Existence of solution is discussed in literature in two cases — when $\nu \geq 0$ and when $\nu < 0$. For $\nu \geq 0$, Pazy (see [93], page 233) has given existence and uniqueness of global solution for $u_0(x) \in H^2(\Omega)$. For $\nu < 0$, a soliton-type analytical solution is derived by Scott *et al.* [104]. Zakharov and Shabat [125, 126] derived soliton-type analytical solution for $\nu < 0$ (self-focusing) and $\nu > 0$ (de-focusing) for an initial condition $u(t_0,x) = f(x)$, where $u_x(t_0,x) \to 0$ for $|x| \to \infty$. These solutions are valid under the localized traveling wave assumption. Another soliton-type solution for $\nu = -1$ is obtained by Argyris and Haase [7] for $u, \ u_x \to 0$ whenever $|x| \to \infty$. Some other authors also have solved the equations analytically using several other techniques, for example, inverse scattering transformation, Bäcklund and Darboux transformations, bilinear and Lie group methods [75, 89], symbolic computation aided transformations [80], representation of solution in terms of Volterra series [43]. The solutions obtained by these methods are often too complicated and involved. This acts as a constraint on their applicability to physical situations. However, the soliton solutions have fairly simple form. Therefore, in the first part of this chapter, we obtain soliton solutions of the equation for all cases of parameters.

Due to involvement of non-linearity, either the exact solutions are not possible to obtain or these are too complicated to derive any physical significance out of them. Most of the solutions obtained so far have some particular form like soliton-type. Numerical solutions provide a way out of this situation. Different methods and techniques are used to find out

numerical solutions of the equation to sufficient degree of accuracy. In this order, some of the important works include finite difference method [121], Petrov-Galerkin finite element method [7], discontinuous Galerkin method [74], local discontinuous Galerkin method [47], adaptive Galerkin method [9], improved complex variable moving least-squares Ritz method [127], cubic B-spline functions based collocation method [33], modified cubic B-spline differential quadrature method [11], quadratic B-spline finite element method [22], orthogonal spline collocation method [98], differential quadrature method [64], dynamic adaptive wavelet method [13].

Ismail [50] discussed stability and accuracy of Galerkin finite element solution of this kind of equations. He used Newton's method to resolve non-linearity in the equation. However, as may be noticed the method is quite involved and computationally costly. Petrov-Galerkin method used in [7] to solve the equation is a non-conforming method, that is, the space in which the solution is approximated may not be a subspace of the original solution space. Petrov-Galerkin method is suitable for the differential equations which have odd order spatial derivatives. In such a case, the test space and the solution space may not be the same. However, the Eq. (5.1) does not involve odd order space derivatives. Therefore, the hardship and the extra computational cost incurred while applying Petrov variant of Galerkin method is not compensated for. On the contrary, classical Galerkin method is easy to work with and offers fairly good accuracy.

To overcome the cubic non-linearity involved in the equation, several techniques are used in literature, for instance, the Euler modified method, lagging the non-linearity to previous known level *etc.* These techniques are only first order accurate which makes the calculation inefficient. Therefore some more efficient second order accurate techniques like Newton's method (secant scheme) are better suited for good results [50]. Further, the extra cost of computation involved in Newton's method is minimized by using the P-C scheme, which is also second order accurate.

5.2 Some Soliton-Type Analytical Solutions

Before, we proceed to find out analytic solutions to the equation, it is important to state a comprehensive result by Pazy [93] about existence and uniqueness of global solution of Eq. (5.1).

Theorem 5.2.1. *Let $u_0(x) \in H^2(\mathbb{R}^2)$. If $\nu \geq 0$ then the initial value problem (5.1) with $u(0,x) = u_0(x)$ has a unique global solution $u \in C([0,\infty); H^2(\mathbb{R}^2)) \cap C^1([0,\infty); L^2(\mathbb{R}^2))$.*

Proof. See [93], page 233. ∎

In order to obtain an analytical solution, we set $u(t,x) = \mathscr{U}(t,x)e^{i(ax+bt)}$ in Eq. (5.1),

$$-b\mathscr{U}e^{i(ax+bt)} + i\mathscr{U}_t e^{i(ax+bt)} + \mathscr{U}_{xx}e^{i(ax+bt)} + 2ia\mathscr{U}_x e^{i(ax+bt)} - a^2\mathscr{U}e^{i(ax+bt)} - \nu\mathscr{U}^3 e^{i(ax+bt)} = 0.$$

Equating real and imaginary parts to zero separately, we have

$$-b\mathscr{U} + \mathscr{U}_{xx} - a^2\mathscr{U} - \nu\mathscr{U}^3 = 0, \tag{5.2}$$

and

$$\mathscr{U}_t + 2a\mathscr{U}_x = 0. \tag{5.3}$$

Eq. (5.3) is a transport equation, the solution to which may be given in terms of a function as,

$$\mathscr{U} = \mathcal{U}(x - 2at). \tag{5.4}$$

Plugging in $\mathscr{U}$ from Eq. (5.4) into Eq. (5.2), for $\xi = x - 2at$, we have

$$\mathcal{U}_{\xi\xi} = k_1\mathcal{U} + \nu\mathcal{U}^3, \tag{5.5}$$

where $k_1 = b + a^2$. Multiplying Eq. (5.5) by $\mathcal{U}_\xi$ and integrating w.r.t. ξ, we obtain,

$$\mathcal{U}_\xi^2 = k_1\mathcal{U}^2 + \frac{\nu}{2}\mathcal{U}^4. \tag{5.6}$$

Since u and u_x goes to zero as $|x| \to \infty$, we take constant of integration as zero.

Case 1: $\nu = 0$

This case reduces Eq. (5.1) to a linear partial differential equation for which solution may be easily worked out by some technique, for example, separation of variables technique.

Case 2: $k_1 \geq 0,\ \nu > 0$

For this case, we follow from Eq. (5.6) that,

$$\frac{d\mathcal{U}}{\mathcal{U}\sqrt{2k_1 + \nu\mathcal{U}^2}} = \frac{d\xi}{\sqrt{2}}.$$

Substitution $\mathcal{U} = \sqrt{\frac{2k_1}{\nu}}\tan\theta$ yields,

$$\begin{aligned}
\csc\theta d\theta &= \sqrt{k_1}d\xi, \\
\implies \csc\theta + \cot\theta &= e^{-\sqrt{k_1}\xi}, \\
\implies \frac{\sqrt{2k_1 + \nu\mathcal{U}^2} + \sqrt{2k_1}}{\sqrt{\nu}\mathcal{U}} &= e^{-\sqrt{k_1}\xi}, \\
\implies \mathcal{U} &= \sqrt{\frac{2k_1}{\nu}}\text{csch}(-\sqrt{k_1}\xi).
\end{aligned}$$

From Eq. (5.4), $\mathscr{U} = \sqrt{\frac{2k_1}{\nu}}\text{csch}\left(-\sqrt{k_1}(x-2at)\right)$. Finally, the solution becomes

$$u(t,x) = \sqrt{\frac{2k_1}{\nu}}\text{csch}\left(-\sqrt{k_1}(x-2at)\right)e^{i(ax+bt)},$$

where $k_1 = b + a^2$.

Case 3: $k_1 \geq 0,\ \nu < 0$

Replacing ν by $-\lambda$ in Eq. (5.6),

$$\frac{d\mathcal{U}}{\mathcal{U}\sqrt{2k_1 - \lambda\mathcal{U}^2}} = \frac{d\xi}{\sqrt{2}}.$$

Substitution $\mathcal{U} = \sqrt{\frac{2k_1}{\lambda}}\sin\theta$ yields,

$$\begin{aligned}
\csc\theta d\theta &= \sqrt{k_1}d\xi. \\
\implies \csc\theta + \cot\theta &= e^{-\sqrt{k_1}\xi}, \\
\implies \frac{\sqrt{2k_1} + \sqrt{2k_1 - \lambda\mathcal{U}^2}}{\sqrt{\lambda}\mathcal{U}} &= e^{-\sqrt{k_1}\xi}, \\
\implies \mathcal{U} &= \sqrt{\frac{2k_1}{\lambda}}\text{sech}\left(\sqrt{k_1}\xi\right).
\end{aligned}$$

Therefore, the solution in this case is

$$u(t,x) = \sqrt{\frac{2k_1}{\lambda}}\text{sech}\left(\sqrt{k_1}(x-2at)\right)e^{i(ax+bt)}, \tag{5.7}$$

where $k_1 = b + a^2$.

Case 4: $k_1 < 0,\ \nu > 0$

Replacing k_1 by $-m_1$ in Eq. (5.6),

$$\frac{d\mathcal{U}}{\mathcal{U}\sqrt{\nu\mathcal{U}^2 - 2m_1}} = \frac{d\xi}{\sqrt{2}}.$$

Substitution $\mathcal{U} = \sqrt{\frac{2m_1}{\nu}}\sec\theta$ yields,

$$d\theta = \sqrt{m_1}d\xi.$$
$$\implies \mathcal{U} = \sqrt{\frac{2m_1}{\nu}}\sec(\sqrt{m_1}\xi).$$

Thus, the solution becomes,

$$u(t,x) = \sqrt{\frac{2m_1}{\nu}}\sec\left(\sqrt{k_1}(x-2at)\right)e^{i(ax+bt)},$$

where $k_1 = b + a^2$.

Remark: It may be noted that these cases are exhaustive since $k_1 < 0,\ \nu < 0$ is not possible from Eq. (5.6).

5.3 Truncation of Domain

The boundary conditions $u,\ u_x \to 0$ for $|x| \to \infty$ need to be replaced by some boundary conditions on a finite interval. For example, Wang and Liang [121] achieved this by introducing artificial boundary conditions. The solution (5.7) is a soliton solution which diminishes fast as $|x|$ becomes large. We utilize this fact and try to observe that how big an interval we need to consider for making sure that $|u| < \epsilon$, for some given small $\epsilon > 0$.

From (5.7), $|u|< \epsilon$ implies

$$\text{sech}\left(\sqrt{k_1}(x-2at)\right) < \epsilon\sqrt{\frac{\lambda}{2k_1}}. \tag{5.8}$$

Taking $k_1 \neq 0$, since $k_1 = 0$ may be considered separately and $|u_x|< \epsilon$ implies

$$\sqrt{a^2 + k_1\text{tanh}^2\left(\sqrt{k_1}(x-2at)\right)}\ \text{sech}\left(\sqrt{k_1}(x-2at)\right) < \epsilon\sqrt{\frac{\lambda}{2k_1}}. \tag{5.9}$$

If $\sqrt{a^2 + k_1\text{tanh}^2\left(\sqrt{k_1}(x-2at)\right)} \geq 1$, the Eq. (5.9) is redundant and we proceed with Eq. (5.8). In this case, using expansion of sech upto two terms,

$$1 - \frac{1}{2}k_1(x-2at)^2 < \epsilon\frac{\lambda}{2k_1},$$

$$\text{or} \qquad 2at - \sqrt{\frac{2}{k_1} - \frac{\epsilon\lambda}{k_1^2}} < x < 2at + \sqrt{\frac{2}{k_1} - \frac{\epsilon\lambda}{k_1^2}}.$$

If ϵ is arbitrarily small, then $2at - \sqrt{\frac{2}{k_1}} < x < 2at + \sqrt{\frac{2}{k_1}}$.
If $\sqrt{a^2 + k_1\text{tanh}^2\left(\sqrt{k_1}(x-2at)\right)} < 1$, then Eq. (5.8) is redundant and we may proceed with Eq. (5.9). Since, $\sqrt{k_1}\text{tanh}\left(\sqrt{k_1}(x-2at)\right) < \sqrt{a^2 + k_1\text{tanh}^2\left(\sqrt{k_1}(x-2at)\right)}$, we have from Eq. (5.9),

$$\text{tanh}\left(\sqrt{k_1}(x-2at)\right)\text{sech}\left(\sqrt{k_1}(x-2at)\right) < \frac{\epsilon}{k_1}\sqrt{\frac{\lambda}{2}}.$$

Using expansions for tanh and sech upto second degree,

$$2at - \epsilon\sqrt{\frac{\lambda}{2k_1^3}} < x < 2at + \epsilon\sqrt{\frac{\lambda}{2k_1^3}}.$$

5.4 Numerical Demonstrations and Discussions

In this section, we find out numerical solution of Eq. (5.1). First, we split the solution into real and imaginary parts, that is, $u(t,x) = u_1(t,x) + iu_2(t,x)$ and then approximate these parts treating them as coupled components of the consequent reaction diffusion equations:

$$u_{1,t} + u_{2,xx} - \nu(u_1^2 + u_2^2)u_2 = 0, \tag{5.10}$$

$$u_{2,t} - u_{1,xx} + \nu(u_1^2 + u_2^2)u_1 = 0. \tag{5.11}$$

We consider the domain for the problem big enough so that $u(t,x)$ may be taken zero on boundary of domain as discussed in the earlier section. Thus, we take $\Omega = (a,b)$ and

$$u_1(a,t) = 0 = u_2(a,t) = 0 \text{ and } u_1(b,t) = 0 = u_2(b,t) = 0. \tag{5.12}$$

Furthermore, suppose the initial conditions are $u_1(0,x) = u_{10}(x)$ and $u_2(0,x) = u_{20}(x)$, for $x \in \Omega$.

We reformulate the problem (5.10)-(5.11) with boundary conditions (5.12) in its weak form. The weak form essentially weakens the regularity requirement on the solution, and thereby, enabling us to try even those functions as potential candidate for solution which lack enough regularity. In other words, this formulation broadens the solution space. To evaluate weak form, we push the derivatives of solution to a chosen smooth test function.

The weak formulation to the problem is obtained by multiplying the Eqs. (5.10) and (5.11) by some function (called test function) $w \in H_0^1(\Omega)$ and then integrating w.r.t. space variable x over Ω. The use of integration by parts together with homogeneous boundary conditions (5.12) yields the following weak formulation:

We say that functions (u_1, u_2) such that

$$u_1,\ u_2 \in L^2(0,T;H_0^1(\Omega)) \text{ with } u_1',\ u_2' \in L^2(0,T;H^{-1}(\Omega)) \tag{5.13}$$

is a weak solution of (5.10)-(5.11) if

$$(u_1',\phi) - (u_{2,x},\phi_x) - \nu(u_1^2u_2,\phi) - \nu(u_2^3,\phi) = 0,\ \forall\phi \in H_0^1(\Omega), \tag{5.14}$$

$$(u_2',\phi) + (u_{1,x},\phi_x) + \nu(u_1^3,\phi) + \nu(u_1u_2^2,\phi) = 0,\ \forall\phi \in H_0^1(\Omega), \tag{5.15}$$

and

$$u_1(0,x) = u_{10}(x),\ u_2(0,x) = u_{20}(x). \tag{5.16}$$

Here, u' represents derivative of u with respect to t.

Theorem 5.4.1. *Suppose* $u \in L^2(0,T;H_0^1(\Omega))$ *with* $u' \in L^2(0,T;H^{-1}(\Omega))$. *Then* $u \in$

$C([0,T];L^2(\Omega))$ *and*

$$\max_{0\le t\le T}||u(t)||\le C(||u||_{L^2(0,T;H_0^1)}+||u'||_{L^2(0,T;H^{-1})}).$$

Proof. See [30], Chapter 5, Section 5.9. ∎

By Theorem 5.4.1, we see the point values in Eq. (5.16) make sense.

In view of (5.13) and Theorem 5.4.1, the solution space of the problem is $\mathcal{S} = C(0,T;L^2(\Omega))$, which is infinite dimensional space since it contains polynomials of all degrees. To get an approximation of the solution by Galerkin method, we take a finite dimensional subspace V_m of $\mathcal{S}$, characterized by discretization parameter h, which is $\max_{j\in\{1,2,...,m-1\}}(x_{j+1}-x_j)$ for a discretization $\{x_i\}_{i=1}^m$ of Ω, where $a=x_1<x_2<...<x_m=b$.

Taking a Lagrange basis $\{\phi_i\}_{i=1}^m$ of linear polynomials for V_m, we write

$$u_1(t,x)=\sum_{i=1}^m c_i(t)\phi_i(x),\ u_2(t,x)=\sum_{i=1}^m d_i(t)\phi_i(x), \tag{5.17}$$

where $\phi_i(x)=\frac{x-x_{i-1}}{x_i-x_{i-1}}$, for $x_{i-1}<x<x_i$, $2\le i\le m$ and $\phi_i(x)=\frac{x_{i+1}-x}{x_{i+1}-x_i}$ for $x_i<x<x_{i+1}$, $1\le i\le m-1$. Putting u_1 and u_2 from Eq. (5.17) into (5.14)-(5.15) and taking $\phi=\phi_j(x)$, we get the following matrix form,

$$Ac'-Bd-\nu e(c,d)-\nu p(d)=0, \tag{5.18}$$

$$Ad'+Bc+\nu f(c)+\nu q(d,c)=0, \tag{5.19}$$

where matrices A and B are assembled from element matrices A^e and B^e, which are given in earlier chapters. The vector q which depends on unknowns c and d and is assembled from the following element vector

$$q^e(c,d)=\left(\frac{h}{60}\right)\begin{bmatrix} 12c1^2d1+3c2^2d2+2(c2^2d1+2c1c2d2)+3(c1^2d2+2c1c2d1)\\ 3d1c1^2+12d2c2^2+3(c2^2d1+2c1c2d2)+2(c1^2d2+2c1c2d1)\end{bmatrix},$$

where $c1$ and $c2$ represent the values of c at end nodes of an element $e=[x_i,x_{i+1}]$, $d1$ and $d2$ represent the values of d at end nodes of the element e. The vector p which depends on

unknown d only, is assembled from the following element vector

$$p^e(d) = \left(\frac{h}{60}\right) \begin{bmatrix} 12d1^3 + 3d2^3 + 9d1^2d2 + 6d1d2^2 \\ 3d1^3 + 12d2^3 + 6d1^2d2 + 9d1d2^2 \end{bmatrix}.$$

Matrices A, B are assembled diagonally from element matrices A^e, B^e. To make the assembly process clear, we give the assembled matrix A here,

$$A = \begin{bmatrix} h/3 & h/6 & 0 & \dots & 0 \\ h/6 & 2h/3 & h/6 & \dots & 0 \\ 0 & h/6 & 2h/3 & \dots & 0 \\ \vdots & \vdots & \vdots & \ddots & \vdots \\ 0 & 0 & 0 & h/6 & h/3 \end{bmatrix}.$$

Applying C-n method at $t^{k-1/2}$ to Eqs. (5.18)-(5.19), we get

$$\frac{A}{dt}c^k = \frac{A}{dt}c^{k-1} + Bd^{k-1/2} + \nu q(c^{k-1/2}, d^{k-1/2}) + \nu p(d^{k-1/2}), \tag{5.20}$$

$$\frac{A}{dt}d^k = \frac{A}{dt}d^{k-1} - Bc^{k-1/2} - \nu q(c^{k-1/2}) - \nu p(d^{k-1/2}, c^{k-1/2}). \tag{5.21}$$

To resolve the problem of non-linearity involved in vectors p and q, P-C method is resorted to, which is illustrated in the following algorithm:

(i) having c^0, d^0 from the initial profile, put $k = 1$ in (5.20)-(5.21) and replace $c^{1/2}$, $d^{1/2}$ with c^0, d^0; denote c^1 and d^1 so obtained by $c^{1,p}$ and $d^{1,p}$ respectively, indicating predicted values of c^1 and d^1,

(ii) again put $k = 1$ in (5.20)-(5.21) and now replace $c^{1/2}$, $d^{1/2}$ with $\frac{c^0+c^{1,p}}{2}$, $\frac{d^0+d^{1,p}}{2}$; the values of c^1 and d^1 so obtained may be treated as correct values of c^1 and d^1,

(iii) put $k = 2$ in (5.20)-(5.21) and find c^2 and d^2 by replacing $c^{3/2}$, $d^{3/2}$ with $\frac{3c^1-c^0}{2}$, $\frac{3d^1-d^0}{2}$ respectively,

repeating step (iii), we reach to any time level.

Example 1.

In this example, we consider Eq. (5.1) for $\nu < 0$. The solution in this case follows from Eq.

(5.7),

$$u(t,x) = \sqrt{\frac{2k_1}{\lambda}}\text{sech}\left(\sqrt{k_1}(x-2at)\right)e^{i(ax+bt)}, \tag{5.22}$$

where $\nu = -\lambda$, $k_1 = b + a^2$ and a, b are independent parameters. If we write $ax + bt$ as $a(x - \frac{-b}{a}t)$, then $\frac{-b}{a}$ represents soliton wave speed. Taking $\lambda = 2$, $a = 2$, $b = -3$, then $k_1 = 1$. Taking initial and boundary conditions from this solution, we plot the solution in Fig. 5.1. We observe in the Fig. 5.1 that the wave speed for the real and imaginary parts is $\frac{-b}{a}$; however, the wave speed for $|u|$ is $2a$, *i.e.*, 4 in this case. As we see in time $t = 4$, the wave reaches to $x = 16$. This speed $2a$ is also evident from Eq. (5.22), where $|u|$ has a factor $(x - 2a)$ in the argument of function.

Example 2.

In this example, we observe the interaction of two solitons. We consider two soliton-type solutions just like in the previous example. If $u(t,x)$ is solution of Eq. (5.1), then $u^s(t,x) = u(t, x - x_s)$ for some fixed x_s, is also a solution of Eq. (5.1), since $u^s_t = u_t$ and $u^s_x = u_x$. Therefore,

$$u_j(t,x) = \sqrt{\frac{2k_{1j}}{\lambda}}\text{sech}\left(\sqrt{k_{1j}}((x-x_j) - 2a_jt)\right)e^{i(a_i(x-x_j)+b_jt)}, \tag{5.23}$$

are also solutions of Eq. (5.1), where $j = 1, 2$ and $k_{1j} = b_j + a_j^2$. Taking $x_1 = -10$, $x_2 = 10$, $\lambda = 2$, $a_1 = 2$, $a_2 = -2$, $b_j = -3$, for both $j's$. Therefore, $k_{1j} = 1$, $j = 1, 2$. Considering the initial conditions $u(0,x) = u_1(0,x) + u_2(0,x)$, we plot interactions between solitons in Fig. 5.2. We note that at time $t = 0$ solitons peaks are at $x = -10$ and $x = 10$. As time progresses solitons begin to move towards each other with wave velocity $a_1(= 2)$ and $a_2(= -2)$ and at $t = 2.5$ the super-imposition kind of situation observed. The opposite direction of movement of solitons is accounted for by the opposite sign of a_1 and a_2. Thereafter, the solitons move apart. 3D plot of the absolute value of the solution $|u|$ is plotted in Figure 5.3 and its contour version is Figure 5.4.

Example 3.

In this example, we demonstrate that the proposed computational scheme works well even with the case where the coefficients of the Eq. (5.1) are time dependent. Therefore, we

consider the following problem,

$$iu_t + \left(\frac{1}{2}\cos t\right) u_{xx} + \left(\frac{\cos t}{\sin t + 3}\right) |u|^2 u = 0,\ x \in [-20, 20],\ t > 0. \tag{5.24}$$

Considering homogeneous boundary conditions on the domain Ω, an exact solution is given by [25],

$$u(t,x) = \frac{1}{\sqrt{\sin t + 3}} \text{sech}\left(\frac{x}{\sin t + 3}\right) e^{i\left(\frac{x^2-1}{2(\sin t+3)}\right)}. \tag{5.25}$$

Taking initial conditions from the exact solution, the numerical simulations are plotted in Fig. 5.5 for different times. 3D plot of the absolute value of the solution $|u|$ is plotted in Figure 5.6 and its contour version is Figure 5.7. We do not see any movement of solitons in this example because the effect of time is being modulated by the presence of sine function.

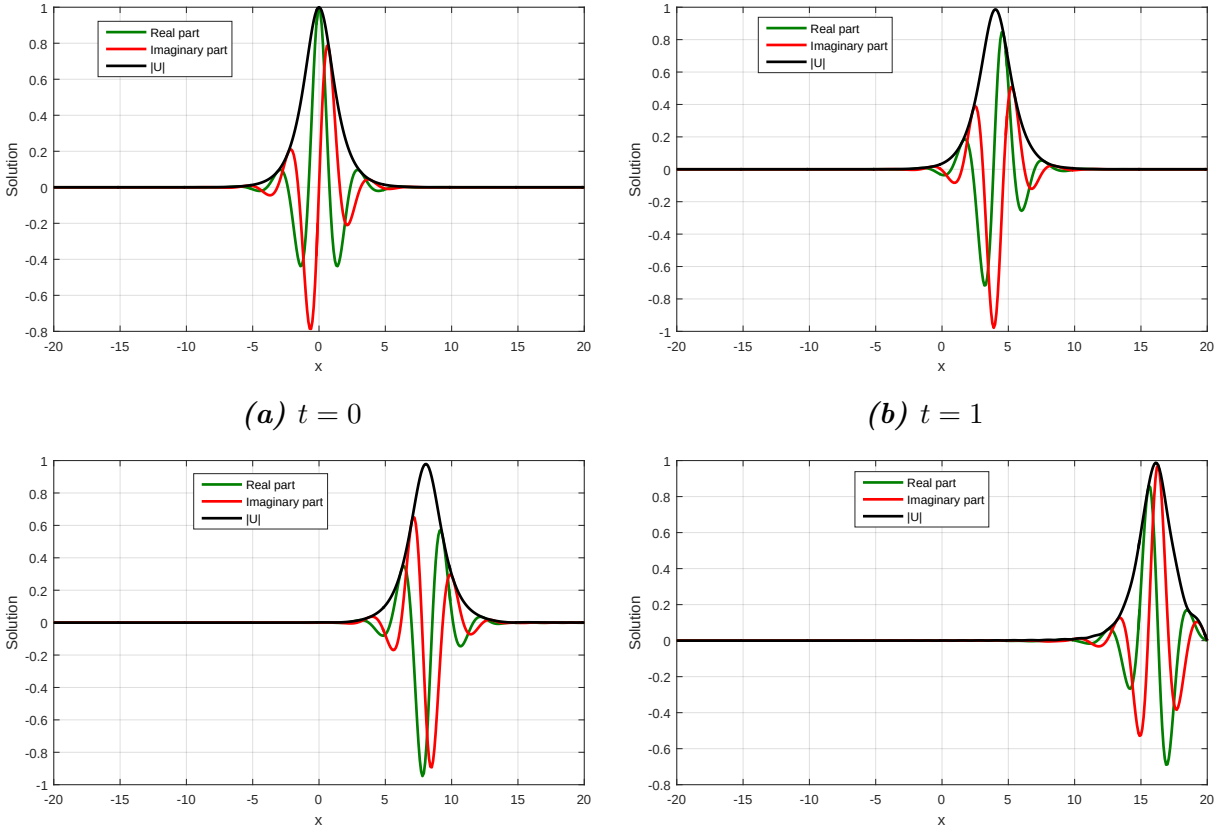

(a) $t = 0$ ***(b)*** $t = 1$

(c) $t = 2.5$ ***(d)*** $t = 4$

Figure 5.1: *Soliton solution of Example 1 for different times. We note from Section 4 that* $\sqrt{a^2 + k_1 tanh^2\left(\sqrt{k_1}(x - 2at)\right)} \geq 1$ *since* $a = 2$ *and* $k_1 = 1 > 0$. *Therefore, the domain should include the interval* $[4t - \sqrt{2}, 4t + \sqrt{2}]$. *This figure validates this result as most the variation in* U *is confined to this interval. Computational parameters:* $\Delta t = 0.0001$, $h = \frac{1}{10}$.

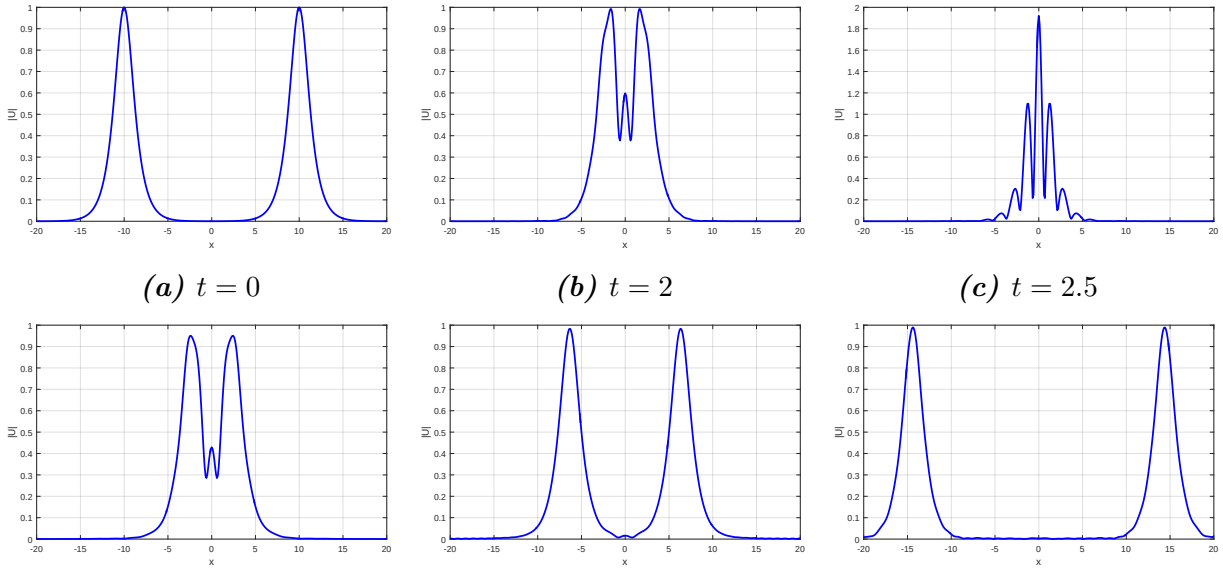

(a) $t = 0$ ***(b)*** $t = 2$ ***(c)*** $t = 2.5$

(d) $t = 3$ ***(e)*** $t = 4$ ***(f)*** $t = 6$

Figure 5.2: *Soliton solution of Example 2 at different times. The solitons in (a) starts moving towards each other, interacts at* $t = 2.5$ *in (c), then move away. We observe that solitons switch positions in (a) and (e)— the left one in (a) is the right one in (e). Computational parameters:* $\Delta t = 0.00001$, $h = \frac{1}{10}$.

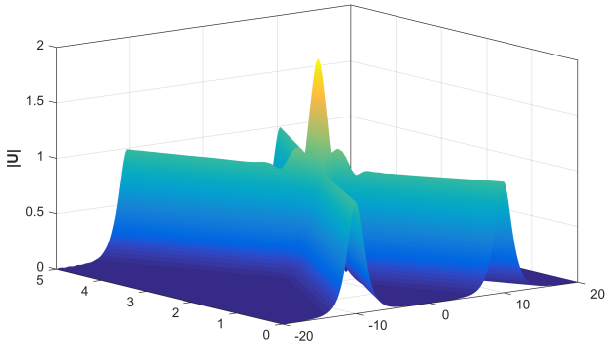

Figure 5.3: *3D plot of* $|u| = \sqrt{u_1^2 + u_2^2}$, *where* u_1, u_2 *represent real and imaginary parts of the solution w.r.t. space* $x \in [-20, 20]$ *and time* $t \in [0, 2]$, $\Delta t = 0.00001$, $h = \frac{1}{10}$.

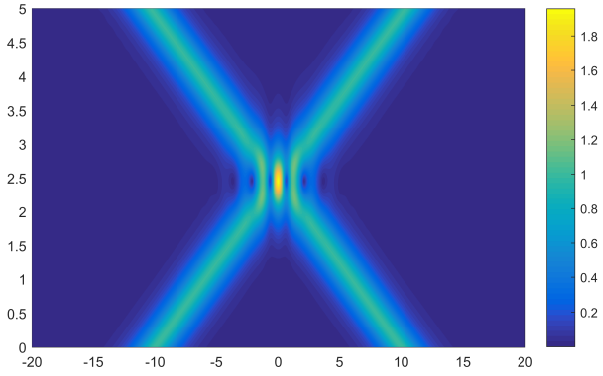

Figure 5.4: *Contour plot of Figure 5.3*

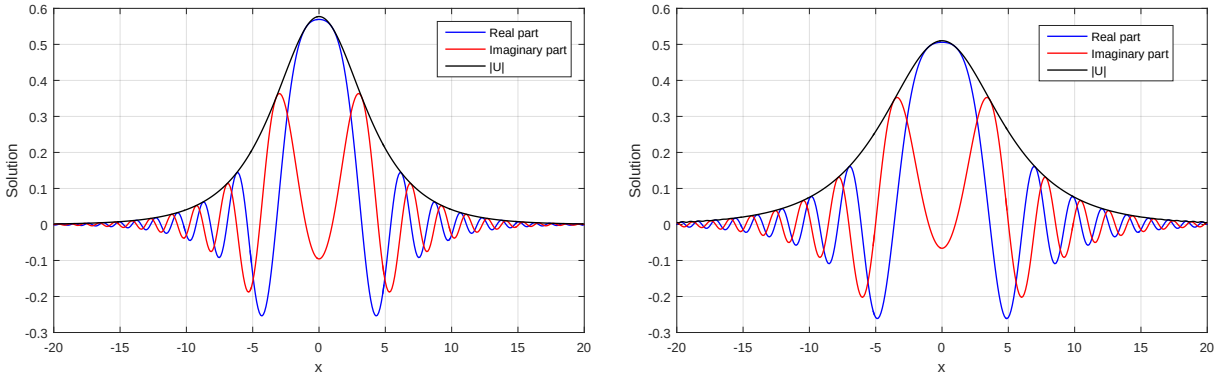

(a) $t = 0$ ***(b)*** $t = 1$

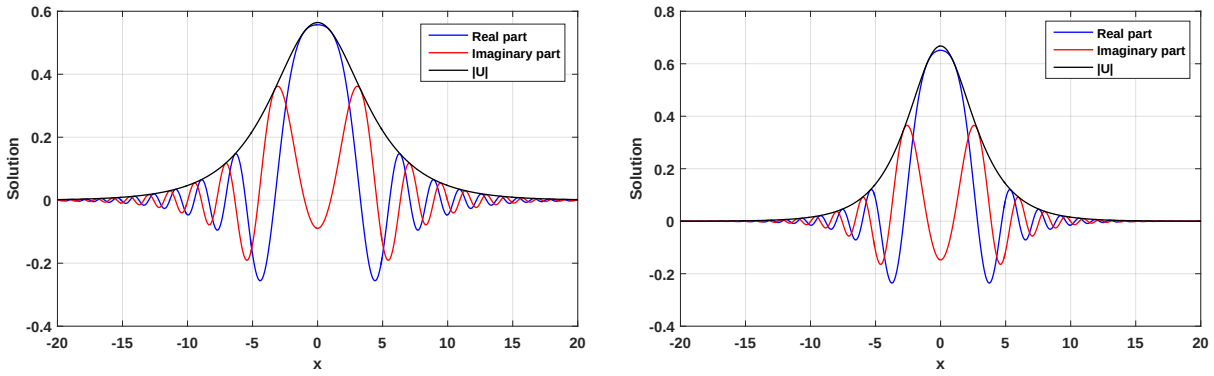

(c) $t = 3$ ***(d)*** $t = 4$

Figure 5.5: *Soliton solution of Example 3 at different times. Computational parameters:* $\Delta t = 0.00001$, $h = \frac{1}{10}$.

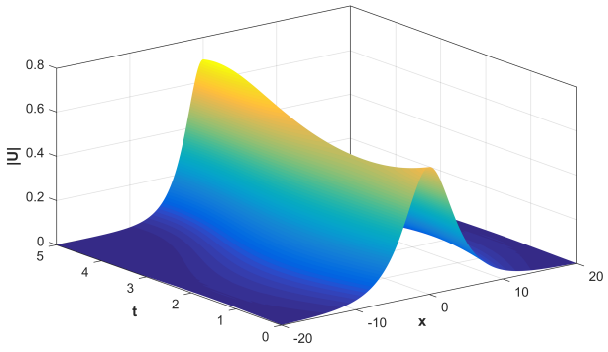

Figure 5.6: *3D plot of* $|u| = \sqrt{u_1^2 + u_2^2}$, *where* u_1, u_2 *represent real and imaginary parts of the solution w.r.t. space* $x \in [-20, 20]$ *and time* $t \in [0, 5]$, $\Delta t = 0.00001$, $h = \frac{1}{10}$.

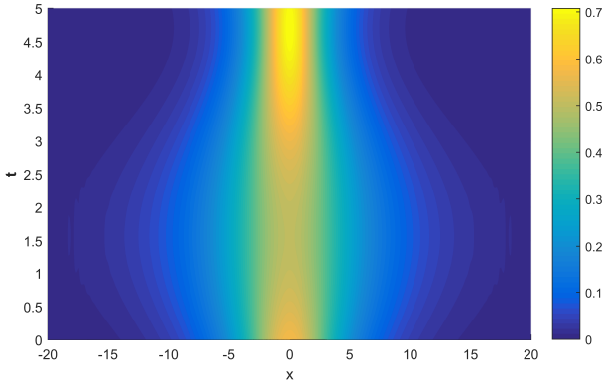

Figure 5.7: *Contour plot of Figure 5.6.*

Chapter 6

Reaction Diffusion Advection Models

In this chapter, we present finite element approximation of generalized semilinear reaction-diffusion-advection equation $u_t(t,x) - d\Delta u(t,x) + f(u, \nabla u) = 0$, where f is Lipschitz continuous in both of its arguments. In Sec. 6.3, existence of the solution is discussed by Banach fixed point theorem and uniqueness is done by using a simple transformation. Then, a priori L^2 error estimates of a Galerkin finite element approximation to the solution is given for semi-discrete in Sec. 6.4. In Sec. 6.6, computational modeling is done using C-N method and the non-linearity is handled by P-C scheme .

6.1 Introduction

Non-linear reaction diffusion (RD) equations are one of the most important classes of PDEs modeling real world problems from different disciplines of the science and engineering. For example, Sherratt and Murray [107] describe how modeling of wound healing process gives rise to RD equations. Chaplain [19] studies role of the reaction diffusion equation in the process tumor invasion. In an another article, Harrison [45] explains the mechanism of pattern formation in living organisms. The models used in these pattern-forming dynamics are usually described by non-linear RD equations.

We wish to analyze the following semi-linear unsteady reaction-diffusion-advection equation:

$$u_t(t,x) - d\Delta u(t,x) + f(u, \nabla u) = 0, \ (t,x) \in (0,T] \times \Omega, \tag{6.1}$$

$$u(t,x) = 0, \ (t,x) \in (0,T] \times \partial\Omega, \tag{6.2}$$

$$u(0,x) = u_0(x),\ x \in \Omega, \tag{6.3}$$

where d is the diffusion coefficient, $u_0(x) \in H_0^1(\Omega)$ vanishes on the boundary $\partial\Omega$, Ω is a domain of $\mathbb{R}^n$, $n = 1, 2$ and $f(u, \nabla u)$ is Lipschitz continuous in u and ∇u, that is,

$$|f(v_1, w_1) - f(v_2, w_2)| \leq C\sqrt{|v_1 - v_2|^2 + |w_1 - w_2|}, \tag{6.4}$$

for $v_1, v_2 \in \mathbb{R}$ and $w \in \mathbb{R}^n$.

Here, $u : \{0\} \cup \mathbb{R}^+ \times \mathbb{R}^n \to \mathbb{R}$ represents an unknown function to be evaluated, $u_0 : \mathbb{R}^n \to \mathbb{R}$, a given initial data and $f : \mathbb{R} \times \mathbb{R}^n \to \mathbb{R}$, a source function.

Existence and uniqueness of $u_t - \Delta u = f(u)$ has been surveyed in introduction. In this chapter, we prove existence and uniqueness of the equation $u_t - d\Delta u = f(u, \nabla u)$ under the more generalized assumption on f, taking $f(u, \nabla u)$ Lipschitz continuous in u and ∇u. Besides, the Banach fixed point theorem is used here to prove existence of the solution under suitable assumptions, which uses theory of partial differential equations and does not require a priori estimates.

The important works regarding the approximation of solution by Galerkin method and a priori estimates for such error of approximation are [27, 66, 123]. In these works, the error estimates are derived for nonlinear equations in divergence form, that is, $u_t - \nabla(a(u)\nabla u) = f(u)$, for f being Lipschitz continuous in u. However, the divergence form can not lead to an arbitrary order of ∇u in the problem. Therefore, we take general f which depends on u and ∇u. Under some restrictions, we establish a priori estimates and found second order convergence in space variable.

With regard to fully discritization, there are different schemes which have been used in literature such as explicit scheme, Euler implicit scheme, C-N scheme, θ methods *etc* [123]. Amongst these schemes, only CN scheme has second order convergence and unconditional stability. But, due to nonlinearity in f, we get a system of nonlinear equations. To resolve this problem, the predictor corrector (PC) method is proposed [27, 113]. In the numerical experiments, we will use this CN cum PC method to get a scheme. Lastly, we consider some examples in 1D as well as in 2D to show the second order convergence.

6.2 Weak Formulation

The weak formulation to the problem (6.1) with boundary condition (6.2), is obtained by multiplying the equation (6.1) by some function $v \in H_0^1(\Omega)$ and then integrating w.r.t. space variable x over Ω. The use of integration by parts yields the following weak formulation: We say that a function

$$u \in L^2(0,T;H^2(\Omega) \cap H_0^1(\Omega)) \text{ with } u' \in L^2(0,T;H^{-1}(\Omega)) \tag{6.5}$$

is a weak solution of (6.1)-(6.3) if

$$< u', \phi > + d(\nabla u, \nabla \phi) + (f(u, \nabla u), \phi) = 0 \tag{6.6}$$

holds for every $\phi \in H_0^1(\Omega)$, and

$$u(0,x) = u_0(x). \tag{6.7}$$

Theorem 6.2.1. *Suppose $f \in L^2(0,T;H_0^1(\Omega))$ with $f' \in L^2(0,T;H^{-1}(\Omega))$. Then $f \in C([0,T];L^2(\Omega))$ and*

$$\max_{0 \le t \le T} ||f(t)|| \le C(||u||_{L^2(0,T;H_0^1(\Omega))} + ||f'||_{L^2(0,T;H^{-1}(\Omega))}).$$

Proof. See [30], Chapter 5, Section 5.9. ∎

In view of the above theorem, the point values in Eq. (6.7) make sense.
For the space $\mathcal{S} = C([0,T];L^2(\Omega))$, we associate the following norm

$$||u(t)||_{\mathcal{S}} = \max_{0 \le t \le T} ||u(t)||.$$

6.3 Existence and Uniqueness of Solution

Theorem 6.3.1. *If $||\nabla u_1(t) - \nabla u_2(t)||_{\mathcal{S}} \le ||(u_1(t) - u_2(t))||_{\mathcal{S}}$, then there exists a weak solution of (6.1)-(6.3).*

Lemma 1. For u satisfying (6.6) and having regularity as in (6.5), u and ∇u belong to $\mathcal{S}$.

Proof. From Theorem 6.2.1, we deduce that $u \in \mathcal{S}$.

As $u \in L^2(0,T;H^2(\Omega) \cap H_0^1(\Omega))$, this implies $u_{x_i} \in L^2(0,T;H_0^1(\Omega))$ and hence $\nabla u \in L^2(0,T;H_0^1(\Omega))$. The assumption (6.4) on f implies $f \in L^2(0,T;H_0^1(\Omega))$. Therefore $\nabla f \in L^2(0,T;L^2(\Omega))$. Thus, from (6.6), component-wise differentiation yields,

$$(\nabla u_t(t), \phi) + d(\nabla^2 u, \nabla\phi) + (\nabla f, \phi) = 0.$$

From characterization of H^{-1} [30], we see that since $||\nabla u_t(t)||_{H^{-1}(\Omega)} < \infty$, therefore $\nabla u_t \in L^2(0,T;H^{-1}(\Omega)$. Now, we call upon Theorem 6.2.1 to see $\nabla u \in V$. ∎

Proof. Continuing with the proof of the theorem, we set $h(t) = f(u(t), \nabla u(t)),\ 0 \le t \le T$. From the Lemma 1, we may note that $h(t) \in L^2(0,T;L^2(\Omega))$.

From the theory of linear PDEs [30], the problem

$$\begin{aligned} w_t(t,x) - \Delta w(t,x) &= h(t,x)\ (t,x) \in (0,T] \times \Omega, \\ w(t,x) &= 0,\ (t,x) \in (0,T] \times \partial\Omega, \\ w(0,x) &= u_0(x),\ x \in \Omega, \end{aligned} \tag{6.8}$$

has a unique weak solution in $L^2(0,T;H_0^1(\Omega))$ with $w' \in L^2(0,T;H^{-1}(\Omega))$. This implies w belongs to $\mathcal{S}$ and w satisfies

$$< w_t, \phi > + (\nabla w, \nabla\phi) = (h, \phi),\ \forall\ \phi \in H_0^1(\Omega), \tag{6.9}$$

for *a.e.* $0 \le t \le T$ and $w(0,x) = u_0(x)$.

Defining operator A such that $Au = w$, we need to show that A is contracting in order to apply Banach fixed point theorem. Towards that end, we start by controlling $w_1 - w_2$. Taking $v = w_1 - w_2$ in (6.9), we have

$$\begin{aligned} \frac{1}{2}\frac{d}{dt}||w_1 - w_2||^2 + ||w_1 - w_2||_{H_0^1}^2 &= (h_1 - h_2, w_1 - w_2) \\ &\le c||h_1 - h_2||^2 + \frac{1}{4c}||w_1 - w_2||^2 \\ &\le c||h_1 - h_2||^2 + \frac{C}{4c}||w_1 - w_2||_{H_0^1}^2. \end{aligned}$$

For $c = C/4$, appropriately large, $0 \leq t \leq T$,

$$\begin{aligned}
\frac{d}{dt}||w_1(t) - w_2(t)||^2 &\leq C||f(u_1, \nabla u_1) - f(u_2, \nabla u_2)||^2 \\
&\leq C(||u_1 - u_2||^2 + ||\nabla u_1 - \nabla u_2||^2). \\
||w_1(t) - w_2(t)||^2 &\leq C(\int_0^t ||u_1(s) - u_2(s)||^2 ds + \int_0^t ||\nabla u_1(s) - \nabla u_2(s)||^2) ds \\
&\leq Ct(\max_{0\leq s\leq t}||u_1(s) - u_2(s)||^2 + \max_{0\leq s\leq t}||\nabla u_1(s) - \nabla u_2(s)||^2) \\
&\leq CT||u_1 - u_2||_{\mathcal{S}}^2, \ 0 \leq t \leq T,
\end{aligned}$$

therefore

$$||w_1 - w_2||_{\mathcal{S}} \leq (CT)^{1/2}||u_1 - u_2||_{\mathcal{S}}.$$

Therefore, $||Au_1 - Au_2||_{\mathcal{S}} = ||w_1 - w_2||_{\mathcal{S}} \leq (CT)^{1/2}||u_1 - u_2||_{\mathcal{S}}$. For sufficiently small T such that $(CT)^{1/2} < 1$, we conclude A is a contracting operator. Appealing to Banach fixed point theorem, we observe that there exists a w such that $w = u$ in (6.8) implying existence of a function satisfying (6.9). ∎

Theorem 6.3.2. *The problem* (6.1) *has a unique solution.*

Proof. Transformation $v = ue^{-\lambda t}$ takes $\Delta u - u_t = f(u, \nabla u)$ to

$$\Delta v - v_t = e^{-\lambda t} f(ve^{\lambda t}, e^{\lambda t}\nabla v) + \lambda v = \tilde{f}(t, x, v, \nabla v).$$

To check if $\tilde{f}$ is monotonically increasing in v, we see, for $v_1 < v_2$

$$\begin{aligned}
\tilde{f}(t, x, v_1, \nabla v) - \tilde{f}(t, x, v_2, \nabla v) &= e^{-\lambda t}(f(t, x, e^{\lambda t}v_1, e^{\lambda t}\nabla v) - f(t, x, e^{\lambda t}v_2, e^{\lambda t}\nabla v)) + \lambda(v_1 - v_2) \\
&\leq e^{-\lambda t}|f(t, x, e^{\lambda t}v_1, e^{\lambda t}\nabla v) - f(t, x, e^{\lambda t}v_2, e^{\lambda t}\nabla v)| + \lambda(v_1 - v_2) \\
&\quad \text{(since } x \leq |x|\text{)} \\
&\leq e^{-\lambda t}M|e^{\lambda t}v_1 - e^{\lambda t}v_2| + \lambda(v_1 - v_2), \text{ from (6.4)} \\
&= -M(v_1 - v_2) + \lambda(v_1 - v_2) = (\lambda - M)(v_1 - v_2). \qquad (6.10)
\end{aligned}$$

Therefore, we see from (6.10), $\tilde{f}$ is monotonically increasing in v for $\lambda > M$.
Suppose u_1 and u_2 are two solutions of (6.1), which are not identically same, then without loss of generality we can assume $u_1 > u_2$ at some points in the domain. Let $u = u_1 - u_2$.

Clearly, u takes positive maximum in the domain Ω_T. Denoting by (t_0, x_0) a point where the maximum is obtained, then $\nabla u(t_0, x_0) = 0$ implying $\nabla u_1 = \nabla u_2$ at (t_0, x_0). For $L = \Delta - \frac{\partial}{\partial t}$, we have

$$\begin{aligned} Lu(t_0, x_0) &= (Lu_1 - Lu_2)(t_0, x_0) \\ &= \tilde{f}(t_0, x_0, u_1(t_0, x_0), \nabla u_1(t_0, x_0)) - \tilde{f}(t_0, x_0, u_2(t_0, x_0), \nabla u_2(t_0, x_0)) > 0. \end{aligned}$$

But, for linear operators $Lu(t_0, x_0) \leq 0$ for every point of maxima. Hence, a contradiction.

■

6.4 A Priori Error Estimates

In this section, we present a priori error estimates and its order of convergence for Galerkin finite element approximation of the solution $u \in \mathcal{S}$. A finite dimensional subspace V_m of $\mathcal{S}$ is chosen using a discretizing parameter h such that, for some integer $r \geq 2$,

$$\inf_{V \in V_m} \{||v - V|| + h||\nabla(v - V)||\} \leq Ch^s ||v||_s, \text{ for } 1 \leq s \leq r, \tag{6.11}$$

where $v \in H^s \cap H_0^1$.

The semi-discrete problem of (6.6) by Galerkin method is given by: Find $u_m(t) \in V_m$ with some suitable choice of $u_m(0)$ according to the regularity available on u_0, which in most of the cases obtained by interpolation, such that

$$(u_{m,t}, \phi_m) + d(\nabla u_m, \nabla \phi_m) + (f(u_m, \nabla u_m), \phi_m) = 0, \ \forall \ \phi_m \in V_m. \tag{6.12}$$

As described in earlier chapters, error $u_m(t) - u(t)$ is written as $(u_m(t) - U(t)) + (U(t) - u(t)) = \theta(t) + \rho(t)$, where $U(t)$ is an elliptic projection of exact solution $u(t)$ onto V_m, for which the error estimates are available.

To control $\theta(t)$, we see from (6.6) and (6.12), $\forall \phi_m \in V_m$,

$$\begin{aligned} (\theta_t, \phi_m) + d(\nabla\theta, \nabla\phi_m) &= (u_{m,t}, \phi_m) + d(\nabla u_m, \nabla \phi_m) - (U_t, \phi_m) - d(\nabla U, \nabla \phi_m) \\ &= -(f(u_m, \nabla u_m), \phi_m) - (\rho_t + u_t, \phi_m) - d(\nabla u, \nabla \phi_m) \\ &\qquad \text{since } (\nabla \rho, \nabla \phi_m) = 0 \end{aligned}$$

$$= (f(u, \nabla u) - f(u_m, \nabla u_m), \phi_m) - (\rho_t, \phi_m).$$

Since $\theta \in V_m$, therefore, taking $\phi_m = \theta$, we have

$$\begin{aligned}
\frac{1}{2}\frac{d}{dt}||\theta||^2 + d||\nabla\theta||^2 &\leq C(||u - u_m|| + ||\nabla u - \nabla u_m||)||\theta|| + ||\rho_t||||\theta|| \\
&\leq C(||\theta + \rho|| + ||\nabla\theta + \nabla\rho|| + ||\rho_t||)||\theta|| \\
&\leq d||\nabla\theta||^2 + C(||\theta||^2 + ||\rho||^2 + ||\rho_t||^2 + ||\nabla\rho||^2). \\
\frac{1}{2}\frac{d}{dt}||\theta||^2 &\leq C(||\theta||^2 + ||\rho||^2 + ||\rho_t||^2 + ||\nabla\rho||^2). \\
||\theta(t)||^2 &\leq ||\theta(0)||^2 + \int_0^t C(||\theta(s)||^2 + ||\rho(s)||^2 + ||\rho_t(s)||^2 + ||\nabla\rho(s)||^2)ds.
\end{aligned}$$

Using Gronwall inequality,

$$\begin{aligned}
||\theta(t)||^2 &\leq e^{Ct}\Big(||\theta(0)||^2 + \int_0^t C(||\rho(s)||^2 + ||\rho_t(s)||^2 + ||\nabla\rho(s)||^2)ds\Big). \\
||\theta(t)||^2 &\leq K_1||\theta(0)||^2 + K_2\int_0^t (||\rho(s)||^2 + ||\rho_t(s)||^2 + ||\nabla\rho(s)||^2)ds, \quad (6.13)
\end{aligned}$$

where constants K_1 and K_2 may depend on T.

Theorem 6.4.1. *Under appropriate assumptions on u and ρ, we have*

$$\begin{aligned}
||\rho(t)|| + h||\nabla\rho(t)|| &\leq C_1(u)h^2, \ \textit{for } t \in [0, T], \\
||\rho_t(t)|| + h||\nabla\rho_t(t)|| &\leq C_2(u)h^2, \ \textit{for } t \in [0, T].
\end{aligned}$$

Proof. See [113], Chapter 13. ∎

In view of the assumption for existence of solution that $||\nabla u - \nabla U||_{\mathcal{S}} \leq ||u - U||_{\mathcal{S}}$, we see that $||\nabla\theta + \nabla\rho|| \leq ||\theta + \rho|| \leq ||\theta|| + ||\rho||$. From (1.12) and Theorem 6.4.1, we obtain $||\nabla\rho|| \leq Ch^2$, and hence $||\theta(t)||$ has convergence of order h^2.

6.5 Fully Discretization of the Problem

Applying C-N method to (6.12), we obtain

$$\left(\frac{u_m^k - u_m^{k-1}}{\Delta t}, \phi_m\right) + d\left(\frac{u_m^k + u_m^{k-1}}{2}, \nabla\phi_m\right)$$

$$+\left(f\left(\frac{3}{2}u_m^{k-1}-\frac{1}{2}u_m^{k-2},\nabla\left(\frac{3}{2}u_m^{k-1}-\frac{1}{2}u_m^{k-2}\right)\right),\phi_m\right)=0,\ \forall\ \phi_m\in V_m, \quad (6.14)$$

for $k \geq 2$. Here, u_m^k stands for $u_m(t^k)$. We must specify u_m^1 to apply (6.14). To do that, we use P-C method,

$$\left(\frac{u_m^{1,p}-u_m^0}{\Delta t},\phi_m\right)+d\left(\frac{\nabla u_m^{1,p}+\nabla u_m^0}{2},\nabla\phi_m\right)+(f(u_m^0,\nabla u_m^0),\phi_m)=0,$$
$$\left(\frac{u_m^1-u_m^0}{\Delta t},\phi_m\right)+d\left(\frac{\nabla u_m^1+\nabla u_m^0}{2},\nabla\phi_m\right)+\left(f\left(\frac{u_m^{1,p}+u_m^0}{2},\frac{\nabla u_m^{1,p}+\nabla u_m^0}{2}\right),\phi_m\right)=0.$$

We obtain the following semi-discrete system from the analysis presented above.

$$Ac'+Bc=C(c),$$

where c is a column vector containing values of unknown at node points. Here, the element matrices A and B in 1D are

$$\begin{bmatrix} h/3 & h/6 \\ h/6 & h/3 \end{bmatrix},\ \begin{bmatrix} 1/h & -1/h \\ -1/h & 1/h \end{bmatrix}, \quad (6.15)$$

where h represents step-length for space parameter. For 2D case, these matrices are

$$\Delta_e\begin{bmatrix} 1/6 & 1/12 & 1/12 \\ 1/12 & 1/6 & 1/12 \\ 1/12 & 1/12 & 1/6 \end{bmatrix},\ \Delta_e\begin{bmatrix} a_1^2+b_1^2 & a_1a_2+b_1b_2 & a_1a_3+b_1b_3 \\ a_1a_2+b_1b_2 & a_2^2+b_2^2 & a_2a_3+b_2b_3 \\ a_1a_3+b_1b_3 & a_2a_3+b_2b_3 & a_3^2+b_3^2 \end{bmatrix},$$

where Δ_e is elemental area. The matrix C depends on c, nonlinearly. Applying C-N scheme at time $(k-\frac{1}{2})$,

$$A*\left(\frac{c^k-c^{k-1}}{\Delta t}\right)+B*\left(\frac{c^k+c^{k-1}}{2}\right)=C\left(c^{k-\frac{1}{2}}\right). \quad (6.16)$$

The scheme in (6.16) is of second order in time. Resolving non-linearity by using

$$c^{k-\frac{1}{2}}=\frac{3}{2}c^{k-1}-\frac{1}{2}c^{k-2}.$$

But, we must start from $k \geq 2$. Therefore, we need c^0 and c^1 to have c^2. c^0 is known to us from u^0 by interpolation. But in going from c^0 to c^1, we use P-C method as pointed out in

previous chapters.

6.6 Numerical Demonstrations

The spatial domain Ω is discretized into elements. For 1D problems, the elements will be intervals. For 2D problems, the right angled isosceles triangles are taken as elements. Uniform griding is used for both 1D and 2D problems.
We have given L^2 formulae for 1D, corresponding formulas for 2D can easily be arrived at. The L^2 error will be given by

$$\sum_{i=1}^{N} h_i \left(u(t, \frac{x_1+x_2+x_3}{3}, \frac{y_1+y_2+y_3}{3}) - \frac{U(t,x_1,y_1)+U(t,x_2,y_2)+U(t,x_3,y_3)}{3} \right)^2. \quad (6.17)$$

We have implemented the scheme described in the previous section to some problems and found the result fitting to the discussion, that is, second order convergence is observed. To test the accuracy of the scheme, initial and boundary conditions are taken invariably from exact solutions.

Example 1

Consider the Burgers' problem in 1D:

$$u_t - du_{xx} + \alpha u u_x = 0, \ (t,x) \in [0,T] \times (-10,10). \quad (6.18)$$

The initial and boundary conditions are taken from exact solution of (6.18) [84]. A traveling wave solution to (6.18) is given by $u(t,x) = \frac{\nu}{\alpha} - \frac{2d}{\alpha}\tanh(x-\nu t)$, where the parameter ν represents wave speed. Taking $\nu = 1/2$, we explain how the approximate solution is obtained. After applying Galerkin's finite element method, we obtain the following matrix form of (6.18),

$$Ac' + dBc + \alpha C(c) = 0, \quad (6.19)$$

where A and B are given as in (6.15). And

$$C(i) = \int_{x_i}^{x_{i+1}} ((c_i\phi_i + c_{i+1}\phi_{i+1})(c_i\phi_{i,x} + c_{i+1}\phi_{i+1,x}), \phi_i)dx,$$

where ϕ_i and ϕ_{i+1} are the hat functions, given by

$$\phi_i(x) = \frac{x - x_{i+1}}{x_i - x_{i+1}},\ \phi_{i+1}(x) = \frac{x - x_i}{x_{i+1} - x_i},$$

for the generic element (x_i, x_{i+1}). Taking the parameters $d = 1$, $\alpha = -1$, $\Omega = (-10, 10)$ and $T = 1$, the exact and the approximate solutions are plotted in Fig. 6.1a and order of convergence is depicted in Fig. 6.1b. The L^2 and L^∞ errors with their order of convergence are tabulated in Table 6.1.

Another solution to (6.18) is

$$u(t, x) = \frac{2d\pi e^{-\pi^2 dt}\sin\pi x}{\alpha + 2d\pi e^{-\pi^2 dt}\cos\pi x},\ \alpha > 1.$$

Taking initial and boundary conditions from the exact solution, we evaluate the Galerkin finite element approximation of $u(t)$ for different parameters. The results are compared with the results available in literature and we find the proposed scheme offering slightly better results. Table 6.2 presents the comparison of the present results with the results obtained by semi implicit finite-difference method (SIFDM) [96] and the results obtained by modified cubic B-splines collocation method (MCSCM) [84].

Example 2.

Consider 2D Burgers' problem given as follows

$$u_t - d(u_{xx} + u_{yy}) + u(u_x + u_y) = 0,\ (t, x, y) \in [0, T] \times (0, 1) \times (0, 1). \tag{6.20}$$

Following exact solution to (6.20) is considered [86],

$$u(t, x, y) = \frac{1}{1 + e^{\frac{x+y-t}{2d}}}.$$

The parameter h, to refine the mesh, is taken as square root of area. On each refinement the parameter h is halved. Time step Δt is taken as proportional to h. Taking the parameters $d = 0.05$, $T = 1$, the order of convergence is shown in Figure 6.2. The L^2 and L^∞ errors are tabulated in Table 6.3.

Example 3.

Consider 2D Burgers'-Huxley problem of the form,

$$u_t - (u_{xx} + u_{yy}) + \alpha u(u_x + u_y) - u(1-u)(u-\gamma) = 0,\ (t,x,y) \in [0,T]\times(10,20)\times(10,20). \quad (6.21)$$

An exact solution to (6.21) is given by [29],

$$u(t,x,y) = \frac{1}{2} - \frac{1}{2}\tanh\left(\frac{z - \nu t}{r - \bar{\alpha}}\right),$$

where $\bar{\alpha} = \alpha\sqrt{2}$, $r = \sqrt{\bar{\alpha}^2 + 8}$ and $\nu = (2\bar{\alpha} + (\bar{\alpha} - r)(2\gamma - 1))/4$. Taking the parameters $\alpha = 0.4$, $\gamma = 0.4$, $T = 1$, $\Delta t = 0.1h$, the order of convergence is depicted in Figure 6.3. The L^2 and L^∞ errors are tabulated in Table 6.3.

Table 6.1: *L^2 and L^∞ Errors and their Orders of Convergence*

m	h	L^2	Order	L^∞	Order
100	0.2	8.887e-3	-	2.036e-3	-
200	0.1	2.222e-3	1.99	5.129e-4	1.99
400	0.05	5.575e-4	1.99	1.279e-4	2.00
800	0.025	1.393e-4	2.00	3.202e-5	1.99
1600	0.0125	3.482e-5	2.00	8.016e-6	1.99

Table 6.2: *Comparison of L^2 and L^∞ errors ($d = 0.01$, $\alpha = 100$, $T = 1$, $h = 1/m$, $\Delta t = 0.01$)*

	SIFDM [96]		MCSCM [84]		Present Method	
m	L^2	L^∞	L^2	L^∞	L^2	L^∞
10	3.454e-7	4.881e-7	3.284e-7	4.628e-7	3.251e-7	4.587e-7
20	1.012e-7	1.430e-7	8.192e-8	1.164e-7	8.110e-8	1.148e-7
40	4.003e-8	5.668e-8	2.047e-8	2.907e-8	2.027e-8	2.874e-8
80	2.471e-8	3.499e-8	5.119e-9	7.271e-9	5.068e-9	7.187e-9

Table 6.3: *L^2 and L^∞ errors with their orders of convergence for 2D Burgers' and Burgers'-Huxley problem*

		Burgers' Problem				Burgers'-Huxley problem			
h	Δt	L^2	Order	L^∞	Order	L^2	Order	L^∞	Order
0.1250	0.0125	8.397e-3	-	1.361e-3	-	3.828e-7	-	2.645e-8	-
0.0625	0.00625	2.125e-3	1.98	6.504e-4	1.94	9.401e-8	2.02	6.690e-9	1.98
0.0313	0.00313	5.336e-4	1.99	9.104e-5	1.99	2.349e-8	2.00	1.714e-9	1.96
0.0156	0.00156	1.336e-4	2.00	2.647e-5	1.99	5.989e-9	1.97	3.851e-10	2.15

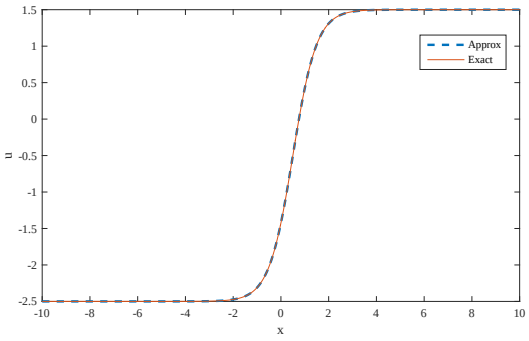

(a) *Comparison of solutions*

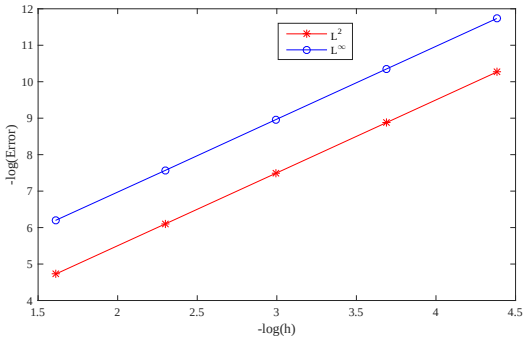

(b) *Order of convergence*

Figure 6.1: *1D Burgers' equation (Ex 1)*

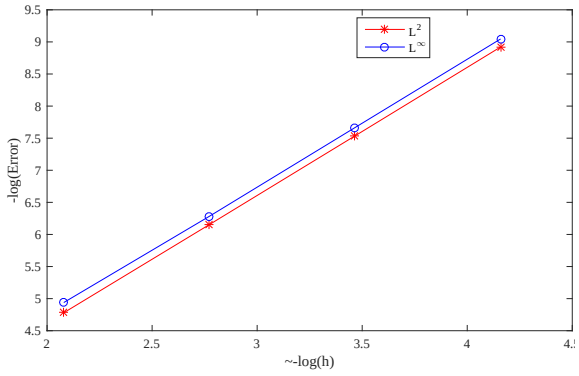

Figure 6.2: *Order of convergence (Ex 2)*

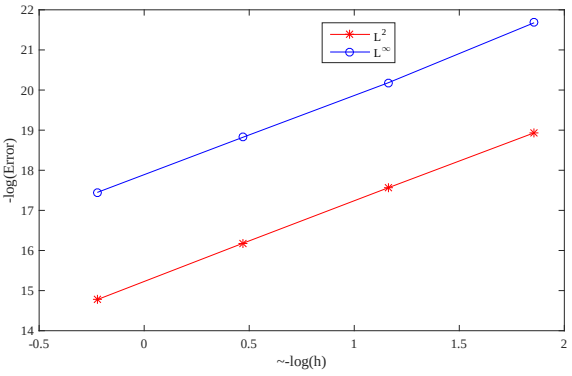

Figure 6.3: *Order of convergence (Ex 3).*

Chapter 7

Conclusions and Future Scopes

7.1 Conclusions

In this thesis, we analyze and approximate some non-linear parabolic PDEs using Galerkin finite element method. Existence of solutions to such PDEs is proved and a priori error estimates for these approximations are also given in most cases. Some examples are also considered in each chapter to validate the analytical findings and to compare the FEM solution with the solutions available in literature.

In **Chapter 2**, we extend finite element analysis available for forced Fisher equation to Burgers'-Fisher equation. We establish existence, uniqueness of solution, a priori error estimate for the approximation and propose a finite element scheme which preserves the positivity of the solution. The scheme offers a good accuracy and efficiency. Other methods available for such equations, for example, Adonian decomposition method, homotopy analysis method, variation iteration method *etc.* use complicated iterations on polynomials to get numerical solutions. But, the present scheme is free from this drawback. Therefore, the scheme offers a good alternative to find approximations of nonlinear problems.

In **Chapter 3**, coupled reaction diffusion equations are analyzed for which the error analysis is not available for a general case. We also prove the existence and uniqueness of the solutions using Banach fixed point theorem, and observe that if the solutions remain bounded in the domain, the solutions exist. Next, we observe second-order convergence of the approximate solutions $u_m(t)$ and $v_m(t)$, i.e. $||u_m(t)-u(t)||\leq K_1h^2$ and $||v_m(t)-v(t)||\leq K_2h^2$. This is verified in `MATLAB` simulations. Furthermore, it is demonstrated that the non-uniform

grids improve the accuracy considerably without much extra computational cost for the kinds of problems considered in this chapter. Numerical results are compared with those available from literature and we find that the proposed method offers better results. Turing patterns are also plotted for some cases, which are found similar to the earlier patterns.

In **Chapter 4**, we approximate Brusselator model when cross-diffusion is present. We know the diffusion in the model induces instability of equilibrium state. This diffusion driven instability is called 'the Turing instability'. We study the effect of cross-diffusion on the stability of the model. We find that the wave number associated to the solution increases in case of cross-diffusion. Approximate solution is obtained and an a priori error estimate for approximation is given. Numerical simulations of some examples are also presented to corroborate the analytical findings.

In **Chapter 5**, we consider the Schrödinger equation with cubic non-linearity. The equations is convertible to a coupled form of the reaction diffusion equation. We obtain some new soliton-type analytical solutions of the equation for all ranges of parameters. Further, some issues related to truncation of domain to finite interval are discussed and the estimates are found. These estimates are verified in the numerical simulations presented by using Galerkin method for spatial discretization and C-N method with P-C scheme for time discretization.

In **Chapter 6**, reaction-diffusion-advection equation is considered for analysis and approximation. The existence and uniqueness of solution to the generalized equation is proved under the assumption that solution varies moderately, that the Lipschitz type condition holds. A priori error estimates are also discussed in the chapter and second order convergence is observed. Some numerical examples are considered and the results are compared with the results from literature, and found slightly better convergence and accuracy.

7.2 Future Scopes

We briefly outline some interesting aspects that may be studied in future.

7.2.1 Adaptivity Analysis

In most of the chapters, we find a priori error estimates for approximations. These bounds serve the purpose of establishing convergence and order of accuracy. However, the estimates usually contains some parameters and constants for which the estimates are usually not available or the estimates are largely coarse and imprecise. Therefore, we intend to find error estimates which are achievable and more importantly refinable. Such estimates are obtained in terms of approximate solutions. Such analysis is called the *adaptivity analysis*. This type of error estimates are known as a posteriori error estimates. These errors may be refined by either refining the mess (*h-adaptivity*) or by increasing the degree of basis polynomials (*p-adaptivity*) or by using some combination of these two (*hp-adaptivity*). These issues are available for exploration in future.

7.2.2 Extension to 2D

We considered some 2D examples in Chapter 6 and we saw that method may be extended to 2D problems. Further, we may extend the method to some other problems like coupled problems in 2D. This may be studied with higher degree basis as well.

7.2.3 More general basis

As we pointed out, we considered linear continuous Lagrange polynomials as basis V_m. The space V_m satisfies (1.7), which is second order accurate. However, if higher order basis be chosen then the order of accuracy can be improved. In this way, we can take a quadratic basis for V_m and V_m satisfies

$$\inf_{\chi \in V_m} \{||v-\chi|| + h||\nabla(v-\chi)||\} \leq Ch^3||v||_3, \tag{7.1}$$

for all $v \in H^3 \cap H_0^1$. If the solution has enough regularity, say H^3, we get more accuracy. But in this case, we also need to take a third order accurate scheme for time discretization. Taking a cue from the P-C scheme

$$c^k = \frac{3}{2}c^{k-1} - \frac{1}{2}c^{k-2},$$

we plan to use the following scheme:

$$c^k = \frac{15}{8}c^{k-1} - \frac{5}{4}c^{k-2} + \frac{3}{8}c^{k-3},\ k \geq 3.$$

But, we have c^0 only and need to supply c^1 and c^2 to evaluate c^3. We may use some other third order accurate method like one of the Runge-Kutta methods to find c^1 and c^2. Once we have these starting values, the rest process is easy and computationally efficient. These schemes could be considered in future.

Bibliography

1. Adomian, G. The diffusion-Brusselator equation. *Comput. Math. Appl.* **29,** 1–3 (1995).

2. Almeida, R. M. P., Antontsev, S. N., Duque, J. C. M. & Ferreira, J. A reaction-diffusion model for the non-local coupled system: existence, uniqueness, long-time behaviour and localization properties of solutions. *IMA J. Appl. Math.* **81,** 344–364 (2016).

3. Alqahtani, A. M. Numerical simulation to study the pattern formation of reaction-diffusion Brusselator model arising in triple collision and enzymatic. *J. Math. Chem.* **56,** 1543–1566 (2018).

4. Alt, H. W. & Luckhaus, S. Quasilinear elliptic-parabolic differential equations. *Math. Z.* **183,** 311–341 (1983).

5. Amann, H. Existence and regularity for semilinear parabolic evolution equations. *Ann. Scuola Norm. Sup. Pisa Cl. Sci. (4)* **11,** 593–676 (1984).

6. Ang, W.-T. The two-dimensional reaction–diffusion Brusselator system: a dual-reciprocity boundary element solution. *Engineering analysis with boundary elements* **27,** 897–903 (2003).

7. Argyris, J. & Haase, M. An engineer's guide to soliton phenomena: application of the finite element method. *Comput. Methods Appl. Mech. Engrg.* **61,** 71–122 (1987).

8. Ashbourn, J. M. A., Geris, L., Gerisch, A. & Young, C. J. S. Numerical simulation of two-dimensional and three-dimensional axisymmetric advection-diffusion systems with complex geometries using finite-volume methods. *Proc. R. Soc. Lond. Ser. A Math. Phys. Eng. Sci.* **466.** With supplementary data available online, 1621–1643 (2010).

9. Ávila, A. I., Meister, A. & Steigemann, M. An adaptive Galerkin method for the time-dependent complex Schrödinger equation. *Appl. Numer. Math.* **121,** 149–169 (2017).

10. Babolian, E. & Saeidian, J. Analytic approximate solutions to Burgers, Fisher, Huxley equations and two combined forms of these equations. *Commun. Nonlinear Sci. Numer. Simul.* **14,** 1984–1992 (2009).

11. Bashan, A., Yagmurlu, N. M., Ucar, Y. & Esen, A. An effective approach to numerical soliton solutions for the Schrödinger equation via modified cubic B-spline differential quadrature method. *Chaos Solitons Fractals* **100,** 45–56 (2017).

12. Bawa, R. K. & Natesan, S. An efficient hybrid numerical scheme for convection-dominated boundary-value problems. *Int. J. Comput. Math.* **86,** 261–273 (2009).

13. Behera, R. & Mehra, M. A dynamic adaptive wavelet method for solution of the Schrodinger equation. *J. Multiscale Model.* **6,** 1450001, 22 (2015).

14. Benilan, P. & Wittbold, P. On mild and weak solutions of elliptic-parabolic problems. *Adv. Differential Equations* **1,** 1053–1073 (1996).

15. Biancalani, T., Fanelli, D. & Di Patti, F. Stochastic Turing patterns in the Brusselator model. *Physical Review E* **81,** 046215–1–046215–8 (2010).

16. Bray, W. C. A periodic reaction in homogeneous solution and its relation to catalysis. *Journal of the American Chemical Society* **43,** 1262–1267 (1921).

17. Brenner, S. C. & Scott, L. R. *The mathematical theory of finite element methods* Third, xviii+397 (Springer, New York, 2008).

18. Brezis, H. & Browder, F. Partial differential equations in the 20th century. *Adv. Math.* **135,** 76–144 (1998).

19. Chaplain, M. A. Reaction–diffusion prepatterning and its potential role in tumour invasion. *Journal of Biological Systems* **3,** 929–936 (1995).

20. Chou, C.-S., Zhang, Y.-T., Zhao, R. & Nie, Q. Numerical methods for stiff reaction-diffusion systems. *Discrete Contin. Dyn. Syst. Ser. B* **7,** 515–525 (2007).

21. Das, P. & Natesan, S. Higher-order parameter uniform convergent schemes for Robin type reaction-diffusion problems using adaptively generated grid. *Int. J. Comput. Methods* **9,** 1250052, 27 (2012).

22. Dağ, I. A quadratic B-spline finite element method for solving nonlinear Schrödinger equation. *Comput. Methods Appl. Mech. Engrg.* **174,** 247–258 (1999).

23. Debnath, L. *Nonlinear partial differential equations for scientists and engineers* Third, xxiv+860 (Birkhäuser/Springer, New York, 2012).

24. Dehghan, M. & Abbaszadeh, M. Variational multiscale element free Galerkin (VMEFG) and local discontinuous Galerkin (LDG) methods for solving two-dimensional Brusselator reaction-diffusion system with and without cross-diffusion. *Comput. Methods Appl. Mech. Engrg.* **300,** 770–797 (2016).

25. Dehghan, M. & Taleei, A. A compact split-step finite difference method for solving the nonlinear Schrödinger equations with constant and variable coefficients. *Comput. Phys. Comm.* **181,** 43–51 (2010).

26. Din, Q. A novel chaos control strategy for discrete-time Brusselator models. *J. Math. Chem.* **56,** 3045–3075 (2018).

27. Douglas, J. Jr. & Dupont, T. Galerkin methods for parabolic equations. *SIAM J. Numer. Anal.* **7,** 575–626 (1970).

28. Ersoy, O. & Dag, I. Numerical solutions of the reaction diffusion system by using exponential cubic B-spline collocation algorithms. *Open Physics* **13,** 414–427 (2015).

29. Ervin, V. J., Macías-Díaz, J. E. & Ruiz-Ramírez, J. A positive and bounded finite element approximation of the generalized Burgers-Huxley equation. *J. Math. Anal. Appl.* **424,** 1143–1160 (2015).

30. Evans, L. C. *Partial differential equations* xviii+662 (American Mathematical Society, Providence, RI, 1998).

31. Fisher, R. A. The wave of advance of advantageous genes. *Annals of eugenics* **7,** 355–369 (1937).

32. Friedman, A. *Partial differential equations of parabolic type* xiv+347 (Prentice-Hall, Inc., Englewood Cliffs, N.J., 1964).

33. Gardner, L. R. T., Gardner, G. A., Zaki, S. I. & El Sahrawi, Z. *B*-spline finite element studies of the nonlinear Schrödinger equation. *Comput. Methods Appl. Mech. Engrg.* **108,** 303–318 (1993).

34. Garvie, M. R. Finite-difference schemes for reaction-diffusion equations modeling predator-prey interactions in MATLAB. *Bull. Math. Biol.* **69,** 931–956 (2007).

35. Gasser, I. & Rybicki, M. Modelling and simulation of gas dynamics in an exhaust pipe. *Appl. Math. Model.* **37,** 2747–2764 (2013).

36. Gerisch, A. & Chaplain, M. A. J. Robust numerical methods for taxis-diffusion-reaction systems: applications to biomedical problems. *Math. Comput. Modelling* **43,** 49–75 (2006).

37. Gerisch, A., Lang, J., Podhaisky, H. & Weiner, R. High-order linearly implicit two-step peer—finite element methods for time-dependent PDEs. *Appl. Numer. Math.* **59,** 624–638 (2009).

38. Golbabai, A. & Javidi, M. A spectral domain decomposition approach for the generalized Burger's-Fisher equation. *Chaos Solitons Fractals* **39,** 385–392 (2009).

39. Gowrisankar, S. & Natesan, S. An efficient robust numerical method for singularly perturbed Burgers' equation. *Appl. Math. Comput.* **346,** 385–394 (2019).

40. Goyal, K. & Mehra, M. A fast adaptive diffusion wavelet method for Burger's equation. *Comput. Math. Appl.* **68,** 568–577 (2014).

41. Gray, P & Scott, S. Autocatalytic reactions in the isothermal, continuous stirred tank reactor: isolas and other forms of multistability. *Chemical Engineering Science* **38,** 29–43 (1983).

42. Gunzburger, M. D., Hou, L. S. & Zhu, W. Modeling and analysis of the forced Fisher equation. *Nonlinear Anal.* **62,** 19–40 (2005).

43. Guo, L. Z., Guo, Y. Z., Billings, S. A., Coca, D. & Lang, Z. Q. The use of Volterra series in the analysis of the nonlinear Schrödinger equation. *Nonlinear Dynam.* **73,** 1587–1599 (2013).

44. Gupta, A. K. & Saha Ray, S. On the solutions of fractional Burgers-Fisher and generalized Fisher's equations using two reliable methods. *Int. J. Math. Math. Sci.* Art. ID 682910, 16 (2014).

45. Harrison, L. G. Kinetic theory of living pattern. *Endeavour* **18,** 130 –136 (1994).

46. Hartman, P. *Ordinary differential equations* xiv+612 (John Wiley & Sons, Inc., New York-London-Sydney, 1964).

47. Hong, J., Ji, L. & Liu, Z. Optimal error estimate of conservative local discontinuous Galerkin method for nonlinear Schrödinger equation. *Appl. Numer. Math.* **127,** 164–178 (2018).

48. Ilati, M. & Dehghan, M. Application of direct meshless local Petrov–Galerkin (DMLPG) method for some Turing-type models. *Engineering with Computers* **33,** 107–124 (2017).

49. Ismail, H. N. A., Raslan, K. & Rabboh, A. A. A. Adomian decomposition method for Burger's-Huxley and Burger's-Fisher equations. *Appl. Math. Comput.* **159,** 291–301 (2004).

50. Ismail, M. S. Numerical solution of coupled nonlinear Schrödinger equation by Galerkin method. *Math. Comput. Simulation* **78,** 532–547 (2008).

51. Javidi, M. Spectral collocation method for the solution of the generalized Burger-Fisher equation. *Appl. Math. Comput.* **174,** 345–352 (2006).

52. Jiwari, R. A hybrid numerical scheme for the numerical solution of the Burgers' equation. *Comput. Phys. Commun.* **188,** 59–67 (2015).

53. Jiwari, R. & Yuan, J. A computational modeling of two dimensional reaction-diffusion Brusselator system arising in chemical processes. *J. Math. Chem.* **52,** 1535–1551 (2014).

54. Jiwari, R., Mittal, R. C. & Sharma, K. K. A numerical scheme based on weighted average differential quadrature method for the numerical solution of Burgers' equation. *Appl. Math. Comput.* **219,** 6680–6691 (2013).

55. Jiwari, R., Singh, S. & Kumar, A. Numerical simulation to capture the pattern formation of coupled reaction-diffusion models. *Chaos Solitons Fractals* **103,** 422–439 (2017).

56. Jiwari, R., Koksal, M. E. & Akca, H. Recent trends in computational and theoretical aspects in differential and difference equations [Editorial]. *J. Math.* Art. ID 3406716, 1 (2017).

57. Jiwari, R., Tomasiello, S. & Tornabene, F. A numerical algorithm for computational modelling of coupled advection-diffusion-reaction systems. *Engineering Computations* **35,** 1383–1401 (2018).

58. Johnson, C., Larsson, S., Thomée, V. & Wahlbin, L. B. Error estimates for spatially discrete approximations of semilinear parabolic equations with nonsmooth initial data. *Math. Comp.* **49,** 331–357 (1987).

59. Joseph, K. T. & Vasudeva Murthy, A. S. Hopf-Cole transformation to some systems of partial differential equations. *NoDEA Nonlinear Differential Equations Appl.* **8,** 173–193 (2001).

60. Kadalbajoo, M. K., Sharma, K. K. & Awasthi, A. A parameter-uniform implicit difference scheme for solving time-dependent Burgers' equations. *Appl. Math. Comput.* **170,** 1365–1393 (2005).

61. Kang, H. & Pesin, Y. Dynamics of a discrete Brusselator model: escape to infinity and Julia set. *Milan J. Math.* **73,** 1–17 (2005).

62. Kesavan, S. *Functional analysis* Second corrected reprint of the 2009 original [MR2475358], xii+269 (Hindustan Book Agency, New Delhi, 2017).

63. Kesavan, S. & Vasudeva Murthy, A. S. On some boundary element methods for the heat equation. *Numer. Math.* **46,** 101–120 (1985).

64. Korkmaz, A. & Dağ, I. A differential quadrature algorithm for simulations of nonlinear Schrödinger equation. *Comput. Math. Appl.* **56,** 2222–2234 (2008).

65. Kumar, V., Kaur, L., Kumar, A. & Koksal, M. E. Lie symmetry based-analytical and numerical approach for modified Burgers-KdV equation. *Results in physics* **8,** 1136–1142 (2018).

66. Larsson, S., Thomée, V. & Zhang, N. Y. Interpolation of coefficients and transformation of the dependent variable in finite element methods for the nonlinear heat equation. *Math. Methods Appl. Sci.* **11,** 105–124 (1989).

67. Leppänen, T. The theory of Turing pattern formation. *in book Current Topics In Physics: In Honor of Sir Roger J Elliott,* 199–227 (2005).

68. Li, Y. Hopf bifurcations in general systems of Brusselator type. *Nonlinear Anal. Real World Appl.* **28,** 32–47 (2016).

69. Liao, W. An implicit fourth-order compact finite difference scheme for one-dimensional Burgers' equation. *Appl. Math. Comput.* **206,** 755–764 (2008).

70. Liao, W., Zhu, J. & Khaliq, A. Q. M. An efficient high-order algorithm for solving systems of reaction-diffusion equations. *Numer. Methods Partial Differential Equations* **18,** 340–354 (2002).

71. Liao, W., Yong, P., Dastour, H. & Huang, J. Efficient and accurate numerical simulation of acoustic wave propagation in a 2D heterogeneous media. *Appl. Math. Comput.* **321,** 385–400 (2018).

72. Lin, Z., Ruiz-Baier, R. & Tian, C. Finite volume element approximation of an inhomogeneous Brusselator model with cross-diffusion. *J. Comput. Phys.* **256,** 806–823 (2014).

73. Liu, W. Existence and uniqueness of solutions to nonlinear evolution equations with locally monotone operators. *Nonlinear Anal.* **74,** 7543–7561 (2011).

74. Lu, W., Huang, Y. & Liu, H. Mass preserving discontinuous Galerkin methods for Schrödinger equations. *J. Comput. Phys.* **282,** 210–226 (2015).

75. Ma, W.-X. & Chen, M. Direct search for exact solutions to the nonlinear Schrödinger equation. *Appl. Math. Comput.* **215,** 2835–2842 (2009).

76. Macías-Díaz, J. E. & González, A. E. A convergent and dynamically consistent finite-difference method to approximate the positive and bounded solutions of the classical Burgers-Fisher equation. *J. Comput. Appl. Math.* **318,** 604–615 (2017).

77. Madzvamuse, A. Time-stepping schemes for moving grid finite elements applied to reaction-diffusion systems on fixed and growing domains. *J. Comput. Phys.* **214,** 239–263 (2006).

78. Malik, S. A., Qureshi, I. M., Amir, M., Malik, A. N. & Haq, I. Numerical Solution to Generalized Burgers'-Fisher Equation Using Exp-Function Method Hybridized with Heuristic Computation. *PloS one* **10,** e0121728 (2015).

79. Mehra, M. & Rathish Kumar, B. V. Time accurate fast three-step wavelet-Galerkin method for partial differential equations. *Int. J. Wavelets Multiresolut. Inf. Process.* **4,** 65–79 (2006).

80. Meng, G.-Q., Gao, Y.-T., Yu, X., Shen, Y.-J. & Qin, Y. Multi-soliton solutions for the coupled nonlinear Schrödinger-type equations. *Nonlinear Dynam.* **70,** 609–617 (2012).

81. Mittal, R. C. & Jain, R. K. Numerical solutions of nonlinear Burgers' equation with modified cubic B-splines collocation method. *Appl. Math. Comput.* **218,** 7839–7855 (2012).

82. Mittal, R. C. & Jiwari, R. Numerical solution of two-dimensional reaction-diffusion Brusselator system. *Appl. Math. Comput.* **217,** 5404–5415 (2011).

83. Mittal, R. C. & Jiwari, R. Numerical study of two-dimensional reaction-diffusion Brusselator system by differential quadrature method. *Int. J. Comput. Methods Eng. Sci. Mech.* **12,** 14–25 (2011).

84. Mittal, R. C. & Jiwari, R. A differential quadrature method for numerical solutions of Burgers'-type equations. *Internat. J. Numer. Methods Heat Fluid Flow* **22,** 880–895 (2012).

85. Mittal, R. C. & Rohila, R. Numerical simulation of reaction-diffusion systems by modified cubic B-spline differential quadrature method. *Chaos Solitons Fractals* **92,** 9–19 (2016).

86. Mittal, R. & Tripathi, A. Numerical solutions of two-dimensional Burgers equations using modified Bi-cubic B-spline finite elements. *Engineering Computations* **32,** 1275–1306 (2015).

87. Mittal, R., Jiwari, R. & Sharma, K. K. A numerical scheme based on differential quadrature method to solve time dependent Burgers' equation. *Engineering Computations* **30,** 117–131 (2012).

88. Moghimi, M. & Hejazi, F. S. A. Variational iteration method for solving generalized Burger-Fisher and Burger equations. *Chaos Solitons Fractals* **33,** 1756–1761 (2007).

89. Neugebauer, G. & Meinel, R. General N-soliton solution of the AKNS class on arbitrary background. *Phys. Lett. A* **100,** 467–470 (1984).

90. Nohara, B. T. Governing equations of envelopes created by nearly bichromatic waves on deep water. *Nonlinear Dynam.* **50,** 49–60 (2007).

91. Olmos-Liceaga, D. & Segundo-Caballero, I. An implicit pseudospectral scheme to solve propagating fronts in reaction-diffusion equations. *Numer. Methods Partial Differential Equations* **32,** 86–105 (2016).

92. Patel, V. K., Singh, S., Singh, V. K. & Tohidi, E. Two dimensional wavelets collocation scheme for linear and nonlinear Volterra weakly singular partial integro-differential equations. *Int. J. Appl. Comput. Math.* **4,** Art. 132, 27 (2018).

93. Pazy, A. *Semigroups of linear operators and applications to partial differential equations* viii+279 (Springer-Verlag, New York, 1983).

94. Prigogine, I. & Lefever, R. Symmetry breaking instabilities in dissipative systems. II. *The Journal of Chemical Physics* **48,** 1695–1700 (1968).

95. Quarteroni, A. *Numerical models for differential problems* Second. Translated from the fifth (2012) Italian edition by Silvia Quarteroni, xx+656 (Springer, Milan, 2014).

96. Rahman, K., Helil, N. & Yimin, R. Some new semi-implicit finite difference schemes for numerical solution of Burgers equation. *in International Conference on Computer Application and System Modeling (ICCASM)* **14,** V14–451 (2010).

97. Rashidi, M. M., Ganji, D. D. & Dinarvand, S. Explicit analytical solutions of the generalized Burger and Burger-Fisher equations by homotopy perturbation method. *Numer. Methods Partial Differential Equations* **25,** 409–417 (2009).

98. Robinson, M. P. The solution of nonlinear Schrödinger equations using orthogonal spline collocation. *Comput. Math. Appl.* **33,** 39–57 (1997).

99. Rodin, E. Y. On some approximate and exact solutions of boundary value problems for Burgers' equation. *J. Math. Anal. Appl.* **30,** 401–414 (1970).

100. Ruiz-Ramírez, J. & Macías-Díaz, J. E. A skew symmetry-preserving computational technique for obtaining the positive and the bounded solutions of a time-delayed advection-diffusion-reaction equation. *J. Comput. Appl. Math.* **250,** 256–269 (2013).

101. Ruiz-Ramírez, J. Preserving nonnegativity of an affine finite element approximation for a convection-diffusion-reaction problem. *J. Comput. Appl. Math.* **306,** 286–299 (2016).

102. Sari, M., Gürarslan, G. & Dağ, I. A compact finite difference method for the solution of the generalized Burgers-Fisher equation. *Numer. Methods Partial Differential Equations* **26,** 125–134 (2010).

103. Schrödinger, E. An undulatory theory of the mechanics of atoms and molecules. *Physical review* **28,** 1049–1070 (1926).

104. Scott, A. C., Chu, F. Y. F. & McLaughlin, D. W. The soliton: a new concept in applied science. *Proc. IEEE* **61,** 1443–1483 (1973).

105. Shakeri, F. & Dehghan, M. The finite volume spectral element method to solve Turing models in the biological pattern formation. *Comput. Math. Appl.* **62,** 4322–4336 (2011).

106. Sharma, N., Khebchareon, M., Sharma, K. & Pani, A. K. Finite element Galerkin approximations to a class of nonlinear and nonlocal parabolic problems. *Numer. Methods Partial Differential Equations* **32,** 1232–1264 (2016).

107. Sherratt, J. A. & Murray, J. Models of epidermal wound healing. *Proceedings of the Royal Society of London B: Biological Sciences* **241,** 29–36 (1990).

108. Singh, S., Patel, V. K., Singh, V. K. & Tohidi, E. Application of Bernoulli matrix method for solving two-dimensional hyperbolic telegraph equations with Dirichlet boundary conditions. *Comput. Math. Appl.* **75,** 2280–2294 (2018).

109. Singh, V. K., Pandey, R. K. & Singh, S. A stable algorithm for Hankel transforms using hybrid of Block-pulse and Legendre polynomials. *Comput. Phys. Comm.* **181,** 1–10 (2010).

110. Tang, S. & Weber, R. O. Numerical study of Fisher's equation by a Petrov-Galerkin finite element method. *J. Austral. Math. Soc. Ser. B* **33,** 27–38 (1991).

111. Tatari, M., Sepehrian, B. & Alibakhshi, M. New implementation of radial basis functions for solving Burgers-Fisher equation. *Numer. Methods Partial Differential Equations* **28,** 248–262 (2012).

112. Thomée, V. & Vasudeva Murthy, A. S. A numerical method for the Benjamin-Ono equation. *BIT* **38,** 597–611 (1998).

113. Thomée, V. *Galerkin finite element methods for parabolic problems* Second, xii+370 (Springer-Verlag, Berlin, 2006).

114. Tomasiello, S. DQ-based simulation of weakly nonlinear heat conduction processes. *Comm. Numer. Methods Engrg.* **24,** 1523–1532 (2008).

115. Tomasiello, S. Numerical solutions of the Burgers-Huxley equation by the IDQ method. *Int. J. Comput. Math.* **87,** 129–140 (2010).

116. Turing, A. M. The chemical basis of morphogenesis. *Philos. Trans. Roy. Soc. London Ser. B* **237,** 37–72 (1952).

117. Twizell, E. H., Gumel, A. B. & Cao, Q. A second-order scheme for the "Brusselator" reaction-diffusion system. *J. Math. Chem.* **26,** 297–316 (2000) (1999).

118. Tyson, J. J. Some further studies of nonlinear oscillations in chemical systems. *The Journal of Chemical Physics* **58,** 3919–3930 (1973).

119. Ul Islam, S., Ali, A. & Haq, S. A computational modeling of the behavior of the two-dimensional reaction-diffusion Brusselator system. *Appl. Math. Model.* **34,** 3896–3909 (2010).

120. Verma, A., Jiwari, R. & Koksal, M. E. Analytic and numerical solutions of nonlinear diffusion equations via symmetry reductions. *Adv. Difference Equ.* 2014:229, 13 (2014).

121. Wang, B. & Liang, D. The finite difference scheme for nonlinear Schrödinger equations on unbounded domain by artificial boundary conditions. *Appl. Numer. Math.* **128,** 183–204 (2018).

122. Wang, X. Y. & Lu, Y. K. Exact solutions of the extended Burgers-Fisher equation. *Chinese Phys. Lett.* **7,** 145–147 (1990).

123. Wheeler, M. F. A priori L_2 error estimates for Galerkin approximations to parabolic partial differential equations. *SIAM J. Numer. Anal.* **10,** 723–759 (1973).

124. Xiao, A., Zhang, G. & Zhou, J. Implicit-explicit time discretization coupled with finite element methods for delayed predator-prey competition reaction-diffusion system. *Comput. Math. Appl.* **71,** 2106–2123 (2016).

125. Zakharov, V. E. & Shabat, A. B. Exact theory of two-dimensional self-focusing and one-dimensional self-modulation of waves in nonlinear media. *Ž. Èksper. Teoret. Fiz.* **61,** 118–134 (1971).

126. Zakharov, V. & Shabat, A. Interaction between solitons in a stable medium. *Sov. Phys. JETP* **37,** 823–828 (1973).

127. Zhang, L. W. & Liew, K. M. An element-free based solution for nonlinear Schrödinger equations using the ICVMLS-Ritz method. *Appl. Math. Comput.* **249,** 333–345 (2014).

128. Zhang, R., Yu, X., Zhu, J. & Loula, A. F. D. Direct discontinuous Galerkin method for nonlinear reaction-diffusion systems in pattern formation. *Appl. Math. Model.* **38,** 1612–1621 (2014).

129. Zhang, R., Zhu, J., Loula, A. F. D. & Yu, X. A new nonlinear Galerkin finite element method for the computation of reaction diffusion equations. *J. Math. Anal. Appl.* **434,** 136–148 (2016).

130. Zhang, R., Zhu, J., Loula, A. F. D. & Yu, X. A new nonlinear Galerkin finite element method for the computation of reaction diffusion equations. *J. Math. Anal. Appl.* **434,** 136–148 (2016).

131. Zhang, T., Feng, X. & Yuan, J. Implicit–explicit schemes of finite element method for the non-stationary thermal convection problems with temperature-dependent coefficients. *International Communications in Heat and Mass Transfer* **76,** 325–336 (2016).

132. Zhao, H.-q. & Yuan, J. A semi-discrete integrable multi-component coherently coupled nonlinear Schrödinger system. *J. Phys. A* **49,** 275204, 17 (2016).

133. Zorsahin Gorgulu, M. & Dag, I. Exponential B-splines Galerkin Method for the Numerical Solution of the Fisher's Equation. *Iran. J. Sci. Technol. Trans. A Sci.* **42,** 2189–2198 (2018).